UC Berkeley
UC Berkeley Electronic Theses and Dissertations

Title
Limit Shapes in the Six Vertex Model

Permalink
https://escholarship.org/uc/item/6k51w95x

Author
Sridhar, Ananth

Publication Date
2016

Peer reviewed|Thesis/dissertation

eScholarship.org Powered by the California Digital Library
University of California

Limit Shapes in the Six Vertex Model

by

Ananth Sridhar

A dissertation submitted in partial satisfaction of the

requirements for the degree of

Doctor of Philosophy

in

Physics

in the

Graduate Division

of the

University of California, Berkeley

Committee in charge:

Professor Yasunori Nomura, Co-chair
Professor Nicolai Reshetikhin, Co-chair
Professor Joel Moore
Professor John Lott

Fall 2016

Abstract

Limit Shapes in the Six Vertex Model

by

Ananth Sridhar

Doctor of Philosophy in Physics

University of California, Berkeley

Professor Yasunori Nomura, Co-chair

Professor Nicolai Reshetikhin, Co-chair

The purpose of this thesis is to present some new results about the six-vertex model and dimer model, andi in particular some aspects of the limit shapes that form in the thermodynamic limit and the partial differential equations that arise in their study. Chapter 1 provides a detailed introduction to limit shape phenomena and its mathematics. Chapter 2 reviews basic facts about the six-vertex model and dimer model and their properties in the thermodynamic limit.

Chapter 3 investigates the role of integrability of the six vertex model in the formation of limit shapes. By integrability we mean, on one hand the discrete integrability of the six-vertex model in the sense of commutative families of transfer matrices, and on the other hand the integrability in the continuum limit in the Liouville sense of Poisson commutative families of functions (integrals of motion) on the phase space. The main result is to show that the partial differential equations describing the limit shape have an infinite number of conserved quantities. For the dimer model, the partial differential equations are related to the inviscid Burgers equation.

Chapter 4 explains the results of the previous chapter in a more general setting. The main result is a straightforward theorem in Hamiltonian mechanics, which gives conditions for the Poisson commutativity of two Hamiltonian functions in terms of their principal action functions. It suggests a generalization of our previous results to other integrable lattice models, for example, the generalizations of the six-vertex model related to other Lie algebras.

Chapter 5 studies the six-vertex model for a special class of weights called the stochastic six-vertex model, for which the six vertex model is closely related to interacting particle models. For these weights, the transfer matrix of the model satisfies the Markov property and defines the transition matrix for a stochastic process that can be seen as a discrete time generalization of the asymmetric exclusion process. The main result of this chapter is the derivation for the partial differential equations for the height function of this stochastic process on the cylinder.

Chapter 6 studies models at the intersection of discrete geometry and statistical mechanics. The main result is the asymptotic expansion of the discrete Laplacian that

approximate Laplace operators induced by a Riemannian metric. These Laplacians arise as a discretization of the Gaussian free field and are closely related to Dimer models that can be regarded as a discretization of Dirac operators in a background metric.

Contents

Contents **i**

1 Introduction **1**
1.1 Preface . . . 1
1.2 Limit Shapes . . . 1
1.3 The Six-vertex and Dimer Model . . . 4
1.4 Outline of Thesis . . . 6
Chapter 2 . . . 6
Chapter 3 . . . 7
Chapter 4 . . . 7
Chapter 5 . . . 7
Chapter 6 . . . 8

2 The Six Vertex and Dimer Model **9**
2.1 Surface Graphs . . . 9
Square Lattice Surface Graphs . . . 9
2.2 The Six Vertex Model . . . 10
The Basics . . . 10
Transfer Matrices . . . 14
The Thermodynamic Limit . . . 17
2.3 The Dimer Model . . . 18
The Basics . . . 18
The Kasteleyn Theory . . . 22
The Thermodynamic Limit . . . 22
2.4 Limit Shapes and the Variational Principle . . . 23
Approximating Surfaces Graphs . . . 23
Normalized Height Functions . . . 24
Stabilizing Boundary Conditions . . . 24
The Variational Principle . . . 24

3 Integrability of Limit Shapes in the Six Vertex Model **25**
3.1 Hamiltonian Framework on the Cylinder . . . 25
3.2 Bethe Ansatz Equations for the Hamiltonian . . . 27
Partial Derivatives of the Hamiltonian . . . 29

3.3 Commuting Hamiltonians . . . 32
Homogenous Hamiltonians . . . 32
Inhomogenous Hamiltonians . . . 34
3.4 The Dimer Model and Burger's Equation. . . . 35
3.5 The Hexagonal Dimer Model and the Five Vertex Model . . . 38
The Dimer Model on the Hexagonal Lattice . . . 38
5-vertex limits of the 6-vertex model . . . 39
3.6 Free Fermionic Point Six Vertex Model . . . 42
The Dimer City . . . 42

4 Semiclassical Limits in Quantum Integrable Systems 46
4.1 Integrable Systems . . . 46
4.2 Commuting Actions and Hamiltonians . . . 49
Glued Actions . . . 50
Commuting Actions . . . 51

5 Limit Shapes in the Stochastic Six Vertex Model 54
5.1 The Stochastic Six Vertex Model . . . 54
The Weights . . . 55
The Transfer Matrix . . . 55
The Markov Process . . . 57
The ASEP Limit . . . 59
5.2 Limit Shapes in the Stochastic 6-vertex model . . . 62
The Variational Problem . . . 62
The Surface Tension Function for $\Delta > 1$ . . . 62
Degeneration to a Parabolic PDE . . . 63
The ASEP Limit and Burgers Equations . . . 65
5.3 Solutions to the Limit Shape equations . . . 66
Characteristics for Conservation Equations . . . 66
Limit Shapes of the Stochastic Six Vertex Model with Domain Wall Initial Conditions . . . 68
5.4 Conclusion . . . 72

6 Asymptotic Determinants of Discrete Laplace Operators 73
6.1 Discrete Laplacians . . . 74
Riemannian Structures on Graphs . . . 75
The Combinatorial Laplacian . . . 76
Gaussian Field Theories on Graphs . . . 77
6.2 Combinatorial Laplacians in Rectangular Graphs . . . 81
6.3 Inverse of Combinatorial Laplacian . . . 83
Smooth Green's Function . . . 83
Combinatorial Green's Function . . . 85
6.4 Asymptotic Determinant of Laplacian . . . 89
Determinant . . . 95

6.5 Conclusions 96

Bibliography **97**

Chapter 1

Introduction

1.1 Preface

The main purpose of this thesis is to present some new results about the six-vertex model and dimer model. In particular, we investigate some aspects of the limit shapes that form in the thermodynamic limit and the partial differential equations that arise in their study. These results are contained in chapters 3-6, each of which is based on research papers and preprints available independently.

The first two chapters provide background and preliminaries. Chapter 1 is intended to give a broad overview of the limit shape phenomena and its mathematics. We motivate and describe the basic ideas of the variational approach that we study for a large part of the thesis. Some aspects of this variational principle, strictly speaking, are still conjectural. We then briefly summarize our main results and outline the remainder of the text. Chapter 2 reviews basic facts about the six-vertex model and dimer model and their properties in the thermodynamic limit.

1.2 Limit Shapes

An important problem in mathematical physics is to understand the relationship between the deterministic laws that describe physics at a macroscopic scale and the statistical laws that describe the same phenomenon at the microscopic scale. For example, each particle of a fluid executes a random walk as it collides with other particles, yet the fluid at the large scale is described by the partial differential equations of hydrodynamics. A rigorous derivation of these equations from the microscopic point-of-view by Boltzmann and many others was a great triumph of statistical mechanics. More broadly, from the mathematical perspective, the emergence of deterministic laws from random processes can be seen as a manifestation of a sort of law of large numbers.

An exciting and flourishing area of mathematical physics today is in developing a similar theory for certain geometric phenomena. It has been observed that a large class of random "stepped" surface models on the lattice, in the continuum limit, converge in probability to non-random surfaces called the *limit shapes*. It turns out that the limit

shapes in these models can be obtained as solutions to certain *variational problems*, structurally similar to those from the classical theory of soap bubbles, elastic sheets, and other physical surfaces and interfaces. We can illustrate the basic principles of this approach with an easy example:

Example: Limit Shapes The Random Walk

Consider a one dimensional random walk $X = \{X_i\}_{i=0\cdots T}$ of T steps on the line $\mathbb{Z}$, conditioned to begin at the origin and end at a point X_T. We can imagine the trace of the random walk as a path on the square lattice $\mathbb{Z}^2$, beginning at the origin and ending at (X_T, T). We would like to study the continuum limit of the random walk, found by scaling the lattice $\mathbb{Z}^2$ by a mesh ϵ tending to zero, while keeping the starting and ending points (viewed as points in the underlying spacetime) of the random walk fixed.

Letting the continuum coordinates $x = \epsilon X$ and $t = \epsilon T$, in the limit $\epsilon \to 0$, the set of all random walks converge to the set of continuum paths $x(t) : [0, t_f] \to \mathbb{R}$ that satisfy the Lipshitz constraint:

$$|x(t) - x(t')| \leq |t - t'|$$

We can ask: in the continuum limit what is the most probable path the particle takes in his random walk? More generally, fixing a continuum path $x(t)$, what is the probability of our particle taking a random walk "near" $x(t)$?

We can answer these questions along the lines of the following calculation. Consider first the random walk conditioned to begin at the origin (and free at the other end), but biased by a "magnetic field" $p \in \mathbb{R}$ so that:

$$\mathrm{P}[\text{step right}] \propto e^{p/2} \qquad \mathrm{P}[\text{step left}] \propto e^{-p/2}$$

Equivalently, the probability of a particular walk X is given by:

$$\mathrm{P}[X] = \frac{1}{Z}\, W(X)$$

where the weight W is:

$$\begin{aligned} W(X) &= e^{(\#\text{ right steps})\, p/2}\; e^{-(\#\text{ left steps})\, p/2} \\ &= e^{vpt/\epsilon} \end{aligned}$$

where $v = X_t/T$ is the average velocity of the walk, and the partition function Z is:

$$\begin{aligned} Z &= \sum_{\text{paths } X} W(X) \\ &= (e^p + e^{-p})^{t/\epsilon} \end{aligned}$$

It is useful to define the normalized free energy density

$$f(p) = \frac{\epsilon}{t} \log(Z) \tag{1.2.1}$$

We can calculate the partition function alternately, by partitioning the sum of all paths by their average velocity:

$$\begin{aligned} Z &= \sum_{\text{paths } X} W(X) \\ &= \sum_{\text{velocities } v} \left(\sum_{\text{paths } X \text{ with velocity } v} W(X) \right) \\ &= \sum_{\text{velocities } v} e^{tvp/\epsilon} \sum_{\text{paths } X \text{ with velocity } v} 1 \\ &= \sum_{\text{velocities } v} \exp\left(\frac{t}{\epsilon} \left(vp - \sigma(v) \right) \right) \end{aligned}$$

Here we defined the surface tension:

$$\sigma(v) = -\epsilon \log \left(\#\text{ paths with velocity } v \right)$$

In the limit $\epsilon \to 0$, the sum over velocities is dominated by the velocity maximizing the exponent.

$$\sum_{\text{velocities } v} \exp\left(\frac{t}{\epsilon} \left(vp - \sigma(v) \right) \right) \sim \exp\left(\frac{t}{\epsilon} \max_v \left(vp - \sigma(v) \right) \right) \left(1 + o(1) \right)$$

Equating to (1.2.1) gives:

$$f(p) = \max_v \left(vp - \sigma(v) \right)$$

In other words, the free energy $f(p)$ and the surface tension $\sigma(v)$ are Legendre duals. We can then take the inverse Legendre transform of $f(p)$ using formula (1.2.1) to calculate:

$$\sigma(v) = \frac{1+v}{2} \log\left(\frac{1+v}{2} \right) - \frac{1-v}{2} \log\left(\frac{1-v}{2} \right)$$

Note that σ is strictly convex.

Now, given a continuum path $x(t)$, we can rectify the path by line segments small compared to the curve but large compared to the lattice. The log of the number of paths near $x(t)$ is roughly equal to the sum of the surface tensions of the slopes/velocities along each line segment. Taking (carefully) the limit to a Riemann integral, we find then that the number of random walks "near" a continuum curve $x(t)$ is given by $\exp(S[x(t)]/\epsilon)$, where:

$$S[x(t)] = -\frac{1}{\epsilon} \int_0^t \sigma\left(\frac{dx}{dt}(t') \right) dt' \tag{1.2.2}$$

In the limit $\epsilon \to 0$, by the same arguments as those above, it is easy to see that the partition function is dominated by the path that minimizes the action $S[x(t)]$. The

minimizing path is the *limit shape*. Moreover, the probability of finding a macroscopic deviation from the limit shape vanishes like $\exp(-1/\epsilon)$ as $\epsilon \to 0$.

The function σ is very important, has many names: in the theory of surfaces, σ is called the *surface tension function*. In statistical mechanics, it is called the *entropy function*. In statistics and large deviations theory, it is called the *rate function*.

In this example, the Euler-Lagrange equations are easily calculated to find the differential equation:

$$\begin{aligned} \frac{\ddot{x}}{1-\dot{x}} &= 0 \\ x(0) &= 0 \\ x(t) &= x_f \end{aligned}$$

The limit shape in this example, is as expected, a straight line.

The above calculations can be made rigorous without too much additional effort. At the loss of some rigor, we can go further to study small fluctuations around the limit shape. The probability of a small fluctuation $\sqrt{\epsilon}\ \delta x$ about the limit shape is found by expanding the action (1.2.2):

$$\mathrm{P}[x + \sqrt{\epsilon}\ \delta x] \propto \exp\left(- \int_0^t \sigma'(\dot{x}(t))\ (\delta \dot{x})^2\ dt \right)$$

We are tempted to say that the fluctations are described by path integral quantization of the classical action S. Indeed, by the standard heuristic path integral techniques one can easily reproduce the answers obtained by taking the asymptotics of exact formulas in terms of binomial coefficients.

1.3 The Six-vertex and Dimer Model

The study of limit shapes in recent years was sparked by the discovery and study of "arctic circles" in tiling models [CEP]. Figure 1 shows random tilings of a hexagonal region by lozenges of decreasing size. Note that a tiling when viewed as a stack of cubes, can equally be interpreted as a stepped surface. As the lozenges become small, each region outside of the arctic circle becomes frozen, only one type of tile is present. Within the arctic circle, the stepped surface converges to the smooth limit shape that can be obtained by minimizing the functional [CKP]

$$\int \sigma(\partial_x h, \partial_y h)\ \ dx\ dy$$

subject to the boundary conditions and various gradient constraints.

The six-vertex model and the dimer model are generalizations of these tiling models. They first arose in classical statistical mechanics as simple models of molecular bonding.

The dimer model takes place on a graph, in which each vertex represents a molecule and each edge a possible bond. A configuration of the model is a choice of bonds

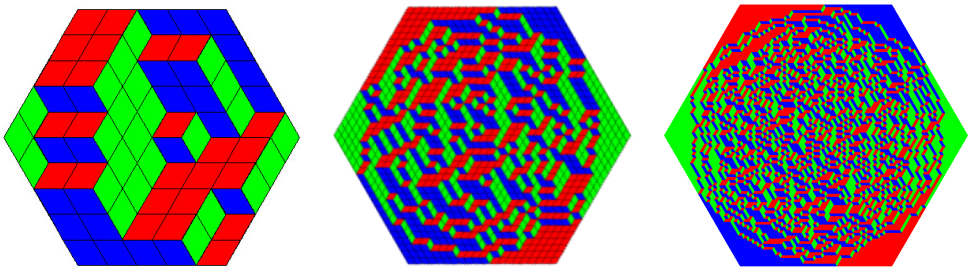

Figure 1.1: The limit shapes in lozenge tilings

(edges of the graph) such that each molecule (vertex) is bonded to exactly one of his neighbors. The dimer model is closely related to the tilings: for example, replacing each bond of the dimer model on a hexagonal graph with a lozenge of the same orientation produces a tiling, see Figure 1.2. The dimer model defines a stepped surface via this interpretation.

The six vertex model takes place on the square lattice, in which each vertex represents a water molecule, and each edge represents a hydrogen bond. In each bond, the hydrogen atom is closer to one of the two water molecules. A microstate of the model is an assignment of hydrogen atoms in each bond, represented by arrows, such that each water molecule has two hydrogens. By mapping rightward and upward arrows to bold edges, a six vertex configuration can be viewed as a set of paths, see Figure 1.3. A six vertex configuration can be reformulated as a stepped surface, whose contour lines are the paths.

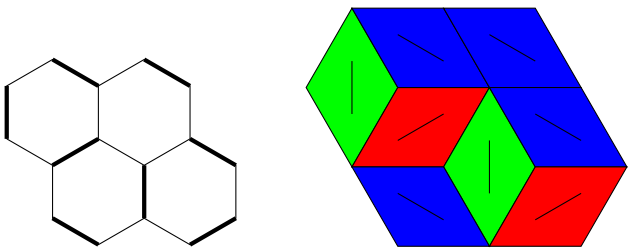

Figure 1.2: A dimer configuration on the hexagonal lattice, and the dual tiling

The six vertex model and the dimer model are especially remarkable in that they are *integrable* or *exactly solvable* models. In the case of the dimer model, this means that the partition function and correlation functions can be computed as the Pfaffians of certain adjacency matrices of the lattice called Kasteleyn matrices. In the case of the six-vertex model, integrability means that the Boltzmann weights and transfer matrices for the model satisfy various algebraic relations that play a deep role in simplifying the computation of partition functions and correlation functions. In particular, the integrability of these models makes the study of the free energy and the surface tension tractable.

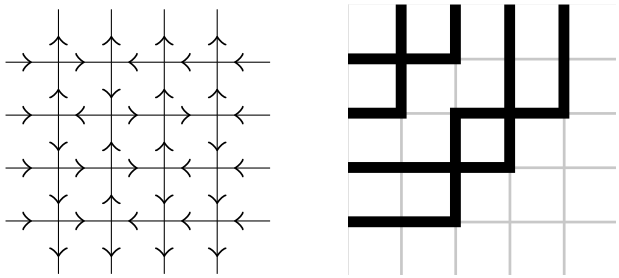

Figure 1.3: A six vertex configuration with domain wall boundary conditions, and the interpretation as lattice paths.

The variational principle for the limit shapes in the dimer/tiling models are rigorously understood by the work of [CKP], [CEP], [KO]. For the six-vertex model, the variational principle is conjectural, but supported by considerable numerical and analytical results.

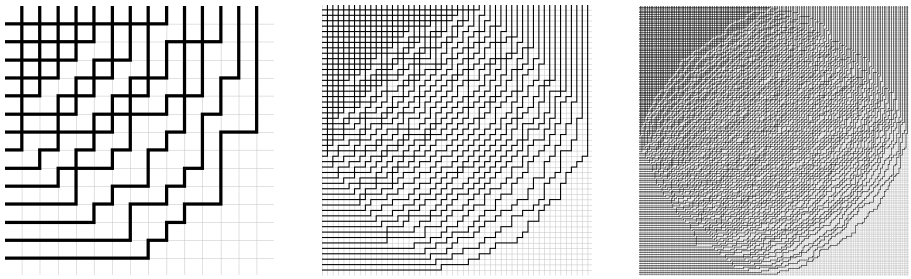

Figure 1.4: The limit shape in the six vertex model with domain wall boundary condition.

1.4 Outline of Thesis

Here is an outline of the thesis and summary of our main results.

Chapter 2

This chapter collects together all prerequisite material needed to understand the remaining chapters. We define the six-vertex model, its reformulation in terms of stepped surfaces called height functions, and the construction of commutative families of transfer matrices. We study the asymptotic partition on the torus via the Bethe ansatz, and describe the properties of the free energy and the surface tension in the thermodynamic limit.

Similarly, for the dimer model, we define the model, the height functions, and the Kasteleyn method for solving the model. We sketch the computation of the toroidal partition function and surface tension.

Finally, we review the limit shape theorem and the variational principle for the six-vertex and dimer model.

Chapter 3

In this chapter, we investigate the role of integrability of the six vertex model in the formation of limit shapes. By integrability we mean, on one hand the discrete integrability of the six-vertex model in the sense of commutative families of transfer matrices, and on the other hand the integrability in the continuum limit in the Liouville sense of Poisson commutative families of functions (integrals of motion) on the phase space.

We first reformulate the variational principle for limit shape as an infinite dimensional Hamiltonian system. We show that the commutative families of transfer matrices for the six-vertex model correspond to commutative families of Hamiltonians. In other words, the partial differential equations describing the limit shape have an infinite number of conserved quantities. We conjecture on this basis that the limit shape is determined by an integrable system. We then turn to the dimer model, for which the limit shape equation is related to the complex Burgers equation, which can be solved by the method of complex characteristics. Finally, we study the free fermionic point $\Delta = 0$ of the 6-vertex model, where it can be reformulated as a dimer model.

Chapter 4

This chapter proves a straightforward theorem in Hamiltonian mechanics, which gives conditions for the Poisson commutativity of two Hamiltonian functions in terms of their principal action functions. In the context of the limit shapes, in which the principal action is asymptotic free energy of the model, the theorem gives a heuristic explanation for the existence of commutative families Hamiltonians corresponding to commutative families of transfer matrices. It suggests a generalization of our previous results to other integrable lattice models, for example, the generalizations of the six-vertex model related to other Lie algebras.

Chapter 5

This chapter studies the six-vertex model for a special class of weights introduced by [BCG], called the stochastic six-vertex model. With these weights, the transfer matrix can be normalized to satisfy the Markov property and then can be regarded as the collection of transition probabilities for a stochastic process on a row of vertical edges of the model. The corresponding Markov process is a discrete time generalization of the asymmetric exclusion process (ASEP). The model has recently been studied by many authors (see for example [A] and references therein), using techniques developed by Tracy and Widom for studying interacting particle systems.

Our main result in this chapter is the derivation for the partial differential equations for the height function of the stochastic 6-vertex model. This result is derived from the conjectural variational principle for the 6-vertex model. The limit shape equations

turn out to be a first order differential equations of the Burger's type, which can be solved by the method of characteristics. In the ASEP limit of the 6-vertex model, we recover the inviscid Burgers equation as computed by [BF] [Rez][GS]. As an example, we compute the height function exactly for domain wall type boundary conditions on the cylinder. When the initial condition is a step function, our solution converges to the limit shape found in [BCG] in the limit when the circumference of the cylinder goes to infinity.

Chapter 6

This chapter turns to a slightly different topic, at the intersection of discrete geometry and statistical physics. We study generalized graph laplacians in $\mathbb{Z}^2$ that can be regarded as finite difference approximations of Laplace-Beltrami operators induced by a Riemannian metric g. The Laplacians arise as a discretization of the action of the Gaussian free field over a background metric. They are closely related to Kasteleyn matrices that can be regarded as a discretization of Dirac operators in a background metric.

The partition function for the discretized Gaussian action is given in terms of the determinant of the discrete Laplacian. We study asymptotics of the the determinant as the mesh ϵ of the approximation tends to zero, and show that the determinant of Δ^i has the asymptotic expansion:

$$\log\det\Delta^\epsilon = \frac{1}{\epsilon^2}\int_M F(g)\ dx\ dy + \frac{1}{\epsilon}\int_{\partial M} B(g)\cdot ds + \frac{1}{2}\log(\epsilon) + O(1) \tag{1.4.1}$$

where the functions F and B are given in equation (6.2.2).

The discrete Guassian field theories are known to be conformally invariant in the scaling limit $i \to \infty$, and consequently the asymptotic expansion of the form (6.0.3) is generally anticipated by the theory of finite size scaling [CaPes]. In particular, the coefficient of the logarithmic term is universally related to the universal charge of the limiting conformal field theory and the Euler characteristic of the underlying space.

The leading order density F can be computed via the variational principle for the dimer model. The subleading terms in the asymptotic expansion suggest a strengthening of the variational principle, although we do not pursue that here.

Some work has been done on relating the constant terms in the asymptotics of the determinant of discretized or finite difference laplacians with regularized functional determinants of analytic laplacians. In one-dimension, there are many positive results, for example [For92], [BFK]. In two dimensions, for some particular cases such as flat rectangles and flat torii, with particular choice of discretized laplacians, the constant term is known to be equal to the zeta-regularized determinant of the analytic laplacian, [DD],[CJK10]. We do not attempt to calculate the constant term in the asymptotic determinant (6.0.3) and its investigation for further work. Identifying such a condition would be a step towards defining a free Gaussian field theory as the regularized limit of discrete Gaussian field theories.

Chapter 2

The Six Vertex and Dimer Model

Here is a lightning review of the Six Vertex Model and Dimer Model. For further details about the six vertex model, see [Re], [PR], [Ba] and the references therein. For further details about the dimer model, see [Ken09], [KOS] and the references therein.

2.1 Surface Graphs

Let $\Gamma = (V, E)$ be a simple graph with vertex set V and edge set E. The set of *boundary vertices* denoted as ∂V are the univalent vertices of Γ. The non-boundary vertices are called *internal vertices*. The set of *boundary edges* denoted as ∂E are those edges adjacent to boundary vertices.

A *bipartite graph* is a graph whose vertices can be partitioned into disjoint sets of black vertices B and white vertices W, such that each edge is adjacent to one black vertex and one white vertex. A bipartite graph has a natural orientation on edges, with each edge oriented from its black vertex to the white vertex.

A *surface graph* Γ is a simple graph embedded in a compact, oriented surface Σ such that: a) the boundary vertices of Γ are embedded on the boundary of Σ. b) the complement of Γ in Σ is the union of a finite set F of open sets each homeomorphic to a disc, called *faces*. A surface graph has a natural orientation on faces, consistent with the orientation of Σ. The set of *boundary faces* are those adjacent to boundary vertices.

Square Lattice Surface Graphs

An important class of surface graphs for the six vertex and dimer model are those in which alll internal vertices are of degree four. We will call such graphs *square lattice surface graphs*.

Here are some particular examples that we will keep in mind. In the following, by $\mathbb{Z}^2$ we mean the graph embedded in the plane $\mathbb{R}^2$ with vertices at positions $(m, n) \in \mathbb{R}^2$ for $m, n \in \mathbb{Z}$ and edges joining all vertices distance 1 apart.

a) Planar Domain Graph: Fix a domain U in $\mathbb{R}^2$ whose boundary ∂U intersects all edges of $\mathbb{Z}^2$ generically. Subdivide the edges at intersection points. The square lattice surface graph is the subgraph of consisting of all vertices in U.

b) The *cylinder graph* $\mathcal{C}_{MN}$ is the quotient of the subgraph $\{0, \cdots, M\} \times \{0, \cdots, N-1\}$ of $\mathbb{Z}^2$ by the equivalence $(m, n) \sim (m + M, n)$, with the edges along the boundary $n = 0$ and $n = N - 1$ removed.

   The set of boundary vertices ∂V is the union of subsets ∂V_1 and ∂V_2, consist of vertices at positions $(m, 0)$ and $(m, N - 1)$ respectively. The boundary edges ∂E_i consists of edges adjacent to exactly one boundary vertex in ∂V_i. The *boundary faces* ∂F_i are those adjacent to boundary edges in ∂E_i.

c) The *torus graph* $\mathcal{T}_{MN}$ is the quotient of the subgraph $\{0, \cdots, M\} \times \{0, \cdots, N-1\}$ of $\mathbb{Z}^2$ by $(m, n) \sim (m + M, n) \sim (m, n + N)$.

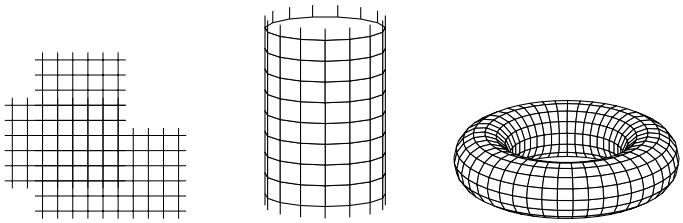

Figure 2.1: A planar graph, cylinder graph, and torus graph.

2.2 The Six Vertex Model

The Basics

Configurations and Weights

The six vertex model is most generally defined on graph Γ all of whose vertices are degree either one or four, i.e. the square lattice graphs. A *configuration* S of the 6-vertex model is a subset of internal and boundary edges satisfying the ice rule: at each internal vertex v, the edges in S adjacent v must be one of six possible local configurations as shown in Figure 2.2. The ice rule implies that a configuration of the 6-vertex model can be seen as an ensemble of paths that do not cross (although they can touch at an a_2 vertex), see Figure 5.1.

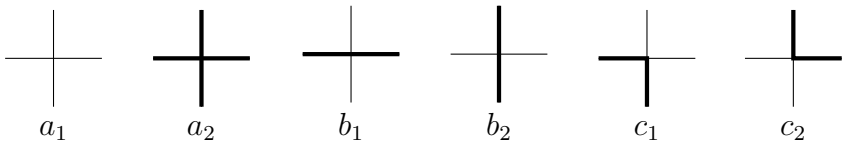

Figure 2.2: Six vertex configurations and their weights.

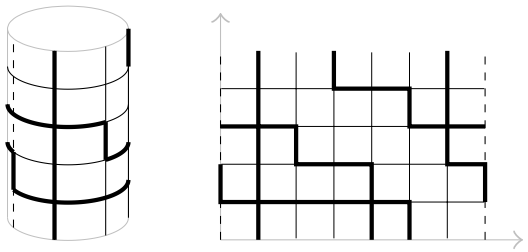

Figure 2.3: A six vertex configuration on a cylindrical graph.

Each vertex v is assigned a vertex weight $w(v, S)$ depending on the configuration of adjacent edges according to Figure 2.2. The Boltzmann weight of S is

$$W(S) = \prod_{v \in \mathrm{int}(V)} w(v, S)$$

Unless otherwise stated, we will assume that the model is *homogenous*: the weights a_i, b_i, c_i do not depend on the vertex.

Boundary Conditions and the Partition Function

The *boundary configuration* ∂S of a configuration S is the restriction of S to the boundary edges ∂E. A *Dirichlet boundary condition* for the 6-vertex model fixes the boundary configurations of S, that is, it is a subset of ∂E. The *partition function* with fixed boundary condition η is:

$$Z_{MN}\big[\eta\big] = \sum_{\substack{\text{configs. } S \\ \partial S = \eta}} W(S) \tag{2.2.1}$$

A boundary condition η is called *admissible* if $Z_{MN}[\eta] \neq 0$.

A *boundary state* is a probability distribution on the set of boundary conditions. We will write $b(\eta)$ for the probability of η in the boundary state b. The partition function with boundary state b.

$$Z_{MN}(b) = \sum_{\eta} b(\eta)\ Z_{MN}[\eta]$$

Here we use round parantheses as opposed to square brackets for the partition function with Dirichlet boundary conditions 2.2.1.

Simple examples of boundary states are:

1) Pure states (Dirichlet boundary conditions) in which the distribution, say b is supported at a single configuration η, $b(\eta) = \delta_{\eta,\eta_0}$.

2) The uniform distribution. In this case $b(\eta) = 2^{-|\partial E|}$.

The partition function $Z_{MN}(b)$ defines a probability measure μ on the set of 6-vertex configurations on $\mathcal{C}_{MN}$, where the probability fof a configuration S is:

$$\mu(S) = \frac{b(\partial S)\ W(S)}{Z_{MN}(b)}$$

The Height Function

To each 6-vertex configuration S on Γ, we associate a height function h_S on the faces of Γ as follows. First fix a reference f of Γ, and set $h_S(f) = 0$. Then, when moving upward or rightward, the h_S changes by $+1$ if crossing an edge in S and -1 otherwise (see Figure 2.4). When Γ is a surface graph of a simply connected surface, the ice rule implies that h_S is a well defined function on faces of Γ, i.e. its value on a particular face does not depend on the path taken to the face. When Γ is not simply connected, it defines a multivalued function on the faces of Γ, i.e. a well defined function after making branch cuts.

Note that (up to an additive constant) the boundary configuration of S determines the values of h_S on boundary faces.

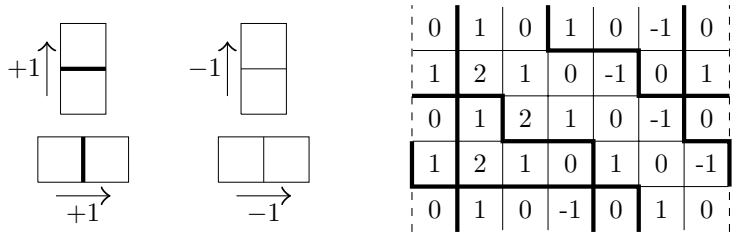

Figure 2.4: The height function rules and an example.

The function h_S satisfies:

$$\begin{aligned} h_S(m+1,n) - h_S(m,n) &= \pm 1 \\ h_S(m,n+1) - h_S(m,n) &= \pm 1 \end{aligned} \tag{2.2.2}$$

A multivalued function h' that satisfies (2.2.2) and $h'(f) = 0$, is called a *height function* for the 6-vertex model. It is clear that there is a bijection between the 6-vertex configurations and height functions.

Remark 1. *One can regard a six vertex state as a* 1*-cycle on the* 2*-dimensional complex of the surface graph in question. In the case when the complex is connected and simply connected, a cycle is the boundary of a* 2*-cycle, which is the height function. But because our interest is mostly the case of a cylinder, we will use somewhat cumbersome notion of a height function on a surface with branch cuts.*

Remark 2. *Many other definitions of the height functions are common in the literature. For example, [BCG] uses a height function where the height function increases by* $+1$ *when crossing a bold edge and does not change when crossing an empty edge.The level sets of this height function are the six vertex paths. Another common definition, used in [RS15] increments or decrements the height function by* $\pm 1/2$*.*

Magnetic Fields

We will assume the following useful parametrization of weights, given in terms of (a, b, c), *magnetic field* (H, V), and λ as:

$$\begin{aligned} a_1 &= a\, e^{H+V} & a_2 &= a\, e^{-H-V} \\ b_1 &= b\, e^{-H+V} & b_2 &= b\, e^{H-V} \\ c_1 &= c\, \lambda & c_2 &= c\, \lambda^{-1} \end{aligned} \tag{2.2.3}$$

The ice rule implies that the difference in the number of c_1 and c_2 vertices in any six vertex configuration depends only on the boundary conditions. In particular, for the cylinder and torus graphs, the c_1 and c_2 vertices occur in equal number. When we assume fixed boundary conditions, there is no loss in generality with setting $\lambda = 1$.

These weights have the following interpretation (see Figure 2.5): vertices are assigned the symmetric weights a, b, c. The vertex weight (depending only on a, b, c) of a configuration is locally invariant when S is replaced by $\Gamma \backslash S$, i.e. by interchanging occupied and unoccupied edges. This symmetry is broken by assigning each occupied horizontal edge a weight $e^{H/2}$ and each unoccupied edge $e^{-H/2}$. Similarly we assign $e^{V/2}$ and $e^{-V/2}$ to occupied and unoccupied vertical edges. The total weight of a state is then the product of weights on edges and weights on vertices.

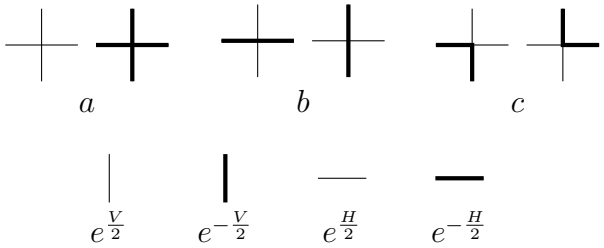

Figure 2.5: The symmetric vertex weights and magnetic fields on edges.

Baxter's Parametrization of Weights

An important characteristic of the 6-vertex model weight is:

$$\Delta = \frac{w_1 w_2 + w_3 w_4 - w_5 w_6}{2\sqrt{w_1 w_2 w_3 w_4}} \quad = \frac{a^2 + b^2 - c^2}{2ab} \tag{2.2.4}$$

A useful parametrization of weights (a, b, c) in terms of (u, γ, r) was introducted by Baxter [Ba]:

a) When $\Delta > 1$:

i If $a > b + c$, let $(a, b, c) = (r \sinh(u + \gamma), r \sinh(u), r \sinh(\gamma))$ with $\gamma > 0$.

ii If $b > a + c$, let $(a, b, c) = (r \sinh(u - \gamma), r \sinh(u), r \sinh(\gamma))$ with $0 < \gamma < u$.

For both of these parametrizations $\Delta = \cosh(\gamma)$.

b) When $|\Delta| < 1$:

   i If $-1 < \Delta \leq 0$, let $(a, b, c) = (r\sin(u-\gamma), r\sin(u), r\sin(\gamma))$ with $0 < \gamma < \pi/2$ and $\gamma < u < \pi/2$.

   ii If $0 < \Delta \leq 1$, let $(a, b, c) = (r\sin(\gamma-u), r\sin(u), r\sin(\gamma))$ with $0 < \gamma < \pi/2$ and $0 < u < \gamma$.

For these parametrizations $\Delta = \pm\cos(\gamma)$.

c) When $\Delta < -1$: let $(a, b, c) = (r\sinh(\gamma-u), r\sinh(u), r\sinh(\gamma))$ with $0 < u < \gamma$. In this case $\Delta = -\cosh(\gamma)$.

We will refer to the variable u as the spectral parameter.

Transfer Matrices

The Six Vertex Model On the Cylinder

In this section, we will focus on the six vertex model on the cylinder graph $\mathcal{C}_{MN}$.

Recall that the boundary ∂E of $\mathcal{C}_{MN}$ is the union of two components ∂E_1 and ∂E_2. A boundary condition on $\mathcal{C}_{MN}$ is a pair (η, η'), where η and η' are boundary configurations (i.e. subsets) of ∂E_1 and ∂E_2, respectively. Similarly, a pair (b_1, b_2) of probability distributions on configurations of ∂E_1 and ∂E_2 define a boundary state on $\mathcal{C}_{MN}$.

A boundary state b (on one boundary component) defines a vector in a Hilbert space $\mathscr{H}_M \simeq (\mathbb{C}^2)^{\otimes M}$ as follows. A boundary configuration η is identified with the element $\psi_\eta \in \mathscr{H}_M$ of the tensor product basis:

$$\psi_\eta = e_{\eta(1)} \otimes e_{\eta(2)} \cdots \otimes e_{\eta(M)}$$

where $i = 1, \cdots, M$ enumerate the boundary edges; $\eta(i) = 1$ if the ith edge is in η and $\eta(i) = 0$ otherwise; and $\{e_0, e_1\}$ is the standard basis for $\mathbb{C}^2$. The 2^M vectors ψ_η form an orthonormal basis for $\mathscr{H}_M$. A local boundary state b is identified with the vector $\sum_\eta b(\eta)\psi_\eta$.

Let $Z_{MN} : \mathscr{H}_M \to \mathscr{H}_M$ be the linear map with matrix elements given by the partition functions $Z_{MN}(\eta, \eta')$. The partition function with boundary states b_1 and b_2 is the inner product:

$$Z_{MN}(b_1, b_2) = \langle b_2, Z_{MN}\, b_1 \rangle \tag{2.2.5}$$

where $\langle b_2, b_1 \rangle = \sum_\eta b_1(\eta) b_2(\eta)$.

Thus, $\mathscr{H}_M$ can be naturally regarded as the space of states corresponding to one end of the cylinder. Boundary states for the cylinder are vectors in $\mathscr{H}_M \otimes \mathscr{H}_M$. Strictly speaking the first factor should be $\mathscr{H}_M^*$ but since we have a scalar product we identify the vector space with its dual.

It is clear that $\mathscr{H}_M$ has the decomposition:

$$\mathscr{H}_M = \oplus_{k=0}^{M} \mathscr{H}_M^{(k)}$$

where $\mathscr{H}_M^{(k)}$, the k-particle sector, is the subspace spanned by boundary configurations with k edges. Because of the 6-vertex rule, Z_{MN} has the block decomposition:

$$Z_{MN} = \oplus_{m=0}^{M} Z_{MN}^{(m)}, \quad Z_{MN}^{(m)} : \mathscr{H}_M^{(m)} \to \mathscr{H}_M^{(m)}$$

The restricted partition function is defined as:

$$Z_{MN}^{(m)}(b_1, b_2) = \langle b_2^{(m)}, Z_{MN}^{(m)}\, b_1^{(m)} \rangle \tag{2.2.6}$$

where $b^{(m)}$ is the orthogonal projection of b to $\mathscr{H}_M^{(m)}$.

The R-Matrix and the Transfer Matrix

The transfer matrix $T_M : \mathscr{H}_M \to \mathscr{H}_M$ is the partition function (2.2.6) with one row, $T_M = Z_{M1}$. It has a more explicit description as follows.

Define the matrix $R : \mathbb{C}^2 \otimes \mathbb{C}^2 \to \mathbb{C}^2 \otimes \mathbb{C}^2$ with matrix elements:

$$R = \begin{pmatrix} ae^{H+V} & 0 & 0 & 0 \\ 0 & be^{-H+V} & c\lambda^{-1} & 0 \\ 0 & c\lambda & be^{-V+H} & 0 \\ 0 & 0 & 0 & ae^{-H-V} \end{pmatrix} \tag{2.2.7}$$

in the standard ordered tensor product basis $\big(e_0 \otimes e_0, e_0 \otimes e_1, e_1 \otimes e_0, e_1 \otimes e_1\big)$ for $\mathbb{C}^2 \otimes \mathbb{C}^2$. The R-matrix (2.2.7) represents a linear operator that maps a state $e_i \otimes e_j$ on the West and South edges adjacent to a vertex to a sum of states $e'_i \otimes e'_j$ on the East and North edges multiplied by the six vertex weight.

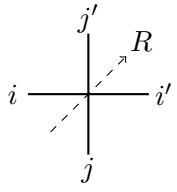

Enumerating the tensor components of $\mathbb{C}^2 \otimes \mathscr{H}_M \simeq (\mathbb{C}^2)^{\otimes(M+1)}$ by $\{0, 1, \cdots M\}$, define $R_{ij} : \mathbb{C}^2 \otimes \mathscr{H}_M \to \mathbb{C}^2 \otimes \mathscr{H}_M$ as the map that acts as R on the ith and jth tensor components and identity on the rest. The transfer matrix is then the trace over the 0th tensor component:

$$T_M = \mathrm{Tr}_0(R_{10} R_{20} \cdots R_{M0})$$

It is clear that the transfer matrix preserves the spaces $\mathscr{H}_M^{(m)}$, and we write $T_M^{(m)}$ for the restriction of the transfer matrix to $\mathscr{H}_M^{(m)}$. The partition functions in terms of the transfer matrix is:

$$Z_{MN}(b_1, b_2) = \langle b_2, (T_M)^N\, b_1 \rangle$$

The Yang-Baxter equation and Commutative Transfer Matrices

Denote by $R(u, H, V)$ the R-matrix (2.2.7) with weights given by the parametrization (2.2), for some fixed Δ. Let $R(u) = R(u, 0, 0)$.

$$R(u, H, V, \lambda) = \left(D^V \otimes D^H\right)\ R(u)\ \left(D^V \otimes D^H\right)$$

where

$$D^\beta = \begin{pmatrix} e^{\beta/2} & 0 \\ 0 & e^{-\beta/2} \end{pmatrix} \tag{2.2.8}$$

The transfer matrix:

$$T(u, H, V) = \mathrm{Tr}_0(R_{10}(u, H, V)R_{20}(u, H, V)\cdots R_{M0}(u, H, V))$$

can be written as:

$$T(u, H, V) = (D_1^{2V}\cdots D_M^{2V})^N\ \mathrm{Tr}_a\left(Q_a(u, H, 0)\right)$$

where the "quantum monodromy matrix"

$$Q_a(u, H, 0) = R_{1a}(u, H, 0)R_{2a}(u, H, 0)\cdots R_{Ma}(u, H, 0))$$

acts on $\mathbb{C}^2 \otimes (\mathbb{C}^2)^{\otimes M}$, where we label the first tensor component by a.

The R-matrices satisfy the Yang-Baxter equation [Ba]:

$$R_{12}(u)R_{13}(u+v)R_{23}(v) = R_{23}(v)R_{13}(u+v)R_{12}(u) \tag{2.2.9}$$

in $\mathbb{C}^2 \otimes \mathbb{C}^2 \otimes \mathbb{C}^2$.

The ice-rule implies that for any diagonal matrix D:

$$(D \otimes D)\ R(u, H, V) = R(u, H, V)\ (D \otimes D) \tag{2.2.10}$$

Together (2.2.10) and (**??**) imply that $R(u, H, V)$ satisfies:

$$\begin{aligned} R_{12}(u, H, 0)R_{32}(u+v, H, 0)R_{31}(v, H, 0) \\ = R_{31}(v, H, 0)R_{32}(u+v, H, 0)R_{12}(u, H, 0) \end{aligned} \tag{2.2.11}$$

The Yang-Baxter equation (2.2.11) implies that

$$Q_a(u, H, 0)\ Q_b(v, H, 0)\ R_{ab}(u-v) = R_{ab}(u-v)\ Q_b(u, H, 0)\ Q_a(v, H, 0)$$

in $\mathbb{C}^2 \otimes \mathbb{C}^2 \otimes (\mathbb{C}^2)^{\otimes M}$, where we label the first tensor component by a, and the second b.

This implies the commutativity of transfer matrices

$$[T(u, H, V), T(v, H, V)] = 0 \tag{2.2.12}$$

Commuting Transfer Matrices with Inhomogenous Weights

It is straightforward to construct the transfer matrices when the weights are inhomogenous. We focus on inhomogenous weights that arise in a particular way as follows [Ba].

To each row, associate a parameter u_i, and to each column, a parameter v_j. The Boltzmann weights of the vertex in the ith row and jth column are the matrix elements of the R-matrix $R(u_i - v_j)$. We assume that for all i and j, $u_i > v_j$ to ensure the positivity of the Boltzmann weights.

The quantum monodromy matrix is defined as:

$$Q_a(u, H, V) = R_{1a}(u - v_1, H, V)R_{2a}(u - v_2, H, V) \cdots R_{Na}(u - v_N, H, V)$$

and the transfer matrix corresponding to the jth row as:

$$T(u_j, H, V) = \mathrm{Tr}_a \, T_a(u_j, H, V)$$

The cylinder partition function then is:

$$Z_{MN}(\eta_1, \eta_2) = \langle \eta_1, T(u_1, H, V)T(u_2, H, V) \cdots T(u_N, H, V)\eta_2 \rangle$$

The Yang-Baxter equation implies that the inhomogenous transfer matrices of different rows commute as in 2.2.12 and therefore the partition function is a symmetric function of u_i.

The Thermodynamic Limit

The Free Energy and Surface Tension

We now focus on the six vertex model on the torus graph $\mathcal{T}_{NN}$, and study the limit $N \to \infty$. The partition function is:

$$Z_{NN} = \mathrm{Tr}\left((T_N)^N\right)$$

The asymptotics of the partition function can be computed by diagonalizing T_N via the Bethe ansatz. We refer the reader to [**?**] for the details and summarise the results.

It is expected[1] that as $N \to \infty$ there exist the limiting density of the free energy

$$f(H, V) = \lim_{N \to \infty} \frac{1}{N^2} \log(Z_{NN}), \tag{2.2.13}$$

We will call $f(H, V)$ the *t*oroidal free energy. Its Legendre transform $\sigma(s, t)$ is the free energy for torus with zero magnetic fields conditioned to having the average magnetization s in the horizontal direction and t in the vertical direction:

$$\sigma(s, t) = \max_{H,V}(sH + tV - f(H, V)), \quad (s, t) \in \mathcal{N} \tag{2.2.14}$$

[1] The evidence for this is overwhelming, though it is hard to point a specific reference where it has been proven with mathematical level of rigor.

where $\mathcal{N} = [-1,1]\times[-1,1]$ is the square. Properties of the toroidal free energy $f(H,V)$ and of $\sigma(s,t)$, are summarized in [PR] (see also references therein). We briefly recall here some of them:

First, it is clear that σ has the following symmetries:

$$\sigma(s,t) = \sigma(t,s) = \sigma(-s,-t)$$

From which we also have $\frac{\partial\sigma}{\partial s}(s,t) = \frac{\partial\sigma}{\partial t}(t,s)$.
In addition, σ has the following analytic structure (see Figure (2.6)). [2]

1. When $\Delta < -1$, σ is convex with corner singularities near the boundary, and an additional conical singularity at $(s,t) = (0,0)$. It is smooth and strictly convex away from $(0,0)$ and the boundary.

2. When $|\Delta| \leq 1$, $\sigma(s,t)$ is strictly convex and smooth for all $-1/2 < s,t < 1/2$, with corner singularities at the boundary.

3. When $\Delta > 1$, σ is convex with corner singularities at the boundary and in addition a groove singularity along $s = t$, when $a > b$, and along $s = -t, -t_0 < t < t_0$ when $a < b$. The function σ is smooth and strictly convex away from these singularities.

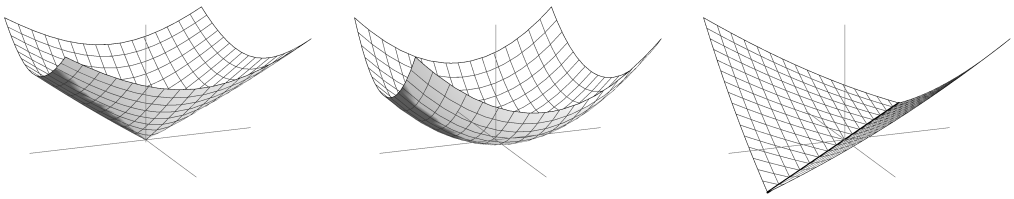

Figure 2.6: Sketch of σ for $\Delta < -1$, $|\Delta| < 1$, and $\Delta > 1$.

2.3 The Dimer Model

The Basics

Configurations and Weights

A *dimer configuration* $\mathcal{D}$ on the graph Γ is a subset of edges, called dimers, such that each internal vertex is adjacent to exactly one edge of $\mathcal{D}$. A dimer configuration is illustrated in Figure 2.3. On a graph with no boundary vertices, a dimer configuration is a *perfect matching*.

[2] Changed these

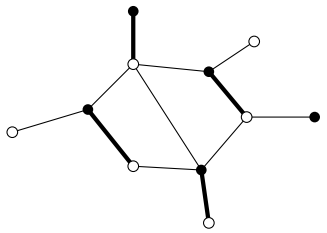

Figure 2.7: A dimer configuration on a bipartite graph.

A positive edge weighting on the graph Γ is a function

$$\begin{aligned} w : & E \to (0, \infty) \\ & e \mapsto w_e \end{aligned}$$

The weight of the dimer configuration $\mathcal{D}$ is then defined as:

$$W(\mathcal{D}) = \prod_{e \in \mathcal{D}} w_e \tag{2.3.1}$$

Boundary Conditions

The boundary configuration $\partial\mathcal{D}$ is the restriction of $\mathcal{D}$ to the boundary edges of Γ. A *boundary condition* η for the dimer model is a subset of boundary edges. A configuration $\mathcal{D}$ respects the boundary condition if $\partial\mathcal{D} = \eta$. Equivalently, if $\mathcal{D}$ restricts to a perfect matching on the subgraph of Γ found by removing the edges in η and their adjacent vertices.

The *Gibbs measure* μ with fixed boundary conditions is a probability measure on the set of dimer configurations satisfying the boundary condition $\partial\mathcal{D} = \eta$ as:

$$\mu(\mathcal{D}) = \frac{W(\mathcal{D})}{Z_{\Gamma,\mathcal{B}}}$$

where the *partition function* is defined as:

$$Z_\Gamma[\eta] = \sum_{\substack{\text{configs } \mathcal{D} \\ \partial\mathcal{D} = \eta}} W(\mathcal{D})$$

A natural generalization to the fixed boundary conditions is as follows. A probability distribution b on boundary conditions is a positive function on the set of boundary conditions satisfying the normalization condition

$$\sum_{\eta \subset \partial E} b(\eta) = 1$$

The Gibbs measure with the boundary condition η is defined by:

$$\mu(\mathcal{D}) = \frac{W(\mathcal{D}) b(\partial\mathcal{D})}{Z_\Gamma(b)}$$

where the partition function $Z_\Gamma(\eta)$ is:

$$Z_\Gamma(b) = \sum_{\text{configs } \mathcal{D}} b(\partial\mathcal{D}) W(\mathcal{D})$$

The case of fixed boundary conditions is recovered by setting b to zero for all but on boundary configurations.

The Partition Function and Dimer Statistics

For each edge e, the random variable χ_e on the set of dimer configurations is defined as:

$$\chi_e(\mathcal{D}) = \begin{cases} 1 & \text{if } e \in \mathcal{D} \\ 0 & \text{otherwise} \end{cases}$$

Abusing the notation a bit, we will write e for χ_e.

The correlation functions of the χ in the Gibbs measure can be computed from the partition function as:

$$\mathbb{E}[e_1 e_2 \cdots e_n] = \frac{w_{e_1} w_{e_2} \cdots w_{e_n}}{Z} \left(\frac{\partial}{\partial w_{e_1}} \frac{\partial}{\partial w_{e_2}} \cdots \frac{\partial}{\partial w_{e_n}} Z \right) \Big|_{w_{e_1} = w_{e_2} \cdots w_{e_3} = 0}$$

Here, we think of Z as a function of the indeterminate edge weights w_{e_i}. It is clear that the partition function can be reconstructed, up to a constant, from all of the correlation functions.

A *gauge transformation* of the dimer model by a function $\lambda : V \to \mathbb{C}$ is a redefinition of weights as:

$$w^\lambda(e) = \exp(\lambda(v))\ w(e)\ \exp(\lambda(v))$$

where w and v are the vertices adjacent to e. A gauge transformation changes the partition function by an overall factor:

$$Z^\lambda_\Gamma[\eta] = \left(\prod_{v \in V} \exp(\lambda(v)) \right) Z$$

A gauge transformation leaves the measure and all correlation functions unchanged.

The Height Function

Two dimer configurations $\mathcal{D}$ and $\mathcal{D}_0$ on a bipartite surface graph Γ define a system of oriented cycles (relative the boundary), written as $(\mathcal{D}, \mathcal{D}_0)$, with edges occupied by $\mathcal{D}$ oriented from black vertices to white vertices and with edges occupied by $\mathcal{D}_0$ from white to black. This is illustrated on Figure 2.8.

For a planar surface graph on a connected simply connected domain, the oriented composition cycle $(\mathcal{D}, \mathcal{D}_0)$ defines a function (up to an overall constant) $h_{\mathcal{D},\mathcal{D}_0}$ on faces of

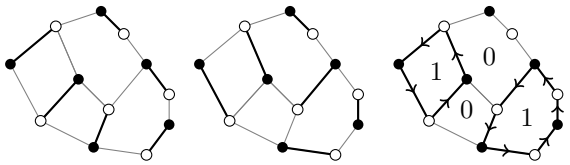

Figure 2.8: Dimer configurations $\mathcal{D}_0$ and $\mathcal{D}$. On the right side is the composition cycle $(\mathcal{D}, \mathcal{D}_0)$ and $h_{\mathcal{D},\mathcal{D}_0}$

$\Gamma \subset D$ with the composition cycles being its level curves; the height function increments when crossing a cycle oriented from left to right. The arbitrary constant can be fixed by fixing its value at a chosen reference face.

As in the 6-vertex model, for surface graphs on non simply-connected surfaces, the height function does not exist as a function of faces. We will assume branch cuts compatible with the graph, so that the height function can be defined on the fundamental polygon.

A more general construction of the height function is as follows. Let C_0 be a cellular one-chain, satisfying

$$\partial C_0 = \sum_{v \in B} v - \sum_{v \in W} v \tag{2.3.2}$$

where B and W are the sets of black and white vertices of Γ. Note that in particular, any dimer configuration can be regarded as a one-chain satisfying (2.3.2). For any dimer configuration $\mathcal{D}$, the chain $\mathcal{D} - C_0$ satisfies $\partial(\mathcal{D} - C_0) = 0$, and so the chain $\mathcal{D} - C_0$ locally integrates to a function on faces $h_{\mathcal{D},C_0}$.

For example, a different height function on 3-valent graphs, arising from the relation to tiling models, is defined as follows:

- Orient all edges of the graph from white vertices to back vertices.
- Using the orientation of the surface define the function $h_{\mathcal{D}}$ on faces adjacent to an inner edge of Γ occupied by a dimer in $\mathcal{D}$ as it is shown below.
- The same definition is used to define $h_{\mathcal{D}}$ on faces adjacent to boundary dimer edges.

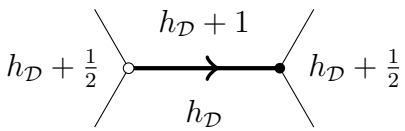

In other words, if $C_0 = \frac{1}{3}\sum_{e \in E(\Gamma)} e$ is the "uniform cover", then

$$h_{\mathcal{D}} = \frac{3}{2} h_{\mathcal{D},\mathcal{C}_0}$$

The Kasteleyn Theory

Omitted, part of the new paper and relevant only to chapter 7.

Kasteleyn Orientations

Kasteleyn Matrix

Local Statistics Theorem

The Thermodynamic Limit

$\mathbb{Z}^2$-periodic dimer models

A $\mathbb{Z}^2$ periodic graph Γ is a graph embedded in the plane such that translations by $\mathbb{Z}^2$ act as graph isomorphisms. The fundamental domain G is the quotient of Γ by the action of $\mathbb{Z}^2$, see figure 2.9) for example.

A $\mathbb{Z}^2$-periodic graph can be seen as the square lattice $\mathbb{Z}^2$, with the fundamental domain G placed at each vertex. Similarly, for each square lattice graph Γ discussed in Section 2.1 we can obtain a graph found by replacing each internal vertex with G, which we will denote $\Gamma(G)$.

Recall that on the torus, the height function $h_{\mathcal{D}}$ of a dimer configuration is a multivalued function with monodromy $\Delta_a h$ and $\Delta_b h$ about the two cycles of on the torus. The *magnetic fields* fields z and w change the weight of a configuration as:

$$W(\mathcal{D}) = z^{\Delta_a h} w^{\Delta_b h} \prod_{e \in \mathcal{D}} w_e$$

The magnetic fields can be absorbed into edge weights. Weight an edge by z if it crosses the vertical edge of the fundamental polygon in the positive direction or z^{-1} if it crosses the edge in the negative direction, and $w^{\pm 1}$ if it crosses a horizontal edge of the fundamental polygon in the positive/negative direction. Here recall that the edges are oriented from black to white. See figure 2.9.

The *spectral polynomial* $P(z, w)$ is the partition function of the dimer model of the fundamental domain Γ. The spectral polynomial is a Laurent polynomial in z and w,

$$P(z, w) = \sum_{(m,n) \in \mathbb{Z}^2} c_{m,n} z^m w^n$$

The *Newton polygon* of the spectral polynomial P is a convex polygon in $\mathbb{R}^2$ defined as:

$$\mathcal{N}_P = \text{convex hull}\{(m, n) \in \mathbb{Z}^2 \mid c_{m,n} \neq 0\}$$

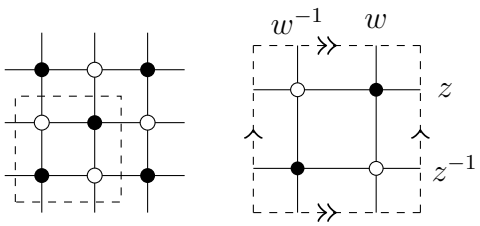

Figure 2.9: The square lattice, and it's fundamental domain and magnetic field weights on the external edges.

The Toroidal Free Energy and the Surface Tension

We focus now on the partition function Z_{NN} of dimer model on $\mathcal{T}_{NN}(G)$ in the limit that $N \to \infty$. The free energy of the dimer model

$$f(H,V) = \lim_{N\to\infty} \frac{1}{N^2} \log(Z_{NN})$$

is the Ronkin function of the spectral curve:

$$f(H,V) = \frac{1}{(2\pi i)^2} \int_{|z|=e^H} \int_{|w|=e^V} \log|P(z,w)|\, dz\, dw$$

The surface tension function is the Legendre transform of the

$$\sigma(s,t) = \max_{H,V}(sH + tV - f(H,V)) \tag{2.3.3}$$

and is defined for all gradients $(s,t) \in \mathcal{N}_P$.

2.4 Limit Shapes and the Variational Principle

In this section, we outline the variational principle for the limit shape. These results were rigorously proven for the planar dimer model by the work of [CEP], [CKP], [KOS], [Sh]. The following generalizations are, strictly speaking, conjectural; ostensibly they can be proven along the same lines of [CKP], but we will not pursue this here. The variational principle for the six vertex model was first studied by [ZJ] and [PR].

Approximating Surfaces Graphs

Let Σ be a Riemannian surface and let $\Sigma^{(\epsilon)}$ be an approximating square lattice surface graph with mesh ϵ. In this section, we will study the six vertex model on the approximating graph as $\epsilon \to 0$. The dimer model is identical but it should be understood that the model is on the graph $\Sigma^{(\epsilon)}(G)$ as defined in 2.3.

In particular, we focus on the three classes of graphs introduced in 2.1.

a) Planar domain: Fix a domain U in $\mathbb{R}^2$. For a mesh ϵ, let U^ϵ be the planar graph as in section 2.1 with the rescaled square lattice $\epsilon\mathbb{Z}^2$.

b) Cylinder: Let $C_{LT} = \mathbb{R} \times [0, T] \,/\, \{(x + L, y) \sim (x, y)\}$ be the cylinder of length T, circumference L with flat metric. For mesh ϵ, we let $C^{\epsilon}_{LT} = \epsilon \mathcal{C}_{[L/\epsilon][T/\epsilon]}$

c) Torus: Let $T_{LT} = \mathbb{R}^2 \,/\, \{(x, y) \sim (x + L, y) \sim (x, y + T)\}$, be the torus of length L and width T with flat metric. For mesh ϵ, we let $T^{\epsilon}_{LT} = \epsilon \mathcal{T}_{[L/\epsilon][T/\epsilon]}$

Normalized Height Functions

The *normalized height function* φ is defined as a piece-wise constant function on Σ, with constant value $\varphi = \epsilon h(f)$ on each face $f \in \Gamma$. As a consequence of the height function rules, the height function satisfy the Lipshitz conditions:

$$\frac{1}{\epsilon} \left(\varphi(x + \epsilon, y) - \varphi(x, y), \varphi(x, y + \epsilon) - \varphi(x, y)\right) \in \mathcal{N} \subset \mathbb{R}^2$$

where for the six vertex model $\mathcal{N}$ is unit square $[-1, 1] \times [-1, 1]$; for the dimer model, it is the Newton polygon of the fundamental domain.

Similarly, a normalized *boundary height function* is a piece-wise constant function on $\partial\Sigma$.

Stabilizing Boundary Conditions

Let $\{\chi^{(\epsilon)}\}$ be a set admissable boundary conditions for the six vertex or dimer model on $\Sigma^{(\epsilon)}$. We say the sequence is stabilizing if the normalized boundary height functions of $\chi^{(\epsilon)}$ converge in the uniform metric to a function $\chi : \partial\Sigma \to \mathbb{R}$ as $\epsilon \to 0$.

The Variational Principle

The variational principle states then that the normalized free energy for the model

$$f = \lim_{\epsilon \to \infty} \frac{1}{\epsilon^2} \ \log \left(Z_{\Sigma^{(\epsilon)}}[\chi^{(\epsilon)}]\right)$$

is given by the maximizing the functional

$$S[\varphi] = \int_{\Sigma} \sigma(\partial_x \varphi, \partial_y \varphi) \, dx \, dy \tag{2.4.1}$$

over the space of piecewise differentiable functions h satisfying the gradient constraint:

$$(\partial_x \varphi, \partial y \varphi) \in \mathcal{N}$$

and subject to the boundary conditions:

$$\varphi\big|_{\partial\Sigma} = \chi + \text{constant}$$

Here, recall that the boundary height functions are defined up to an additive constant.

By the convexity of σ for the dimer model and six vertex model, there is a unique solution φ^* called the *limit shape*. The Gibbs measure of the model concentrates about φ^* with variance exponentially supressed in ϵ^2. It follows that in the limit $\epsilon \to 0$, the normalized height function of the model is almost surely equation to φ^*.

Chapter 3

Integrability of Limit Shapes in the Six Vertex Model

In this chapter, we show that the partial differential equations determining the limit shape of the six vertex model are integrable in a Liouville sense: there are an infinite number of conserved quantities. This chapter is based on the paper [RS15].

In the first section, we first reformulate the variational principle for the limit shape on the cylinder into a Hamiltonian framework. The Hamiltonian function, which generates the evolution of the limit shape in the vertical "time" direction of the cylinder, should be regarded as the continuum limit of the transfer matrix. In the second section, we derive some technical results about the surface tension function of the six vertex model from the Bethe ansatz; this section reviews and extends some results of [NK]. In the third section, we prove the commutativity of Hamiltonians corresponding to commutative transfer matrices. This section improves on [RS15], in that we also consider the six vertex model with inhomogenous weights. In section 4. we sketch the Hamiltonian formulation for the limit shapes in the dimer model. In section 5 and section 6, we study in detail the various dimer model limits of the six vertex model.

3.1 Hamiltonian Framework on the Cylinder

We focus on the variational principle on the cylinder C_{LT}. We will think of the y-direction on the cylinder as time. Let $\mathfrak{H}$ be the space of differentiable functions on $[0, L]$ with periodic derivatives.

As in Lagrangian mechanics, we think of S defined in (**??**) as the action functional on paths $[0, T] \mapsto \mathfrak{H}$. Dirichlet boundary conditions correspond to fixing $\partial_x h(x, 0) = \chi_1(x)$ and $\partial_x h(x, T) = \chi_2(x)$, where χ_i are L-periodic. The function σ is the Lagrangian density function on $T\mathfrak{H}$, with $\partial_x h$ being a tangent vector in the tangent space $T_h\mathfrak{h}$. The free energy f_{C_{LT},η_1,η_2} is the Hamilton-Jacobi action (the critical value) of action functional (**??**).

The Hamiltonian framework is defined in the usual way by passing from Lagrangian densities on $T\mathfrak{H}$ to Hamiltonian densities on $T^*\mathfrak{H}$ via the Legendre transform.

Let $\{h(x)\}_{x=0}^{L}$ be a collection of "coordinate functions" on $\mathfrak{H}$, with $h(x)$ assigning a height function h to its value at x. Let $\{p(x)\}_{x=0}^{L}$ be the collection of "coordinate functions" on $T_h^*\mathfrak{H}$. Since the tangent space $T_h\mathfrak{H}$ consists of periodic functions, we assume $p(x+L) = p(x)$. The canonical Poisson bracket on functionals on $T_h^*\mathfrak{H}$ is defined by its values on the coordinate functions p and h:

$$\begin{aligned}\{h(x), p(x')\} &= \delta(x-x')\\ \{p(x), p(x')\} &= 0\\ \{h(x), h(x')\} &= 0\end{aligned}$$

The Hamiltonian density $\mathcal{H}$ is the Legendre transform with respect to the first argument of the surface tension:

$$\mathcal{H}_u(p,\xi) = \max_{\nu\in\mathbb{R}} \big(p\,\nu - \sigma_u(\xi,\nu) + V\nu\big) \tag{3.1.1}$$

The Hamiltonian describing the evolution of the height function from the bottom of the cylinder to the top is given by:

$$H_u(p,h) = \int_0^L \mathcal{H}_u\Big(p(x)+V,\ \partial_x h(x)\Big)\,dx \tag{3.1.2}$$

for $p, h : [0, L] \to \mathbb{R}$. Here and in the previous formula, we emphasize the dependence of σ and $\mathcal{H}$ on the spectral parameter in Baxter's parametrization since, as we will see below, this is the parameterization of the commutative family of Hamiltonians. Since the dependance of the Hamiltonian on V appears as a change of variable (symplectomorphism) $p \to p+V,\ \partial_x h \to \partial_x h$ we will assume from now on that $V = 0$.

The Hamiltonian equations of motion are:

$$\begin{aligned}\partial_y p(x,y) &= \{p(x,y), H\} = -\frac{\delta H}{\delta h(x)}\big(p(x,y), h(x,y)\big)\\ \partial_y h(x,y) &= \{h(x,y), H\} = \frac{\delta H}{\delta p(x)}\big(p(x,y), h(x,y)\big)\end{aligned} \tag{3.1.3}$$

It is easy to check that they are equivalent to the Euler-Lagrange equations for the height function (**??**).

Note that in the Hamiltonian framework equations of motion are extema of the action functional:

$$S[p,h] = \int_0^T \int_0^L p(x,y)\,\partial_y h(x,y) - \mathcal{H}_u\big(p(x,y), \partial_x h(x,y)\big)\,dx\,dy \tag{3.1.4}$$

for $p, h : C_{LT} \to \mathbb{R}$.

The partial Legendre transform of $\sigma(s,t)$

Let $\mathcal{H}$ be the Legendre transform of σ with respect to the second argument:

$$\mathcal{H}(p,\xi) = \max_{\nu\in\mathbb{R}} \big(p\,\nu - \sigma(\xi,\nu)\big)$$

We assume that σ is strictly convex and smooth except possibly on codimension one strata. Then for generic (p, ξ), the maximum is achieved at $\nu^*(p, \xi)$ defined by:

$$p = \partial_2 \sigma(\xi, \nu^*) \tag{3.1.5}$$

Then:

$$\mathcal{H}(p, \xi) = p\ \nu^*(p, \xi) - \sigma\big(\xi, \nu^*(p, \xi)\big)$$

A simple but useful general fact about the Legendre transform is:

Lemma 1. *The following identity holds:*

$$\frac{\partial_2^2 \mathcal{H}(p, \xi)}{\partial_1^2 \mathcal{H}(p, \xi)} = \partial_1^2 \sigma(\xi, \nu^*)\ \partial_2^2 \sigma(\xi, \nu^*) - \big(\partial_1 \partial_2 \sigma(\xi, \nu^*)\big)^2$$

Proof. We first compute:

$$\partial_1 \mathcal{H} = \partial_p \left(p\nu^* - \sigma(\xi, \nu^*)\right) = \nu^* + p\ \partial_p \nu^* - \partial_2 \sigma(\xi, \nu^*)\ \partial_p \nu^* = \nu^*$$

We used equation (3.1.5). Differentiation (3.1.5) with respect to p gives $1 = \partial_2^2 \sigma(\xi, \nu^*)\ \partial_1 \nu^*$. So:

$$\partial_1^2 \mathcal{H} = \frac{1}{\partial_2^2 \sigma} \tag{3.1.6}$$

Similarly:

$$\begin{aligned} \partial_2 \mathcal{H} &= \partial_\xi \left(p\nu^* - \sigma(\xi, \nu^*)\right) = -\partial_2 \sigma \\ \partial_2^2 \mathcal{H} &= \partial_\xi \left(-\partial_2 \sigma(\xi, \nu^*)\right) = -\partial_2 \partial_1 \sigma - \partial_2^2 \sigma\ \partial_2 \nu^* \end{aligned} \tag{3.1.7}$$

Differentiation (3.1.5) with respect to ξ gives:

$$\partial_2 \nu^*\ \partial_2^2 \sigma + \partial_1 \partial_2 \sigma = 0$$

Solving for $\partial_2 \nu^*$ and substituting into (3.1.7) we obtain:

$$\partial_2 \mathcal{H} = -\partial_2^2 \sigma + \frac{(\partial_1 \partial_2 \sigma)^2}{\partial_2^2 \sigma} \tag{3.1.8}$$

Combining with (3.1.6) we arrive to:

$$\frac{\partial_2^2 \mathcal{H}}{\partial_1^2 \mathcal{H}} = -\partial_1^2 \sigma\ \partial_2^2 \sigma + (\partial_1 \partial_2 \sigma)^2$$

□

3.2 Bethe Ansatz Equations for the Hamiltonian

We will now compute the Hamiltonian and its partial derivatives directly from the Bethe ansatz. This is along the lines of [NK].

Bethe Ansatz Equations

The Bethe ansatz equation for the Q-particle sector is (see [NK], [PR]):

$$z_i^N = (-1)^{Q-1} \prod_{j=1}^{Q} \frac{1 + e^{4h} z_i z_j - 2e^{2h} \Delta z_i}{1 + e^{4h} z_i z_j - 2e^{2h} \Delta z_j}$$

which give eigenvalues of the transfer matrix:

$$\Lambda = \Lambda_L + \Lambda_R \tag{3.2.1}$$

$$\Lambda_R = w_1^{N-Q} \prod_{j=1}^{Q} \left(w_3 - \frac{w_5 w_6}{w_4 - w_1 z_j} \right) \tag{3.2.2}$$

$$\Lambda_L = w_4^{N-Q} \prod_{j=1}^{Q} \left(w_2 + \frac{w_5 w_6 z_j}{w_4 - w_1 z_j} \right) \tag{3.2.3}$$

Define $\Theta(p, p')$ by:

$$e^{i\Theta(p,p')} = \frac{1 + e^{ip+ip'} - 2\Delta e^{ip}}{1 + e^{ip+ip'} - 2\Delta e^{ip'}}$$

For each range of Δ, there is a change of variables $p = p(\alpha)$ that makes Θ a difference kernel, i.e. $\Theta(p(\alpha), p(\beta)) \to \Theta(\alpha - \beta)$.

1. For $\Delta > 1$

   Weights:

   $$a : b : c = \sinh \frac{1}{2}(u - \eta) : \sinh \frac{1}{2}(\eta + u) : \sinh \eta$$

   The change of variables is:

   $$z(\alpha) = e^{ip(\alpha)} = \frac{e^{\eta+\alpha} - 1}{e^{\alpha} - e^{\eta}}$$

   We then have:

   $$\Phi_R(\alpha) = \log \left(-\frac{e^{u+\eta} - e^{\alpha-\eta}}{e^{\alpha} - e^{u}} \right) \qquad \Phi_L(\alpha) = \log \left(-\frac{e^{u-\eta} - e^{\alpha+\eta}}{e^{\alpha} - e^{u}} \right) \tag{3.2.4}$$

2. For $-1 < \Delta < 1$:

   Weights:

   $$a : b : c = \sin \frac{1}{2}(\eta - u) : \sin \frac{1}{2}(\eta + u) : \sin \eta$$

   The change of variables is:

   $$z(\alpha) = e^{ip(\alpha)} = \frac{e^{i\eta+\alpha} - 1}{e^{i\eta} - e^{\alpha}}$$

We then have for Θ:

$$e^{i\Theta(\gamma)} = \frac{1 - e^{\gamma+2i\eta}}{e^{\gamma} - e^{2i\eta}}$$

$$\Phi_R(\alpha) = \log\left(\frac{e^{iu+i\eta} - e^{\alpha-i\eta}}{e^{\alpha} - e^{iu}}\right) \qquad \Phi_L(\alpha) = \log\left(\frac{e^{iu-i\eta} - e^{\alpha+i\eta}}{e^{\alpha} - e^{iu}}\right) \tag{3.2.5}$$

3. For $\Delta < -1$: Omitted, essentially the same.

Integral equations

The roots of the Bethe equations lie on a contour that is symmetric to the imaginary axis with end points A and $B = -A^*$. The density of the roots is determined by Z which satisfies the integral equation:

$$Z(\alpha) = p(\alpha) + 2hi - \frac{1}{2\pi}\int_A^B \Theta(\alpha - \beta)\ Z'(\beta)d\beta$$

and normalization condition:

$$Z(B) = \pi q \qquad Z(A) = -\pi q$$

where $q \sim Q/N$. The density of roots ρ is $\partial_\alpha Z$.

The Hamiltonian is then:

$$\mathcal{H}(h,q) = \min_{R,L}\left\{\pm h \pm \frac{\delta}{2} - \frac{1}{2\pi}\int_A^B \Phi_{L,R}(\alpha)\ \partial_\alpha Z(\alpha)\ d\alpha\right\}$$

with $+/-$ for L/R.

.

Partial Derivatives of the Hamiltonian

We now compute the partial derivates of functions of the form:

$$S(h,q,u) = \frac{1}{2\pi}\int_A^B f(\alpha,u)\ \partial_\alpha Z(\alpha)\ d\alpha$$

where f is some function (placeholder for $\Phi_{L,R}$).

First Partial Derivatives

First a few definitions:

We set $F(\alpha, \mu, A, B)$ the function satisfying the integral equation:

$$F(\alpha,\mu) + \frac{1}{2\pi}\int_A^B K(\alpha-\beta)\, F(\beta,\mu)\, d\beta = -\frac{1}{2}\Theta(\alpha-\mu)$$

where $K(z) = \partial_z\Theta(z)$. Also let $\overset{\circ}{F}(\beta,\mu) = \partial_\mu F(\beta,\mu)$.

The dressed charge functions and constants are defined as:

$$\begin{aligned} D(\alpha) &= 1 - \frac{1}{\pi}\big(F(\alpha,B) - F(\alpha,A)\big) \\ D_2(\alpha) &= F(\alpha,A) + F(\alpha,B) \\ D_0 &= D(B) = D(A) \\ D_2 &= D_2(B) = -D_2(A) \end{aligned} \tag{3.2.6}$$

Lemma 2. *First Partial Derivatives of S:*

$$\partial_h S(h,q) = -\frac{iD_0}{\pi}(f(B)-f(A)) - \frac{iD_0}{\pi^2}\int_A^B f(\alpha)(\overset{\circ}{F}(\alpha,B) - \overset{\circ}{F}(\alpha,A))\, d\alpha$$
$$\partial_q S(h,q) = \frac{1}{2D_0}(f(B)+f(A)) + \frac{1}{2\pi D_0}\int_A^B f(\alpha)(\overset{\circ}{F}(\alpha,B) + \overset{\circ}{F}(\alpha,A))\, d\alpha$$

Proof. We start with equation 51, 52 in [NK] for the first partial derivatives:

$$\begin{aligned} \partial_h S(h,q) &= -\frac{i}{\pi}\int_A^B \partial_\alpha f(\alpha) D(\alpha) d\alpha \\ \partial_q S(h,q) &= \frac{1}{2}(f(A)+f(B)) - \frac{1}{2\pi}\int_A^B \partial_\alpha f(\alpha) D_2(\alpha) d\alpha \end{aligned} \tag{3.2.7}$$

Integrate by parts to get:

$$S_h(h,q) = \frac{i}{\pi}\int_A^B f(\alpha)\partial_\alpha D(\alpha) d\alpha - \frac{iD_0}{\pi}(f(A)-f(B))$$
$$S_q(h,q) = \frac{1}{2}(f(A)+f(B)) - \frac{D_2}{2\pi}(f(B)+f(A)) + \frac{1}{2\pi}\int_A^B f(a)\ \partial_\alpha D_2(\alpha) d\alpha$$

To compute $\partial_1 D(\alpha)$ and $\partial_1 D_2(\alpha)$, start with the definition (3.2.6) and use the following formula given in the appendix A of [NK]:

$$\partial_\alpha F(\alpha,\mu) = \overset{\circ}{F}(\alpha,\mu) - \frac{1}{\pi}\left(F(B,\mu)\overset{\circ}{F}(\alpha,B) - F(A,\mu)\overset{\circ}{F}(\alpha,A)\right)$$

Applying this gives:

$$\begin{aligned}-\pi\partial_\alpha D(\alpha) =&\overset{\circ}{F}(\alpha,B)-\frac{1}{\pi}\left(F(B,B)\overset{\circ}{F}(\alpha,B)-F(A,B)\overset{\circ}{F}(\alpha,A)\right)\\&-\left(\overset{\circ}{F}(\alpha,A)-\frac{1}{\pi}\left(F(B,A)\overset{\circ}{F}(\alpha,B)-F(A,A)\overset{\circ}{F}(\alpha,A)\right)\right)\\=&D_0\ \left(\overset{\circ}{F}(\alpha,B)-\ \overset{\circ}{F}(\alpha,A)\right)\end{aligned}$$

Here we used the definition of D_0 (3.2.6).

Similarly:

$$\begin{aligned}\partial_\alpha D_2(\alpha) =&\overset{\circ}{F}(\alpha,B)-\frac{1}{\pi}\left(F(B,B)\overset{\circ}{F}(\alpha,B)-F(A,B)\overset{\circ}{F}(\alpha,A)\right)\\&+\left(\overset{\circ}{F}(\alpha,A)-\frac{1}{\pi}\left(F(B,A)\overset{\circ}{F}(\alpha,B)-F(A,A)\overset{\circ}{F}(\alpha,A)\right)\right)\\=&\left(1-\frac{D_2}{\pi}\right)(\overset{\circ}{F}(\alpha,B)+\overset{\circ}{F}(\alpha,A))\\=&\frac{1}{D_0}(\overset{\circ}{F}(\alpha,B)+\overset{\circ}{F}(\alpha,A))\end{aligned}$$

We used the identity (Appendix B in [NK]):

$$D_0(1-D_2/\pi)=1 \tag{3.2.8}$$

□

Second partial derivatives

We now remember that f depends on parameter u. Define:

$$\begin{aligned}\zeta&=\frac{1}{i\pi\partial_\alpha Z(B)}\left(\int_A^B\partial_\alpha f(\alpha,u)\overset{\circ}{F}(\alpha,B)\,d\alpha+\pi\partial_\alpha f(B)\right)\\\zeta^*&=\frac{1}{i\pi\partial_\alpha Z(A)}\left(\int_A^B\partial_\alpha f(\alpha,u)\overset{\circ}{F}(\alpha,A)\,d\alpha+\pi\partial_\alpha f(A)\right)\end{aligned} \tag{3.2.9}$$

$$\begin{aligned}\eta&=\frac{1}{2\pi D_0}\left(\int_A^B\partial_u f(\alpha,u)\overset{\circ}{F}(\alpha,B)\,d\alpha+\pi\ \partial_u f(B,u)\right)\\\eta^*&=\frac{1}{2\pi D_0}\left(\int_A^B\partial_u f(\alpha,u)\overset{\circ}{F}(\alpha,A)\,d\alpha+\pi\ \partial_u f(A,u)\right)\end{aligned} \tag{3.2.10}$$

Lemma 3. *The second partial derivatives:*

$$\begin{aligned}
\partial_h^2 S(h,q,u) &= \frac{2iD_0^2}{\pi}(\zeta-\zeta^*)\\
\partial_h\partial_q S(h,q,u) &= \zeta+\zeta^*\\
\partial_q^2 S(h,q,u) &= \frac{i\pi}{2D_0^2}(\zeta-\zeta^*)\\
\partial_h\partial_u S(h,q,u) &= \frac{2iD_0^2}{\pi}\,(\eta-\eta^*)\\
\partial_q\partial_u S(h,q,u) &= \eta+\eta^*
\end{aligned} \tag{3.2.11}$$

Proof. The first three are given in [NK]. The last two are easy because only f depends on u. □

Corollary 1. *The hessian of the surface tension σ does not depend on the spectral parameter u.*

3.3 Commuting Hamiltonians

Homogenous Hamiltonians

In this section, we will prove that Hamiltonians (3.1.2) form a commutative family, i.e. for any u and v

$$\{H_u, H_v\} = 0$$

We first compute the Poisson bracket of H_u and H_v with densities $\mathcal{H}_u$ and $\mathcal{H}_v$:

Lemma 4.

$$\begin{aligned}
\{H_u, H_v\} = \int_0^L &\left(\partial_1^2\mathcal{H}_u\;\partial_2\mathcal{H}_v - \partial_1^2\mathcal{H}_v\;\partial_2\mathcal{H}_u\right)\partial_x p(x)\\
&+\left(\partial_1\partial_2\mathcal{H}_u\;\partial_2\mathcal{H}_v - \partial_1\partial_2\mathcal{H}_v\;\partial_2\mathcal{H}_u\right)\partial_x^2 h(x)\;dx
\end{aligned} \tag{3.3.1}$$

Here we abbreviated the arguments, so that by $\mathcal{H}_u$ we mean $\mathcal{H}_u\big(p(x),\partial_x h(x)\big)$, etc.

Proof. It is a straightforward computation:

$$\begin{aligned}
\{H_u, H_v\} &= \int_0^L \int_0^L \left\{\mathcal{H}_u\big(p(x), \partial_x h(x)\big), \mathcal{H}_v\big(p(x'), \partial_{x'} h(x')\big)\right\} dx\, dx' \\
&= \int_0^L \int_0^L \left(\partial_1\mathcal{H}_u(x)\, \partial_2\mathcal{H}_v(x')\, \{p(x), \partial_{x'} h(x')\} + \partial_2\mathcal{H}_u(x)\, \partial_1\mathcal{H}_v(x')\, \{\partial_x h(x), p(x')\}\right) dx\, dx' \\
&= \int_0^L \int_0^L \left(-\partial_1\mathcal{H}_u(x)\, \partial_2\mathcal{H}_v(x')\, \partial_x\delta(x-x') + \partial_2\mathcal{H}_u(x)\, \partial_1\mathcal{H}_v(x')\, \partial_x\delta(x-x')\right) dx\, dx' \\
&= \int_0^L \int_0^L \left(\left(\partial_x\partial_1\mathcal{H}_u(x)\right) \partial_2\mathcal{H}_v(x')\delta(x-x') - \partial_2\mathcal{H}_u(x) \left(\partial_{x'}\partial_1\mathcal{H}_v(x')\right) \delta(x-x')\right) dx\, dx' \\
&= \int_0^L \left(\left(\partial_1^2\mathcal{H}_u\, \partial_x p + \partial_1\partial_2\mathcal{H}_u\, \partial_x^2 h\right) \partial_2\mathcal{H}_v - \partial_2\mathcal{H}_u \left(\partial_1^2\mathcal{H}_v\, \partial_x p + \partial_1\partial_2\mathcal{H}_v\, \partial_x^2 h\right)\right) dx \\
&= \int_0^L \left(\left(\partial_1^2\mathcal{H}_u\, \partial_2\mathcal{H}_v - \partial_1^2\mathcal{H}_v\, \partial_2\mathcal{H}_u\right) \partial_x p + \left(\partial_1\partial_2\mathcal{H}_u\, \partial_2\mathcal{H}_v - \partial_1\partial_2\mathcal{H}_v\, \partial_2\mathcal{H}_u\right) \partial_x^2 h\right) dx
\end{aligned}$$

□

Proposition 1. *For any u and v, the Hamiltonians H_u and H_v Poisson commute if $Hess(\sigma_u) = Hess(\sigma_v)$.*

Proof. Let us rewrite Lemma 3.3.1 as:

$$\{H_u, H_v\} = \int_0^L \left(A\left(p(x), \partial_x h(x)\right)\, \partial_x p + B\left(p(x), \partial_x h(x)\right)\, \partial_x^2 h\right) dx$$

where

$$\begin{aligned}
A &= \partial_1^2\mathcal{H}_u\, \partial_2\mathcal{H}_v - \partial_1^2\mathcal{H}_v\, \partial_2\mathcal{H}_u \\
B &= \partial_1\partial_2\mathcal{H}_u\, \partial_2\mathcal{H}_v - \partial_1\partial_2\mathcal{H}_v\, \partial_2\mathcal{H}_u
\end{aligned}$$

If

$$\partial_2 A(s_1, s_2) - \partial_1 B(s_1, s_2) = 0$$

for $(s_1, s_2) \in [-\frac{1}{2}, \frac{1}{2}] \times [-\frac{1}{2}, \frac{1}{2}]$ then there exists $\mathcal{F}(s_1, s_2)$ such that:

$$\partial_1\mathcal{F} = A, \quad \partial_2\mathcal{F} = B$$

and so:

$$\begin{aligned}
\{H_u, H_v\} &= \int_0^L \left(\partial_1\mathcal{F}(p(x), \partial_x h(x))\, \partial_x p + \partial_2\mathcal{F}(p(x), \partial_x h(x))\, \partial_x^2 h\right) dx \\
&= \int_0^L \partial_x\mathcal{F}(p(x), \partial_x(h))\, dx = 0
\end{aligned}$$

Now we compute $\partial_2 A - \partial_1 B$:

$$\begin{aligned}
\partial_2 A - \partial_1 B &= \partial_2 \left(\partial_1^2 \mathcal{H}_u \partial_2 \mathcal{H}_v - \partial_1^2 \mathcal{H}_v \partial_2 \mathcal{H}_u\right) - \partial_1 \left(\partial_1 \partial_2 \mathcal{H}_u \partial_2 \mathcal{H}_v - \partial_1 \partial_2 \mathcal{H}_v \partial_2\right) \\
&= (\partial_1^2 \partial_2 \mathcal{H}_u \partial_2 \mathcal{H}_v + \partial_1^2 \mathcal{H}_u \partial_2^2 \mathcal{H}_v - \partial_1^2 \partial_2 \mathcal{H}_v \partial_2 \mathcal{H}_u - \partial_1^2 \mathcal{H}_v \partial_2^2 \mathcal{H}_u) \\
&\quad - (\partial_1^2 \partial_2 \mathcal{H}_u \partial_2 \mathcal{H}_v + \partial_1 \partial_2 \mathcal{H}_u \partial_1 \partial_2 \mathcal{H}_v - \partial_1^2 \partial_2 \mathcal{H}_v \partial_2 \mathcal{H}_u - \partial_1 \partial_2 \mathcal{H}_v \partial_1 \partial_2 \mathcal{H}_u) \\
&= \partial_1^2 \mathcal{H}_u \partial_2^2 \mathcal{H}_v - \partial_1^2 \mathcal{H}_v \partial_2^2 \mathcal{H}_u \\
&= \partial_1^2 \mathcal{H}_u \, \partial_1^2 \mathcal{H}_v \left(\frac{\partial_2^2 \mathcal{H}_v}{\partial_1^2 \mathcal{H}_v} - \frac{\partial_2^2 \mathcal{H}_u}{\partial_1^2 \mathcal{H}_u}\right) \\
&= \partial_1^2 \mathcal{H}_u \, \partial_1^2 \mathcal{H}_v \left(\mathrm{Hess}(\sigma_v) - \mathrm{Hess}(\sigma_u)\right)
\end{aligned}$$

In the last line, we used Lemma 1.

□

Together, corollary (1) and (1) imply:

Corollary 2. *The Hamiltonians H_u of the 6-vertex model form a Poisson commuting family.*

Inhomogenous Hamiltonians

Consider the inhomogeneous 6-vertex model on a cylinder as it is described in section 2.2 with inhomogeneity parameters parameters $v_i, i = 1, \cdots M$ corresponding to vertical lines of the lattice.

In the thermodynamical limit when $N = [T/\epsilon], M = [L/\epsilon]$ and $\epsilon \to 0$ we assume that $u_i \to u(y)$ and $v_j \to v(x)$, assuming that $i = [y/\epsilon]$ and $j = [x/\epsilon]$.

The Hamiltonian then is:

$$H_u(p, h) = \int_0^L \mathcal{H}\big(p(x), h_y(x), u(x)\big)\, dx$$

where the spectral parameter u can depend on x.

Fixing $u(x)$ and a constant c, let $\widetilde{u}(x) = u(x) + c$. In this case, we expect that H_u and $H_{\widetilde{u}}$ will Poisson commute, as the transfer matrices do. Straightforward computation, as before, gives (writing $\widetilde{H}$ for $H_{\widetilde{u}}$):

$$\{H, \widetilde{H}\} = \int_0^L A\, \partial_y p + B\, \partial_y^2 h + C\, \partial_y u\, dy \tag{3.3.2}$$

where:

$$\begin{aligned}
A &= \mathcal{H}_{11} \widetilde{\mathcal{H}}_2 - \widetilde{\mathcal{H}}_{11} \mathcal{H}_2 \\
B &= \mathcal{H}_{12} \widetilde{\mathcal{H}}_2 - \widetilde{\mathcal{H}}_{12} \mathcal{H}_2 \\
C &= \mathcal{H}_{13} \widetilde{\mathcal{H}}_2 - \widetilde{\mathcal{H}}_{13} \mathcal{H}_2
\end{aligned} \tag{3.3.3}$$

The integrand in (3.3.2) will be a total derivative if all the mixed derivatives are zero (a closed one form):

$$\begin{aligned} \partial_2 A - \partial_1 B &= 0 \\ \partial_3 A - \partial_1 C &= 0 \\ \partial_3 B - \partial_2 C &= 0 \end{aligned} \tag{3.3.4}$$

This leads to:

Lemma 5. *The bracket* $\{H, \widetilde{H}\} = 0$ *if:*

$$\begin{aligned} \mathcal{H}_{11}\widetilde{\mathcal{H}}_{22} - \widetilde{\mathcal{H}}_{11}H_{22} &= 0 \\ \mathcal{H}_{11}\widetilde{\mathcal{H}}_{23} + \mathcal{H}_{12}\widetilde{\mathcal{H}}_{13} - \mathcal{H}_{13}\widetilde{\mathcal{H}}_{12} - \mathcal{H}_{23}\widetilde{\mathcal{H}}_{11} &= 0 \\ \mathcal{H}_{12}\widetilde{\mathcal{H}}_{23} + \mathcal{H}_{22}\widetilde{\mathcal{H}}_{13} - \mathcal{H}_{13}\widetilde{\mathcal{H}}_{22} - \mathcal{H}_{23}\widetilde{\mathcal{H}}_{12} &= 0 \end{aligned} \tag{3.3.5}$$

Returning to , note that the ζ and η are identical except for a constant prefactor and by $\partial_\alpha f$ instead of $\partial_u f$. Recall that f is really Φ given in (3.2.5), which can be rewritten:

$$\Phi_R(\alpha, u) = \log\left(\frac{e^{i\eta} - e^{\alpha - i\eta - iu}}{e^{\alpha - iu} - 1}\right) \qquad \Phi_L(\alpha, u) = \log\left(\frac{e^{-i\eta} - e^{\alpha + i\eta - iu}}{e^{\alpha - iu} - 1}\right)$$

Since they depend on α and u only via the linear combination $\alpha - iu$, it is immediately clear that $\partial_\alpha \Phi / \partial_u \Phi = i$. It follows immediately:

Corollary 3. *The Hamiltonians satisfy 3.3.5*

Remark 3. *The existence of Hamiltonians H_u is due to limit shape phenomenon, which can be regarded as a semiclassical nature of the thermodynamic limit. The Poisson commutativity of Hamiltonians is a consequence of commutativity of transfer-matrices and thus, of the Yang-Baxter equation for the weights of the 6-vertex model. One can show that for any model with limit shape phenomenon and commutative family of transfer-matrices we have a family of Poisson commutative Hamiltonians for limit shapes on a cylinder. The details will be given elsewhere.*

3.4 The Dimer Model and Burger's Equation.

The limit shape and Burgers' equation

As for the 6-vertex model the free energy of a dimer model on a cylinder is determined by the minimizer of

$$S[h] = \int_0^T \int_0^L \sigma(\partial_x h, \partial_y h)\, dx\, dy$$

over all piecewise differentiable functions h with slopes $(\partial_x h, \partial_y h) \in \mathcal{N}(P)$.

The Euler-Lagrange equations for the limit shape are then:

$$\partial_1^2 \sigma(\partial_x h, \partial_y h)\, \partial_x^2 h + 2\, \partial_1 \partial_2 \sigma(\partial_x h, \partial_y h)\, \partial_x \partial_y h + \partial_2^2 \sigma(\partial_x h, \partial_y h)\, \partial_y^2 h = 0 \tag{3.4.1}$$

Define the new variables:

$$\begin{aligned} z &= \mp \exp(i\pi\partial_x h + \partial_2\sigma(\partial_x h, \partial_y h)) \\ w &= \pm \exp(-i\pi\partial_y h + \partial_1\sigma(\partial_x h, \partial_y h)) \end{aligned} \tag{3.4.2}$$

Then the Euler-Lagrange equations in terms of z and w are

$$\frac{\partial_y z}{z} + \frac{\partial_z w}{w} = 0 \tag{3.4.3}$$

The imaginary part gives the identity $\partial_y\partial_x h = \partial_x\partial_y h$.

The following theorem is essentially proven in [KO] that

Theorem 1. *[KO] Equations (3.4.1) and (3.4.2), for some choice of branch, together imply $P(z, w) = 0$. Conversely, if z and w satisfy $P(z, w) = 0$ and (3.4.3), then $\partial_y h = -\frac{1}{i\pi}\arg(w)$ and $\partial_x h = \frac{1}{i\pi}\arg(z)$ satisfy the Euler-Lagrange equation (3.4.1).*

Let z and w be as in (3.4.2). We can rewrite the Euler-Lagrange equations as:

$$\partial_y z = F(z)\ \partial_x z \qquad F(z) := \frac{z}{w}\frac{\partial_z P\,(z, w)}{\partial_w P\,(z, w)} \tag{3.4.4}$$

The equations of motion for $F(z)$ itself is the complex Burgers' equation.

$$\partial_y F = F\ \partial_x F \tag{3.4.5}$$

Hamiltonian Framework and Holomorphic Factorization

The Hamiltonian framework for the dimer models is completely parallel to the one for the 6-vertex Model. The Hamiltonian is

$$H = \int_0^L \mathcal{H}(p, \partial_x h)\ dx$$

where p is the momentum (Legendre dual to $\partial_x h$) and

$$\mathcal{H}(p, s) = \max_t\,(t\ p - \sigma(s, t)) \tag{3.4.6}$$

The equation of motion (3.4.4) is closely related to the Hamilton's equations in the Hamiltonian framework outlined in Section 3.1. Recall that the Legendre transform of the surface tension induces an identification of TM and T^*M, in particular, it maps $\partial_y h$ to $p = \partial_2\sigma(\partial_x h, \partial_y h)$. Via this identification, define the image of z of equation (3.4.2) in cotangent bundle to the space of height functions as $z(x) = \exp\,(p(x) + i\pi\partial_x h(x))$ and:

$$l(x) = \log(z(x)) = p(x) + i\pi\partial_x h(x)$$

In terms of l, the canonical Poisson bracket can be written:

$$\begin{aligned} \{l(x), l(x')\} &= 2\pi i\ \delta'(x-x') \\ \{l(x), \bar{l}(x')\} &= 0 \\ \{\bar{l}(x), \bar{l}(x')\} &= -2\pi i\ \delta'(x-x') \end{aligned} \tag{3.4.7}$$

Note that the Poisson algebra of functionals in l has Casimir elements. Its Poisson center is generated by $\int_0^L l(x)dx$ and $\int_0^L \bar{l}(x)dx$

The equations of motion for l and $\bar{l}$ are:

$$\partial_y l = F(e^l)\ \partial_x l \quad \partial_y \bar{l}\ = F(e^{\bar{l}})\ \partial_x \bar{l} \tag{3.4.8}$$

where F was defined in equation (3.4.4).

Now let us rewrite the Hamiltonian (3.4.6) in terms of l and $\bar{l}$.

Proposition 2. *The Hamiltonian density satisfies the following differential equations*

$$\frac{\partial^2 \mathcal{H}}{\partial l^2} = 2\pi i\ F(e^l), \quad \frac{\partial^2 \mathcal{H}}{\partial \bar{l}^2} = -2\pi i\ F(e^{\bar{l}}), \quad \frac{\partial^2 \mathcal{H}}{\partial l \partial \bar{l}} = 0 \tag{3.4.9}$$

Proof. Hamiltonian equations of motion with the Poisson brackets (3.4.7) are:

$$\partial_y l(x,y) = \{\mathcal{H}, l(x)\}(x,y) = \int_0^L \frac{\partial \mathcal{H}}{\partial l}(x',y)\ 2\pi i\ \delta'(x-x')\ dx' = 2\pi i \left(\frac{\partial^2 \mathcal{H}}{\partial l^2}\ \partial_x l + \frac{\partial^2 \mathcal{H}}{\partial l \partial \bar{l}}\ \partial_x \bar{l} \right)$$

and a similar equation for $\bar{l}$. Comparing with equations of motion we have equation (3.4.9). □

Corollary 4. *This implies*

$$\mathcal{H}(p, \partial_x h) = G(e^l) + G(e^{\bar{l}}) + Al + \bar{A}\bar{l} + C$$

where $G(l)$ is any (second) antiderivative of $F(l)$. Note that since $\int_0^L l(x)dx$ and $\int_0^L \bar{l}(x)dx$ are Casimir functions, the equations of motion for such Hamiltonian do not depend on A or C.

It is clear that this Hamiltonian Poisson commute with functionals

$$I_n = \int_0^L l^n(x)dx, \quad \bar{I}_n = \int_0^L \bar{l}^n(x)dx$$

form a commuting family and I_n and $\bar{I}_n$ mutually Poisson commute. The existence of these integrals of course is due to the integrability of the Burgers equation.

3.5 The Hexagonal Dimer Model and the Five Vertex Model

The Dimer Model on the Hexagonal Lattice

In this case $\phi_\epsilon(\mathcal{L})$ is the hexagonal lattice embedded into a cylinder with all edge weights being 1.

The spectral curve for the hexagonal dimer model is:

$$P(z,w) = 1 - z - w$$

Three terms correspond to three dimer configurations on the fundamental domain for a hexagonal lattice with periodic boundary conditions, see Figure 3.1.

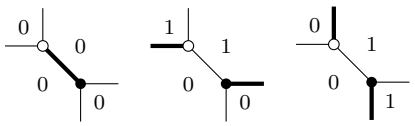

Figure 3.1: The three states on Γ_0 with periodic boundary conditions for the hexagonal lattice.

Surface Tension

The surface tension for the hexagonal dimer model is given in [**?**] as:

$$\sigma(s,t) = -\frac{1}{\pi}\Big(L(\pi s) + L(\pi t) + L(\pi(1-s-t))\Big)$$

where L is the Lobavchesky function:

$$\begin{aligned} L(x) &= -\int_0^x \log(2\sin(x))\,dx \\ &= \frac{1}{2}\Im\left(\mathrm{Li}_2(e^{2ix})\right) \end{aligned}$$

where $\mathrm{Li}_2(z) = \sum_{k=1} \frac{z^k}{k^2}$ is the dilogarithm.

The partial derivatives are:

$$\begin{aligned} \partial_s\sigma(s,t) &= \log\left(\frac{\sin(\pi s)}{\sin(\pi(s+t))}\right) \\ \partial_t\sigma(s,t) &= \log\left(\frac{\sin(\pi t)}{\sin(\pi(s+t))}\right) \end{aligned} \tag{3.5.1}$$

The Euler-Lagrange equations are:

$$\partial_x^2 h\,\frac{\sin(\pi\partial_y h)}{\sin(\pi\partial_x h)} - 2\,\partial_x\partial_y h\,\cos(\pi(\partial_y h + \partial_x h)) + \partial_y^2 h\,\frac{\sin(\pi\partial_x h)}{\sin(\pi\partial_y h)} = 0 \tag{3.5.2}$$

Solving $P(z,w)=0$ for w, we obtain $F(z)=z/(1-z)$. In terms of l-variable the Euler-Lagrange equation become:

$$\partial_x l = -\frac{e^l}{1-e^l}\,\partial_y l$$

Hamiltonian framework

The Legendre transform of the dimer action for this particular case for the homogeneous hexagonal lattice gives:

$$\mathcal{H} = \frac{1}{2\pi i}\,\left(\mathrm{Li}_2(e^l) - \mathrm{Li}_2(e^{\bar{l}})\right) \tag{3.5.3}$$

where $l = p + i\pi h_x$ and $\mathrm{Li}_2(x) = \sum_{k=1}^{\infty} \frac{z^k}{k^2}$.

Indeed, minimizing

$$\mathcal{H}(p, \partial_x h) = p\,\partial_y h - \sigma(\partial_x h, \partial_y h) \tag{3.5.4}$$

with respect to $\partial_x h$ we obtain the equation for the critical point:

$$p(\partial_x h, \partial_y h) = \log\left(\frac{\sin(\pi\partial_y h(x,y))}{\sin\left(\pi(\partial_y h(x,y) + \partial_x h(x,y))\right)}\right) \tag{3.5.5}$$

which is easy to solve for $\partial_y h(x,y)$:

$$\partial_y h(x,y) = \frac{i}{2\pi}\log\left(\frac{1-e^{p(x,y)+i\pi\partial_x h(x,y)}}{1-e^{p(x,y)-i\pi\partial_x h(x,y)}}\right) \tag{3.5.6}$$

Substituting $\partial_y h$ into (3.5.4) and utilizing some dilogarithm identities gives (3.5.3). It is straightforward to check that equations (3.4.9) hold.

5-vertex limits of the 6-vertex model

The 5-vertex model is the limit of the 6-vertex model with the weight $w_2 = 0$. The R-matrix for this model is:

$$R = \begin{pmatrix} ae^{H+V} & 0 & 0 & 0 \\ 0 & be^{H-V} & c & 0 \\ 0 & c & be^{V-H} & 0 \\ 0 & 0 & 0 & 0 \end{pmatrix}$$

Other 5-vertex models are found by setting w_3, w_4, or w_1 each to zero. They are related to model with $w_1 = 0$ by the symmetries that interchange thin vertical edges with thick vertical edges, or thin horizontal edges with thick horizontal edges, or both.

The 5-vertex model an be obtained from the 6-vertex model in the limit that the magnetic fields go to infinity as follows:

1. If $b^2-c^2>0$: using the parametrization with $(a,b,c)=(\sinh\left(u-\gamma\right),\sinh(u),\sinh(\gamma))$, change variables to (ξ,l,m) as:

$$H=\frac{\gamma}{2}+l \qquad V=\frac{\gamma}{2}+m \qquad u=\gamma+\xi$$

Taking the limit $\gamma\to\infty$ the R-matrix converges (up to a constant factor) to:

$$R=\begin{pmatrix} 2\ \sinh(\xi)e^{l+m} & 0 & 0 & 0\\ 0 & e^{\xi-l+m} & 1 & 0\\ 0 & 1 & e^{\xi+l-m} & 0\\ 0 & 0 & 0 & 0 \end{pmatrix}$$

2. If $b^2-c^2=0$: using the parametrization for $(a,b,c)=(r\sin(\gamma-u),r\sin(u),r\sin(\gamma))$, change variables to:

$$H=-\frac{1}{2}\ln(\gamma-u)+l \qquad V=-\frac{1}{2}\ln(\gamma-u)+m$$

then taking the limit $\gamma\to u$, the R-matrix converges to:

$$R=\begin{pmatrix} e^{l+m} & 0 & 0 & 0\\ 0 & \sin(u)e^{l-m} & \sin(u) & 0\\ 0 & \sin(u) & \sin(u)e^{-l+m} & 0\\ 0 & 0 & 0 & 0 \end{pmatrix}$$

3. If $b^2-c^2<0$, using the parametrization with $(a,b,c)=(\sinh(\gamma-u),\sinh(u),\sinh(\gamma))$, change variables to:

$$H=\frac{\gamma}{2}+l \qquad V=\frac{\gamma}{2}+m \qquad u=\gamma-\xi$$

Taking the limit $\gamma\to\infty$ the R-matrix converges (up to a constant factor) to:

$$R=\begin{pmatrix} 2\sinh(\xi)e^{H+V} & 0 & 0 & 0\\ 0 & e^{-\xi+H-V} & 1 & 0\\ 0 & 1 & e^{-\xi+V-H} & 0\\ 0 & 0 & 0 & 0 \end{pmatrix}$$

The 5-vertex model is equivalent to the dimer model with interactions on the hexagonal lattice [HWKK]. At the free fermion point, $b^2-c^2=0$, the five-vertex model is equivalent to the pure dimer model on the hexagonal lattice found by replacing each vertex of the square lattice with the graph:
where the weights are:

$$\alpha=e^{l+m} \qquad \beta=e^{\frac{l-m}{2}} \qquad \gamma=e^{\frac{m-l}{2}}$$

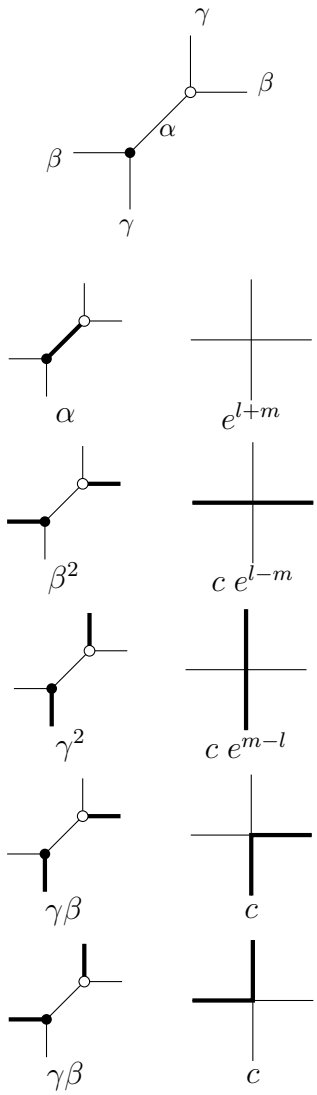

Figure 3.2: The 5-vertex configurations and weights, and the corresponding hexagonal dimer model configurations and weights.

The correspondence of five vertex states and dimer configurations is as shown in Figure (3.2).

It is straightforward to check that as before, the height function of the dimer model and 5-vertex model are related by $\theta^{\text{dimer}} = \theta^{6\text{v}} + x/2 + y/2$.

Thus, the hexagonal dimer model is the limit of the free fermionic 6-vertex model in the limit $u \to \gamma$ and $H, V \to \infty$. Indeed, by taking the limit $u \to 0$ in the PDE (3.6.3) of the limit shape of the free fermionic six vertex model, we recover the PDE (3.5.2) for the hexagonal dimer model.

3.6 Free Fermionic Point Six Vertex Model

The Dimer City

The six-vertex model at the free-fermionic point $\Delta = 0$ is equivalent to a dimer model with the dimer city [MW] placed at each vertex of the square lattice:

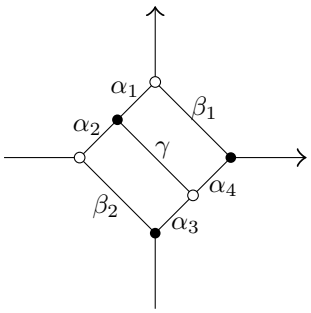

The correspondence of dimer configurations and six vertex states is as shown in Figure 3.3.

In terms of the dimer weights, the weights of the six-vertex configurations are:

$$\begin{aligned} w_1 &= \beta_1\beta_2\gamma + \beta_2\alpha_2\alpha_3 + \beta_1\alpha_1\alpha_4 \\ w_2 &= \gamma \\ w_3 &= \alpha_1\alpha_3 \\ w_4 &= \alpha_4\alpha_2 \\ w_5 &= \alpha_2\alpha_3 + \beta_1\gamma \\ w_6 &= \alpha_1\alpha_4 + \beta_2 \end{aligned}$$

It is straightforward to check that for all choice of parameters, $\Delta = 0$.

The height function for the dimer model was explained in Section (**??**). For the dimer city, we have chosen the first w_1 type vertex as the reference dimer configuration. The height changes are as shown in Figure 3.3.

The characteristic polynomial for the dimer city is computed from dimer configurations satisfying toric boundary conditions. These are the first 6 dimer configurations shown in Figure 3.3, giving:

$$P(z,w) = (\beta_1\beta_2\gamma + \alpha_1\alpha_4\beta_1 + \alpha_2\alpha_3\beta_2) - (\alpha_1\alpha_3)w - (\alpha_2\alpha_4)z^{-1} - \gamma w z^{-1} \qquad (3.6.1)$$

Denote by θ^{dimer} the height function of the dimer model, and by θ^{6v} the height function for the six vertex model. It is clear that:

$$\theta^{\text{dimer}} = \theta^{\text{6v}} + x/2 + y/2$$

It is convenient to choose the following particular weights:

$$\alpha = \sqrt{b} \qquad \beta = \frac{c-b}{a} \qquad \gamma = a$$

Parameterize the six vertex weights as:

$$a = \cos(u) \qquad b = \sin(u) \qquad c = 1$$

The characteristic polynomial, given in (3.6.1) simplifies to:

$$P(z, w) = (wz - 1)\cos(u) + (z + w)\sin(u)$$

Solving $P(z, w) = 0$ for w gives:

$$w = \frac{z\cos u - \sin u}{\cos u + z \sin u}$$

and thus,

$$F(z) = -\frac{z}{(z\cos u + \sin u)(z \sin u - \cos u)}$$

The Surface Tension and Equations of Motion

The formula for the free energy on the torus derived from the Kasteleyn solution is:

$$f(H, V) = \frac{1}{(2\pi i)^2} \int_{|z|=e^V} \int_{|w|=e^H} \log\big((wz - 1)\cos(u) + (z + w)\sin(u)\big) \frac{dz}{z} \frac{dw}{w}$$

It is straightforward to compute the partial derivatives of the free energy:

$$\partial_H f = \frac{1}{\pi} \cos^{-1}\left(\frac{\sinh(V - H)\tan(u) - \sinh(V + H)\cot(u)}{2\cosh(H)}\right)$$
$$\partial_V f = \frac{1}{\pi} \cos^{-1}\left(\frac{\sinh(H - V)\tan(u) - \sinh(V + H)\cot(u)}{2\cosh(V)}\right)$$

This defines the map $\mathbb{R}^2 \to \mathbb{R}^2$, $(H, V) \mapsto (\partial_H f, \partial_V f)$. Partial derivatives of σ define the inverse map $(s, t) \mapsto (\partial_s \sigma, \partial_t \sigma)$. It has the following explicit form:

$$\begin{aligned} \partial_s \sigma(s, t) &= -\sinh^{-1}\left(\frac{\sin(\pi t)\cos(\pi s) - \cos(2u)\cos(\pi t)\sin(\pi s)}{\sin(2u)\sin(\pi s)}\right) \\ \partial_t \sigma(s, t) &= -\sinh^{-1}\left(\frac{\sin(\pi s)\cos(\pi t) - \cos(2u)\cos(\pi s))\sin(\pi t)}{\sin(2u)\sin(\pi t)}\right) \end{aligned} \tag{3.6.2}$$

The Euler-Lagrange equations in the regions where $\partial_x h, \partial_y h \in \left(-\frac{1}{2}, \frac{1}{2}\right)$ are:

$$\begin{aligned} 0 =& \frac{\sin(\pi \partial_y h)}{\sin(\pi \partial_x h)} \, \partial_x^2 h \\ &- 2\left(\cos(\pi \partial_x h)\cos(\pi \partial_y h) + \cos(2u)\sin(\pi \partial_x h)\sin(\pi \partial_y h)\right) \partial_x \partial_y h \\ &+ \frac{\sin(\pi \partial_x h)}{\sin(\pi \partial_y h)} \, \partial_y^2 h \end{aligned} \tag{3.6.3}$$

In the five vertex limit $u \to \pi/2$ (see Section 3.5 for details), we recover the PDE for the limit shape of the hexagonal dimer model (3.5.2). Recall the dimer height function differs from the six vertex height function by a linear term; after shifting $\partial_x h \to \partial_x h - \frac{1}{2}$ and $\partial_y h \to \partial_y h - \frac{1}{2}$, equation (3.6.3) matches with the PDE derived from Bethe ansatz, see [PR], [ZJ].

The Hamiltonian Framework

The Hamiltonian for the free fermionic six vertex model is most easily computed from the Bethe ansatz [PR], [NK]:

$$\mathcal{H} = \frac{1}{2\pi i}\Big(\big(\mathrm{Li}_2(e^l \tan(u)) - \mathrm{Li}_2(-e^l \cot(u))\big) - \big(\mathrm{Li}_2(e^{\bar{l}} \tan(u)) - \mathrm{Li}_2(-e^{\bar{l}} \cot(u))\big)\Big)$$

It is straightforward to check that it satisfies (3.4.9).

We can recover the Hamiltonian (3.5.3) of the hexagonal dimer model by first translating the momentum

$$p \to p + \log(\sin(2u))$$

and then taking the 5-vertex limit $u \to \frac{\pi}{2}$. The translation corresponds to difference of conjugate momenta $p = \partial_t \sigma(s,t)$ of the hexagonal dimer model (3.5.1) and free fermionic six vertex model (3.6.2) in the limit $u \to \frac{\pi}{2}$.

Conclusion

In this paper, we presented infinitely many integrals of motion for the limit shape equations of the 6-vertex model. We conjecture that it defines an integrable system, but this remains to be proven. A proof of integrability would require a transformation to action-angle variables or a Lax pair presentation.

One should notice the analogy between Conformal Field Theory and the free fermionic limit of the six vertex model. In conformal field theory (for example in the Gaussian field theory), the integrals of motion factorize into the sum of holomorphic and antiholomorphic part. When the CFT is perturbed to an integrable QFT [BLZ] , the integrals of motion no longer factorize. We observe the same phenomena in the 6-vertex model. When $\Delta = 0$ the Hamiltonian factorizes into the holomorphic and antiholomorphic part in terms of Burgers variables. But, already terms linear in Δ do not have such structure. This observation goes in line with the discrete holomorphicity of Dimer models (see for example [Sm] and references therein) and suggests that such structure is not fully present in the 6-vertex model, which agrees with [ZJ].

Our results suggest that the equation describing limit shapes in the 6-vertex model (and in Dimer models) is an example of an integrable PDE with gradient constraints. In our proof of Poisson commutativity of the integrals of motion, we assumed that the height function is away from gradient constraints. It is well known that imposing boundary conditions in integrable PDEs destroy the integrability, if the boundary conditions are not of a very special type. It would be interesting to study which sort of gradient constraints in an integrable PDE destroy integrability and which ones preserve it.

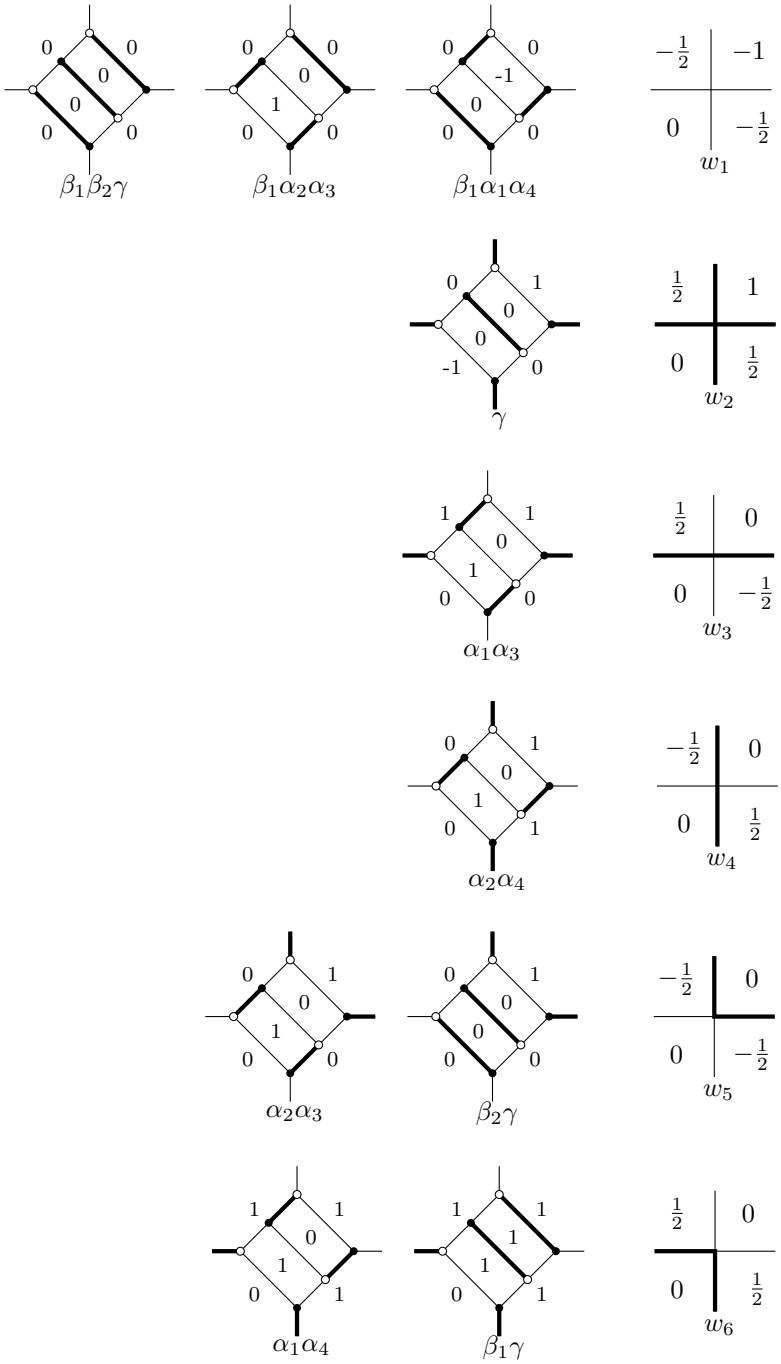

Figure 3.3: The dimer configurations and height changes on the left, and the corresponding six vertex model vertex on the right.

Chapter 4

Semiclassical Limits in Quantum Integrable Systems

The main result of this note is the following theorem in classical mechanics, which gives conditions for the Poisson commutativity of two Hamiltonian functions in terms of their principal action functions. Let M be a configuration space, $L_1, L_2 \in C^\infty(TM)$ be two strictly convex Lagrangian functions, and $S_1, S_2 \in \mathbb{M} \times \mathbb{M} \times \mathbb{R} \to \mathbb{R}$ their corresponding principal action functionals. Let $H_1, H_2 \in C^\infty(T^*M)$ be the corresponding Hamiltonian functions (the Legendre transforms of L_1, L_2 in the cotangent direction) on the phase space T^*M with the canonical Poisson bracket.

Theorem 2. *The Hamiltonian functions Poisson commute, $\{H_1, H_2\} = 0$ if and only if the principal action functions satisfy*

$$\min_q S_1(q_1, q, t_1) + S_2(q, q_2, t_2) = \min_q S_2(q_1, q, t_2) + S_1(q, q_2, t_1) \tag{4.0.1}$$

for all $q_1, q_2 \in M$ and $t_1, t_2 > 0$.

Our interest in this problem arises from studying the presence of integrability in the semiclassical limit of some quantum integrable systems and continuum limits of some solvable lattice models. Let us briefly outline this motivation.

4.1 Integrable Systems

Classical Integrable Systems

Classical integrable systems are most naturally described within the Hamiltonian framework. Here the phase space is a $2n$-dimensional symplectic manifold (N, ω) . The dynamics of the system determined by a Hamiltonian $H \in C^\infty(N)$ and Hamilton's equations for the time evolution of phase space functions (e.g., coordinates of particles):

$$\frac{df}{dt} = \{f, H\}$$

Where the Poisson bracket is given by $\{f, g\} = \omega^{-1}(df, dg)$. A system is *Liouville integrable* if it admits n independent functions $H = I_1, I_2, \cdots, I_n$ all pairwise Poisson commuting, $\{I_i, I_j\} = 0$. The commuting functions can be used to construct action-angle coordinates, in which the Hamiltonian dynamics are trivial.

Quantum Integrable Systems

In a quantum mechanical system, the phase space is replaced by a a Hilbert space of states $\mathscr{H}$, and Hamiltonian by a Hermitian operator $\hat{H} : \mathscr{H} \to \mathscr{H}$ called the quantum Hamiltonian. The time evolution of observables, in the Heisenberg pictures, is given by:

$$\frac{d\hat{O}}{dt} = \frac{i}{\hbar}[\hat{H}, \hat{O}]$$

In analogy to the classical case, a *quantum integrable system* can be characterized by the existence of "many" commuting Hamiltonians. The commuting Hamiltonians, in some sense, underly the solutions by the quantum inverse scattering method and Bethe ansatz [Sk].

The semiclassical limit is found by taking $\hbar \to 0$. It is immediate from the quantization principle

$$[\hat{H}_1, \hat{H}_2] = i\hbar\{H_1, H_2\} + O(\hbar^2)$$

that the commutative quantum Hamiltonians lead in the classical limit to Poisson commutative classical Hamiltonians.

One can derive this in a different way as follows. Take for example the quantum mechanics of a classical particle in $\mathbb{R}$. The kernel $U(q_1, q_2, t)$ of the propagator $e^{i\hat{H}t/\hbar}$ has the WKB asymptotic as $\hbar \to 0$:

$$U(q_1, q_2, t) = \left(2\pi i\hbar \, \frac{\partial^2 S}{\partial q_0 \partial q_1}(q_0, q_1, t)\right)^{-\frac{1}{2}} e^{\frac{i}{\hbar}S(q_1, q_2, t)} \, (1 + O(\hbar)) \tag{4.1.1}$$

where S is the principal action function of the classical system. The semigroup law of the propagator $e^{i\hat{H}t_1/\hbar} \, e^{i\hat{H}t_2/\hbar} = e^{i\hat{H}(t_1+t_2)/\hbar}$ implies for U:

$$U(q_1, q_2, t_1 + t_2) = \int_{\mathbb{R}} U(q_1, q, t_1) \, U(q, q_2, t_2) \, dq$$

The commutativity of Hamiltonians $\hat{H}_1$ and $\hat{H}_2$ gives:

$$\int_{\mathbb{R}} U_1(q_1, q, t_2) \, U_2(q, q_2, t_1) \, dq = \int_{\mathbb{R}} U_2(q_1, q, t_1) \, U_1(q, q_2, t_2) \, dq$$

for the corresponding propagators $e^{i\hat{H}_1 t/\hbar}$ and $e^{i\hat{H}_2 t/\hbar}$.

In the semiclassical limit $\hbar \to 0$, using the asymptotic (4.1.1) and computing the integral over q by the tationary phase approximation, it is seen that the commutativity of the quantum Hamiltonians leads to the relation (4.0.1) for their actions. Theorem 1 then implies that the classical Hamiltonians also commute.

Solvable Lattice Models

A different sort of semiclassical limit can be found in the thermodynamic limit of lattice models. Our prototypical example is a vertex model, for whic configuration is an assignments of states to each edge, and each vertex has an energy depending on the states of its adjacent edges.

Consider a model defined on a cylinder square lattice of size $M \times N$. States of an edge are represented by a Hilbert space V, and the state of one row of is represented by the Hilbert space $\mathfrak{H}_{(M)} = V^{\otimes M}$. The analog of the Hamiltonian is the transfer matrix $T_{(M)} \in \mathrm{End}(\mathfrak{H}_{(M)})$, which generates the evolution states in the vertical direction. For two states $v_1, v_2 \in \mathfrak{H}^{(M)}$, the matrix element $(T^N)_{v_1,v_2}$ gives the partition function of the model with boundary conditions v_1 and v_2 on the top and bottom of the cylinder.

In a *solvable vertex model* the weights can be arranged into R-matrices satisfying Yang-Baxter equations, which implies the commutativity of transfer matrices. In analogy to the classical Liouville integrability, a *lattice integrable model* admits commutative families of transfer matrices.

The "semiclassical" limit is found by taking $N, M \to \infty$,with the aspect ratio $t = N/M$ and weights fixed. In this limit, typically [CKP][**?**][KOS], the macrostate of the systems becomes deterministic and described by a classical field theory, with the thermodynamic fluctuations exponentially suppressed.

The space of semiclassical states $\mathfrak{H}$ is some appropriate limit of $\mathfrak{H}_{(M)}$ as $M \to \infty$. Fixing two such states ν_1 and ν_2, on the top and bottom of the cylinder, the matrix elements of the transfer matrix (ie. the partition functions) have the asymptotic:

$$\lim_{\substack{N,M\to\infty \\ N/M=t}} (T^N)_{v_1 v_2} = e^{-N^2 S(\nu_1,\nu_2,t)} \left(1 + o(1)\right)$$

where S is the principal action functional of the field theory:

$$S(\nu_1, \nu_2, t) = \min_{\substack{\varphi\in\mathfrak{H} \\ \varphi(x,0)=\nu_1(x) \\ \varphi(x,t)=\nu_2(x)}} \int_0^t \int_{S_1} \sigma(\partial_x\varphi, \partial_t\varphi)\, dx\, dt$$

Here the minimization is over the space of continuum fields $S^1 \times [0, T] \to \mathbb{R}^k$ (typically satisfying gradient constraints, which we ignore here for simplicity). The function σ is the surface tension function [CKP] or the free energy with fixed magnetization [PR]. When σ is strictly convex the variational problem has a unique minimizer φ^*, which gives the deterministic state of the system.

The commutativity of transfer matrices T_1 and T_2, as in the quantum integrable case, lead to the relation (4.0.1) for the corresponding functions S_1 and S_2. Theorem 1 then implies that after the Lagrangian field theory is reformulated as a Hamiltonian field theory, the corresponding Hamiltonians H_1 and H_2 Poisson commute.

4.2 Commuting Actions and Hamiltonians

We first review some standard concepts of classical mechanics to fix notation and definitions. Let M, a smooth real manifold, be the configuration space.

Lagrangian Mechanics

Let $L : TM \to \mathbb{R}$, $(\xi, q) \mapsto L(\xi, q), \xi \in T_qM$ be the Lagrangian function. The action functional of a path $\gamma : [t_1, t_2] \to M$, $t \mapsto q(t)$ is

$$\mathcal{S}[\gamma] = \int_{t_1}^{t_2} L\left(\dot{q}(t), q(t)\right) dt \tag{4.2.1}$$

where $\dot{q}(t) = \frac{dq}{dt}(t) \in T_{q(t)}M$.

The classical trajectories of the system are determined by the principle of least action. The trajectory starting at $q_1 \in M$ at time t_1 and arriving at $q_2 \in M$ at t_2 is the minimizer of

$$S(q_1, q_2, t_1, t_2) = \min\left\{\mathcal{S}[\gamma] \;\middle|\; \gamma : [t_1, t_2] \to M, \;\; q(t_1) = q_1, \;\; q(t_2) = q_2\right\} \tag{4.2.2}$$

The function S is called Hamilton's principle function, or simply the action function.

We will assume that there is a unique minimum of the action functional for every boundary conditions $(q_1, t_1), (q_2, t_2)$. The solutions satisfy the Euler-Lagrange equations, which in local coordinates:

$$\frac{d}{dt}\frac{\partial L}{\partial \dot{q}}(q(t), \dot{q}(t)) - \frac{\partial L}{\partial q}(q(t), \dot{q}(t)) = 0$$

Hamiltonian Mechanics

The Hamiltonian function $H : T^*M \to \mathbb{R}$ of L is by definition its Legendre transform, in local coordinates:

$$H(p, q) = \min_{\xi \in T_qM}\Big(p \cdot \xi - L(\xi, q)\Big) \tag{4.2.3}$$

The Legendre transform is well defined if $L(q, \cdot)$ is strictly convex in each tangent fiber.

In the Hamiltonian framework, the action functional of a path $\Gamma : [t_1, t_2] \to T^*M$, in local coordinates, with $(p(t), q(t)) = \Gamma(t)$:

$$\mathcal{S}[\Gamma] = \int_{t_1}^{t_2} p(t) \cdot \frac{dq}{dt}(t) - H\left(p(t), q(t)\right) \; dt$$

The classical trajectories are symplectic flow lines of H, in local coordinates $(p(t), q(t))$ of $\Gamma(t)$ satisfy:

$$\frac{dp}{dt} = \{H, p\} \qquad \frac{dq}{dt} = \{H, q\}$$

where the canonical Poisson bracket is:

$$\{f, g\} = \frac{\partial f}{\partial p} \cdot \frac{\partial g}{\partial q} - \frac{\partial g}{\partial p} \cdot \frac{\partial f}{\partial q}$$

for $f, g \in C^\infty(T^*M)$.

The Legendre transform (4.2.3) gives a diffeomorphism of bundles $\varphi : T^*M \to TM$, where $\varphi(p)$ is the critical value of $\dot{q}$ minimizing (4.2.3). The lift $\varphi^{-1}(d\gamma/dt)$ of a path $\gamma : [t_1, t_2] \to M, t \mapsto (p(t), q(t))$ is the conjugate momentum of γ.

The Hamiltonian and Lagrangian frameworks are equivalent in the sense that classical trajectories of the Lagrangian lift to trajectories of the Hamiltonian via φ, and classical trajectories of the Hamiltonian project via $\pi : T^*M \to M$ to trajectories of the Lagrangian .

Let us regard the action (4.2.2) as a function $S : M \times M \times \mathbb{R} \times \mathbb{R} \to \mathbb{R}$. The Hamilton-Jacobi equation states:

$$dS(q_1, q_2, t_1, t_2) = p(t_2) \cdot dq_2 - p(t_1) \cdot dq_1 - H(p(t_1), q(t_2))\ (dt_2 - dt_1) \tag{4.2.4}$$

where p is the conjugate momentum of the critical trajectory γ for the boundary conditions (q_1, t_1), (q_2, t_2); and $H(p(t_1), q(t_1)) = H(p(t_2), q(t_2))$ is constant along the trajectory.

Glued Actions

Let $L, \widetilde{L} : TM \to \mathbb{R}$ be two Lagrangian functions, and $S, \widetilde{S}$ and $H, \widetilde{H}$ the corresponding action functions and Hamiltonian functions.

For $t, \widetilde{t} > 0$, consider the "glued" action functional of paths $\gamma : [-t, \widetilde{t}] \to M$:

$$\mathcal{S}[\gamma] = \int_{-t}^{0} L\left(\frac{d\gamma}{dt'}\right) dt' + \int_{0}^{\widetilde{t}} \widetilde{L}\left(\frac{d\gamma}{dt'}\right) dt'$$

It is clear that minimizing trajectories $\gamma(t')$ of this action functional satisfy Euler-Lagrange equations of L for $t' < 0$, and Euler-Lagrange equations of $\widetilde{L}$ for $t' > 0$. Thus, minimizing $\mathcal{S}[\gamma]$ with fixed boundary conditions q_1, q_2 reduces to minimizing with respect to the intermediate point $\gamma(0)$. This motivates:

Definition 1. *For $q_1, q_2 \in M$ and $t, \widetilde{t} > 0$:*

$$S_g\left(q_1, q_2, t, \widetilde{t};\ S, \widetilde{S}\right) = \min_{q \in M}\left(S\left(q_1, q, -t, 0\right) + \widetilde{S}\left(q, q_2, 0, \widetilde{t}\right)\right) \tag{4.2.5}$$

It is clear that although the minimizing trajectory is continuous, it may not be differentiable at $t' = 0$. However:

Lemma 6. *The conjugate momentum is continuous along the critical trajectory.*

Proof. Using the Hamilton-Jacobi equation (4.2.4) to differentiate with respect to q gives:

$$d_q\left(S(q_1,q,-t,0)+\widetilde{S}(q,q_2,0,\widetilde{t})\right)=\left(p^{(L)}(0)-p^{(\widetilde{L})}(0)\right)dq$$

Here we have written subscripts $p^{(L)}$ and $p^{(\widetilde{L})}$ to emphasize that the momentum is taken with respect to the Legendre transforms of L or $\widetilde{L}$.
Minimizing with respect to q implies that $p^{(L)}(0)=p^{(\widetilde{L})}(0)$. □

In other words, minimizing with respect to $q=\gamma(0)$ is equivalent to demanding equality of conjugate momenta of $\gamma(t'=0)$ at $t'=0$. As a consequence:

Lemma 7. *Viewing S_g as a function $M\times M\times\mathbb{R}\times\mathbb{R}\to\mathbb{R}$:*

$$\begin{aligned}dS_g(q_1,q_2,t,\widetilde{t})=&\left(p(\widetilde{t})\,dq_2-p(-t)\,dq_1\right)\\&-\left(\widetilde{H}(p(\widetilde{t}),q(\widetilde{t}))\,d\widetilde{t}+H(p(-t),q(-t))\,dt\right)\end{aligned}\tag{4.2.6}$$

Proof. Let q^* be the critical value of q minimizing (4.2.5) and p^* be the conjugate momentum at that $t'=0$. Then:

$$S_g(q_1,q_2,t,\widetilde{t})=S\left(q_1,q^*,-t,0\right)+\widetilde{S}\left(q^*,q_2,0,\widetilde{t}\right)\tag{4.2.7}$$

Since q^* depends on q_1,q_2,t and $\widetilde{t}$, differentiating with respect to any of these involves applying the chain rule. However since $p^*=\partial S/\partial q^*=-\partial S/\partial q^*$, these terms all vanish. The remaining terms follow from the Hamilton-Jacobi equation (4.2.4). □

Commuting Actions

Definition 2. *We say that two actions S and $\widetilde{S}$ commute if for all $q_1,q_2\in M$ and $t,\widetilde{t}>0$:*

$$S_g(q_1,q_2,t,\widetilde{t};S,\widetilde{S})=S_g(q_1,q_2,\widetilde{t},t;\widetilde{S},S)\tag{4.2.8}$$

or more explicitly:

$$\min_{q\in M}\left(S\left(q_1,q,-t,0\right)+\widetilde{S}\left(q,q_2,0,\widetilde{t}\right)\right)=\min_{q'\in M}\left(\widetilde{S}\left(q_1,q',-\widetilde{t},0\right)+S\left(q',q_2,0,t\right)\right)\tag{4.2.9}$$

Lemma 8. *Fix $q_1,q_2\in M$ and $t,\widetilde{t}>0$, and let $\gamma=(p(t),q(t))$ and $\gamma'=(p'(t),q'(t))$ be the paths minimizing the left and right side of (4.2.9) respectively. Then,*

$$\begin{aligned}p(-t)&=p'(-\widetilde{t})\\p(t)&=p'(\widetilde{t})\end{aligned}\tag{4.2.10}$$

In other words, γ and γ' start and end at the same points in phase space.

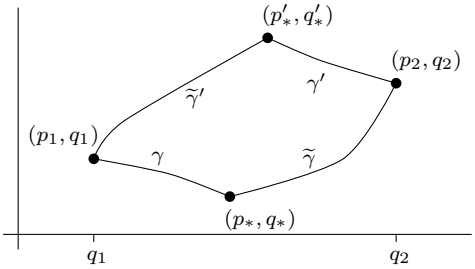

Figure 4.1

The situation is summarized in the figure below. We have let $p_1 = p(-t)$, $p_2 = p(t)$, $(p_*, q_*) = \gamma(0)$ and $(p'_*, q'_*) = \gamma'(0)$. We labeled the segment of $\gamma(t')$ with $t' < 0$ by γ and with $t' > 0$ by $\widetilde{\gamma}$ (and vice versa for γ'). The segments γ, γ' are flow lines of H; and γ'_1, γ_2 flow lines of $\widetilde{H}$.

Proof. Using equation (4.2.6) to differentiate both sides of equation (4.2.8) with respect to q_1 and q_2:

$$\big(p(\widetilde{t})\ dq_2 - p(-t)\ dq_1\big) = \big(p'(t)\ dq_2 - p'(-\widetilde{t})\ dq_1\big)$$

Equating the components gives (4.2.10). □

Lemma 9.

$$\begin{aligned} H(p'_*, q'_*) = H(p_*, q_*) = H(p_1, p_2) = H(p_2, p_2) \\ \widetilde{H}(p'_*, q'_*) = \widetilde{H}(p_*, q_*) = \widetilde{H}(p_1, p_2) = \widetilde{H}(p_2, p_2) \end{aligned} \tag{4.2.11}$$

Proof. Using equation (4.2.6) to differentiate both sides of equation (4.2.8) with respect to t and $\widetilde{t}$ gives:

$$\widetilde{H}(p(\widetilde{t}), q(\widetilde{t}))\ d\widetilde{t} + H(p(-t), q(-t))\ dt = H(p'(-t), q'(-t))\ dt + \widetilde{H}(p'(\widetilde{t}), q'(\widetilde{t}))\ d\widetilde{t}$$

Which can be rewritten more simply as:

$$\widetilde{H}(p_2, q_2)\ d\widetilde{t} + H(p_1, q_1)\ dt = H(p_2, q_2)\ dt + \widetilde{H}(p_1, p_1)\ d\widetilde{t}$$

Equating components gives:

$$\begin{aligned} H(p_1, q_1) &= H(p_2, q_2) \\ \widetilde{H}(p_1, q_1) &= \widetilde{H}(p_2, q_2) \end{aligned}$$

Using the fact that H is conserved along its flow lines γ and γ', and similarly for $\widetilde{H}$ along $\widetilde{\gamma}, \widetilde{\gamma}'$ gives the other equalities in (4.2.11). □

Corollary 5.

$$\{H, \widetilde{H}\} = 0$$

Proof. We show that $\widetilde{H}$ is constant on flow lines of H. Let γ be a flow line of time t starting fro (p_1, q_1). We choose an arbitrary $\widetilde{t}$ and let (p_2, q_2) be given by flowing (p_1, q_1) by H to for time t, and then $\widetilde{H}$ by time $\widetilde{t}$. We can consider the variational problem with the mixed action in the opposite order, which produces a diagram such as (4.1). From (4.2.11), we have $\widetilde{H}(p_1, p_2) = \widetilde{H}(p_*, q_*)$, i.e. $\widetilde{H}$ is equal at the end points of the flow line γ of H. □

Chapter 5

Limit Shapes in the Stochastic Six Vertex Model

This chapter studies the limit shapes of the stochastic six vertex model on the cylinder. It is based on the paper [RS16].

The outline of the chapter is as follows: In the first section, we describe the stochastic weights for the six vertex model, and prove that the transfer matrix with stochastic weights can be normalized to a stochastic matrix. We described the discrete time Markov process associated by the stochastic transfer matrix. This is a natural generalization of ASEP, and how ASEP is obtained as limit of the stochastic six vertex model. In the second section, we describe the variational problem for the limit shape of the Markov process. We take a detour to describe some important properties of the surface tension function at the stochastic point, and then derive the PDEs for the limit shape. In the ASEP limit of the 6-vertex model, we recover the inviscid Burgers equation as computed by [BF] [Rez][GS]. In the last section we give some solutions for the step boundary conditions on the other end of the cylinder, using the method of characteristics. We recover as a special case the limit shape found in [BCG] in the limit when the circumference of the cylinder goes to infinity.

5.1 The Stochastic Six Vertex Model

We focus on the six vertex model defined on the cylinder $\mathcal{C}_{MN}$. Recall that a configuration of the 6-vertex model on the cylinder can be seen as a set of paths of particles that do not cross. Given a six vertex configuration S, we will denote by S_i the configuration (subset) on the ith row of vertical edges; in other words, the configuration of the particles at "discrete time" i. Recall the space $\mathscr{H}_M$ of row configurations decomposes as:

$$\mathscr{H}_M = \oplus_{k=0}^{M} \mathscr{H}_M^{(k)}$$

where $\mathscr{H}_M^{(k)}$ is the subspace spanned by row configurations η with k edges.

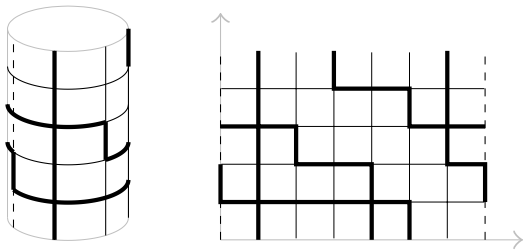

Figure 5.1: A six vertex configuration on a cylindrical graph.

The Weights

The stochastic weights of the six vertex model are parametrized by $b_1, b_2 \in (0,1)$ as:

$$a_1 = 1 \qquad a_2 = 1 \qquad c_1 = 1 - b_1 \qquad c_2 = 1 - b_2 \tag{5.1.1}$$

These values of Boltzmann weights are possible only if $\Delta = (a^2+b^2-c^2)/2ab > 1$, i.e. the region where in Baxter's parametrization $u, \eta > 0$. In terms of this parametrization for the stochastic point we have:

$$a_1 = a_2 = 1, \quad b_1 = \frac{\sinh(u)e^{\pm\eta}}{\sinh(u+\eta)}, \quad b_2 = \frac{\sinh(u)e^{\mp\eta}}{\sinh(u+\eta)}$$

$$c_1 = \frac{\sinh(\eta)e^{\mp u}}{\sinh(u+\eta)}, \quad c_2 = \frac{\sinh(\eta)e^{\pm u}}{\sinh(u+\eta)}$$

For these values of weights $H = -V = \pm\eta/2$ and $\lambda = e^{\mp u}$.

From now on we will assume $b_2 < b_1$ which correspond to $H = \eta > 0$ and will call it the stochastic point. The other sign can be obtained by the reflection which exchanges the edges occupied by paths to empty edges. Note that the transfer matrices on the stochastic line form a commutative family.

The Transfer Matrix

Recall the matrix elements of the transfer matrix $T_M : \mathscr{H}_M \to \mathscr{H}_M$ are the partition functions

$$Z_{MN}(\alpha, \beta) = \langle \alpha, (T_M)^N \beta \rangle$$

with boundary conditions b_1 and b_2. Here we study the partition function with "free" boundary conditions, in other words, summing over all final states β:

Lemma 10. *With the stochastic weights (5.1.7) and fixed state $\alpha \in \mathscr{H}^{(m)}$:*

$$\sum_{\beta \in \mathcal{S}} \langle \beta, T_M \alpha \rangle = 1 + b_1^{M-m} b_2^m$$

Proof. For a boundary configuration α, we will write α_i for the position of the ith particle for $i = 1, \cdots, m$, with the convention that $\alpha_{m+1} = \alpha_1 + M$. For two states α and β, we associate the 6-vertex configuration (α, β) with the ith particle going from α_i to β_i. The ice rule implies that a valid configuration (α, β) must satisfy $\alpha_i \leq \beta_i \leq \alpha_{i+1}$, and $\beta_i \neq \beta_{i+1}$ for all i.

Let us define the weight of a particle's path as:

$$w(\alpha_i, \beta_i) = \begin{cases} b_2 & \text{if } \alpha_i = \beta_i \\ c_1 c_2 \, b_1^{\beta_i - \alpha_i - 1} & \text{if } \beta_i < \alpha_{i+1} \\ b_1^{\beta_i - \alpha_i - 1} & \text{if } \beta_i = \alpha_{i+1} \end{cases} \tag{5.1.2}$$

(Only the third case isn't immediately obvious from 6-vertex weights.) It is straightforward to check that the weight of any valid configuration (α, β) is the product of path weights:

$$W(\alpha, \beta) = \prod_{i=1}^{m} w(\alpha_i, \beta_i)$$

We will compute the sum over all configurations by summing each β_i from α_i to α_{i+1}, and afterward subtracting the overcounted terms corresponding to invalid configurations (when $\beta_i = \beta_{i+1}$ for some i).

Example of two Particles: The sum is easily computed by geometric series:

$$\begin{aligned} \sum_{\beta_i = \alpha_i}^{\alpha_{i+1}} w(\alpha_i, \beta_i) &= b_2 + \sum_{\beta_i = \alpha_i + 1}^{\alpha_{i+1} - 1} c_1 c_2 \, b_1^{\beta_i - \alpha_i - 1} + b_1^{\alpha_{i+1} - \alpha_i - 1} \\ &= b_2 + c_1 c_2 \frac{(1 - b_1)^{\alpha_{i+1} - \alpha_i - 1}}{1 - b_1} + b_1^{\alpha_{i+1} - \alpha_i - 1} \\ &= b_2 + (1 - b_2)(1 - b_1)^{\alpha_{i+1} - \alpha_i - 1} + b_1^{\alpha_{i+1} - \alpha_i - 1} \\ &= 1 + b_1 b_2^{\alpha_{i+1} - \alpha_i - 1} \end{aligned}$$

Here we used $c_1 = 1 - b_1$ and $c_2 = 1 - b_2$. So we have:

$$\begin{aligned} &= (1 + b_1 b_2^{\alpha_2 - \alpha_1 - 1})(1 + b_1 b_2^{\alpha_1 + M - \alpha_2 - 1}) \\ &= 1 + b_1 b_2^{\alpha_2 - \alpha_1 - 1} + b_1 b_2^{\alpha_1 + M - \alpha_2 - 1} + b_1^2 b_2^{M-2} \end{aligned}$$

The middle terms are precisely the weights assigned to the overlap states, $w(\alpha_1, \alpha_2) w(\alpha_2, \alpha_2)$ and $w(\alpha_1, \alpha_1) w(\alpha_2, \alpha_1 + M)$. Subtracting these gives:

$$\sum_{\beta} W(\alpha, \beta) = (1 + b_1 b_2^{M-1})$$

General case: We can compute in the same way as above that:

$$\prod_{i=1}^{m} \sum_{\beta_i = \alpha_i}^{\alpha_{i+1}} w(\alpha_i, \beta_i) = (1 + b_1 b_2^{\alpha_2 - \alpha_1 - 1})(1 + b_1 b_2^{\alpha_3 - \alpha_2 - 1}) \cdots (1 + b_1 b_2^{\alpha_1 + M - \alpha_n - 1}) \tag{5.1.3}$$

We can organize the subtraction of invalid configurations as follows. Writing (5.1.3) as

$$(A_1 + B_1)(A_2 + B_2) \cdots (A_m + B_m)$$

and expanding, a term in the expansion containing $A_i B_{i+1}$ for any i represents sums of weights of states with the ith particle and $(i+1)$th particle overlapping, and invalid case. It follows that what remains is $A_1 \cdots A_m + B_1 \cdots B_m$. We then have:

$$\begin{aligned} A_1 \cdots A_m + B_1 \cdots B_m &= 1 + (b_1 b_2^{\alpha_2 - \alpha_1 - 1})(b_1 b_2^{\alpha_3 - \alpha_2 - 1}) \cdots (b_2^{\alpha_1 + M - \alpha_m - 1}) \\ &= 1 + b_1^n b_2^{M-m} \end{aligned}$$

□

The Markov Process

There is a natural discrete time stochastic process associated with the 6-vertex model, defined as follow. The state space $\mathcal{S}_M^{(m)}$ of the process consist configurations of one row, see Figure 5.2. The stochastic process $\{X_t \mid t \in \mathbb{N}\}$ is then defined by the conditional probabilities:

$$\mathbb{P}[X_t = s' \mid X_0 = s] = Z_{Mt}^{(m)}(s', s)/\mathcal{Z}_{Mt}[s] \tag{5.1.4}$$

$$\mathcal{Z}_t^{(m)}[s] = \sum_{s'' \in \mathcal{S}} Z_{Mt}^{(m)}(s'', s) \tag{5.1.5}$$

Remark 4. *The normalizing factor $\mathcal{Z}$ is proportional to the partition function with Dirichlet boundary conditions on one end of the cylinder and the uniform distribution on the other.*



Figure 5.2: A state of the Markov process

Recall that a discrete time stochastic process over a finite state space is *Markov* if it satisfies

$$\mathbb{P}[X_n = s_n \mid X_{n-1} = s_{n-1}, \cdots, X_0 = s_0] = \mathbb{P}[X_1 = s_n \mid X_0 = s_{n-1}]$$

This means a Markov process is completely defined by "one step" transition probabilities $\mathbb{P}[X_1 = x' \mid X_0 = x] = P_{x'x}$, which satisfy:

$$\begin{aligned} P_{x'x} &\geq 0 && \text{(positivity)} \\ \sum_{x'} P_{x'x} &= 1 && \text{(total probability)} \end{aligned} \tag{5.1.6}$$

The total probability rule can be restated by saying that uniform vector $\mathbb{1}$ is a co-eigenvector (left eigenvector) of P with eigenvalue 1. In other words, a transition matrix defines a Markov if it has nonnegative entries and the uniform distribution is a co-eigenvector of the matrix with the eigenvalue 1.

Proposition 3. *With weights:*

$$a_1 = 1 \quad a_2 = 1 \quad c_1 = 1 - b_1 \quad c_2 = 1 - b_2 \tag{5.1.7}$$

for $b_1, b_2 \in [0, 1]$*, the process defined by (5.1.4) is Markov.*

Proof. Using lemma (10) from Appendix (5.1), we have for $\mathcal{Z}$ as defined in (5.1.5):

$$\mathcal{Z}_1^{(m)}(s) = (1 + b_1^m \, b_2^{M-m})$$

Note in particular that $\mathcal{Z}_1^{(m)}(s)$ is independent of s. It is clear from the definition (5.1.4) that the transition matrix for the process is the normalized transfer matrix

$$P^{(m)} = \frac{1}{1 + b_1^m b_2^{M-m}} T_M^{(m)}$$

which satisfies the Markov conditions (5.1.6). □

In other words, the Markov process with $X_0 = s$ can be sampled by sampling the Gibbs measure with fixed boundary conditions s at the bottom and free boundary conditions at the top, and letting X_i be the ith row configuration.

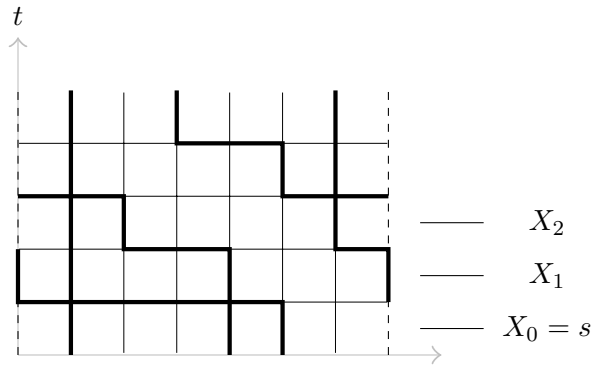

Figure 5.3: The Markov process

The Markov property of the transfer matrix, together with the *uniform boundary condition at the upper end* and fixed boundary condition η at the lower end implies that

- $\mathcal{Z}_{MN}[\eta] = 1$ for any boundary state η.
- The correlation functions of the 6-vertex model:

  $$\mathbb{E}_{MN}\Big[\varphi(x_1, y_1)\varphi(x_2, y_2) \cdots \varphi(x_k, y_k)\Big]$$

  are equal for all $N \geq \max_i y$.

In the thermodynamic limit, the limit shape phenomenon in this case states that the random variable $\varphi(x, y)$ on the cylinder C_{LT} converges in probability to a limit shape $\varphi_0(x, y)$. As a consequence the correlation function written above is expected to converge to

$$\varphi_0(x_1, y_1) \cdots \varphi_0(x_k, y_k)$$

where φ_0 is the solution to the variational problem that we will describe in the next section.

The limit shape $\varphi_0(x, y)$ with this boundary condition is the most probable height function in the bulk and also the most probable boundary height function at the top boundary. The limit shape phenomenon means that random height functions concentrate around φ_0. The limit shape φ_0 is completely determined by the boundary conditions at the lower end of the cylinder. This suggests that it should be determined by a first order PDE (which we will derive in the next section) and that φ_0 is the restriction of a solution to this PDE defined for the half infinite cylinder $[0, L] \times \mathbb{R}^+ \to \mathbb{R}$ to $[0, L] \times [0, T]$.

The ASEP Limit

Here we will show that transition probabilities of the *asymmetric exclusion process* (ASEP) can be obtained from the commuting family of stochastic 6-vertex transfer matrices in a natural limit near the point $u = 0$.

The Asymmetric Exclusion Process on a Ring

Recall that a continuous time Markov process $X(t)$ over a finite state space is defined by a transition matrix W as $dp_i/dt = \sum_{j=1}^{M} W_{ij} p_j$, where $p_i(t) = \mathbb{P}[X(t) = i], i = 1, \cdots, M$ is the probability that system is in the ith state at time t. The transition matrix satisfies:

$$\begin{aligned} W_{ij} > 0 \ \text{ for } i \neq j \qquad & \text{(positivity)} \\ \sum_{j=1}^{M} W_{ij} = 0 \qquad & \text{(total probability)} \end{aligned} \tag{5.1.8}$$

The finite time transition probabilities $P_{ij}(t) = \mathbb{P}[X(t) = i \mid X(0) = j]$ are determined by the differential equation:

$$\begin{aligned} \frac{d}{dt} P_{ij}(t) &= \sum_{k=1}^{M} W_{ik} P_{kj}(t) \\ P_{ij}(0) &= \delta_{i,j} \end{aligned}$$

For any fixed $t > 0$, they satisfy (5.1.6) and define Markov transition probablilities. Note that such process is invariant with respect to transformations $t \mapsto t\lambda^{-1}$, $W_{ij} \mapsto W_{ij}\lambda$ for positive λ. Thus only projective values of W_{ij} are important.

The ASEP is a continuous time stochastic process describing an interacting particle system. The states of the process are configurations of particles on the ring $\mathbb{Z}/M\mathbb{Z}$ with

at most one particle at each lattice site. Each particle waits an exponentially distributed random time, then chooses the adjacent lattice site to the left with probability p, or the right with probability $1-p$. If the chosen site is empty, the particle jumps over; otherwise it remains at the same site.

The transition matrix for ASEP can be written as:

$$W_{ASEP} = \sum_{i}^{M} H_{i,i+1}(p,q)$$

where

$$H(p,q) = \begin{pmatrix} 0 & 0 & 0 & 0 \\ 0 & q & -p & 0 \\ 0 & -q & p & 0 \\ 0 & 0 & 0 & 0 \end{pmatrix}$$

$H_{i,j}(p,q)$ acts as H on the ith and jth components of the tensor product $(\mathbb{C}^2)^{\otimes M}$, and $H_{M,M+1}$ is defined to be $H_{M,1}$ (periodic boundary conditions).

The Relation Between ASEP and the Stochastic 6-vertex Model

The following is a well known relation between the 6-vertex model and the Heisenberg spin chain.

Proposition 4. *The matrix of transition probabilities for the ASEP model is related to the transfer matrix of the stochastic 6-vertex models as follows:*

$$W = \sum_{i=1}^{M} H_{i,i+1}(p,q) = T'_M(0,H,V)T_M(0,H,V)^{-1} - coth(\eta)I$$

where $p = \frac{e^{\eta}}{\sinh(\eta)}$, $q = \frac{e^{-\eta}}{\sinh(\eta)}$. *Note that after rescaling this covers all possible values* $0 < q < p < 1$. *Here* $T'(u,H,V) = \frac{d}{du}T(u,H,V)$.

Proof. First note that as $u \to 0$ we have

$$R(u) = \sinh(\eta)P(1 + u\tilde{H} + O(u^2))$$

where P is the permutation operator, $Px \otimes y = y \otimes x$ and

$$\tilde{H} = \begin{pmatrix} \coth(\eta) & 0 & 0 & 0 \\ 0 & 0 & \operatorname{csch}(\eta) & 0 \\ 0 & \operatorname{csch}(\eta) & 0 & 0 \\ 0 & 0 & 0 & \coth(\eta) \end{pmatrix}$$

From here

$$T_M(0,H,V) = \sinh(\eta)^M (D_1^{2H+2V} \cdots D_M^{H+V})C$$

where C is the cyclic permutation

$$C(x_1 \otimes \cdots \otimes x_M) = x_2 \otimes \cdots \otimes x_N \otimes x_1 \tag{5.1.9}$$

and D^H is the same diagonal matrix as before. For the derivative in u at $u = 0$ we have:

$$T'_M(0, H, V) = \sinh(\eta)^M (D_1^{2H+2V} \cdots D_M^{H+V}) C \sum_{i=1}^{M} U_{i,i+1}$$

where

$$U_{a,b} = D_b^{-H} \tilde{H}_{ba} D_b^H$$

This operator can be written as

$$U = \coth(\eta) I + \sinh(\eta)(I \otimes A - A \otimes I) + H(p, q)$$

where

$$p = \frac{e^{\eta}}{\sinh(\eta)}, \quad q = \frac{e^{-\eta}}{\sinh(\eta)}, \quad A = \begin{pmatrix} 0 & 0 \\ 0 & 1 \end{pmatrix}$$

Taking into account that $\sum_{i=1}^{M}(A_i - A_{i+1}) = 0$ we arrive to

$$W = T'_M(0, H, V) T_M(0, H, V)^{-1} - \coth(\eta)\ I$$

□

ASEP Height Functions and the Thermodynamical Limit

To an ASEP state S, we associate a continuous real valued function on $\mathbb{R}$ as follows. The function h_S is linear on each interval $[i - 1/2, i + 1/2]$ for $i \in \mathbb{N}$, with slope 1 if the ith lattice site is occupied by a particle, and slope -1 otherwise.

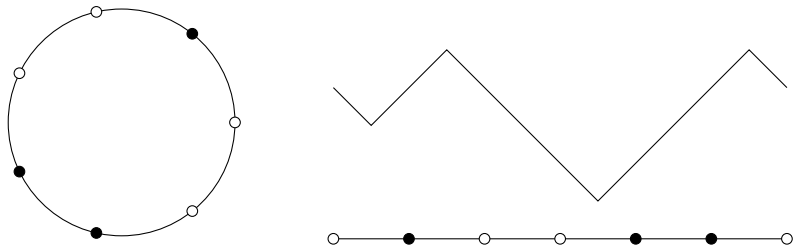

Figure 5.4: An ASEP state and the height function.

As in the stochastic 6-vertex model one can introduce the normalized ASEP height function on $[0, M]$ as $\phi(x) = \epsilon h(\lfloor x/\epsilon \rfloor)$, where the mesh $\epsilon = L/M$. The limit shape phenomenon for the normalized height function of the ASEP model means that as $\epsilon \to 0$, the normalized random height function $\phi(x, t) = \epsilon h(\lfloor x/\epsilon \rfloor, t)$ converges in probability to a deterministic function $\phi_0(x, t)$. In particular, we have:

$$\lim_{\epsilon \to 0} \mathbb{E}_{\lfloor \frac{N}{\epsilon} \rfloor} (\phi(x_1, t_1)\phi(x_2, t_2) \cdots \phi(x_k, t_k)) = \phi_0(x_1, t_1) \cdots \phi_0(x_k, t_k)$$

The function $\phi_0(x,t)$ is called the limit shape. It is been known the limit shape is the solution to the inviscid Burgers equation [BF] [Rez]. We will see that this also can be obtained as a limit of the limit shape equation for the stochastic 6-vertex model.

5.2 Limit Shapes in the Stochastic 6-vertex model

In this section we will study limit shapes for the stochastic 6-vertex model with the uniform distribution at the upper end ($y = T$) and Dirichlet boundary conditions on the the lower end ($y = 0$). The main result of this section is the partial differential equations for the limit shape of the stochastic 6-vertex model.

The Variational Problem

Consider the variation of the action functional with free boundary condition at the upper end of the cylinder and Dirichlet boundary condition at the lower end. In what follows $H_0 = -V_0 = \eta/2$.

$$\delta S[\varphi] = \int_0^L \int_0^T \Big(\partial_1\sigma(\varphi_x,\varphi_y)\delta\varphi_x + \partial_2\sigma(\varphi_x,\varphi_y)\delta\varphi_y + \ V_0\ \delta\varphi_x + \ H_0\ \delta\varphi_y\Big)\ dx\ dy \tag{5.2.1}$$

$$= -\int_0^L \int_0^T \Big(\partial_x\sigma_1(\varphi_x,\varphi_y) + \partial_y\sigma_2(\varphi_x,\varphi_y)\Big)\ \delta\varphi\ dx\ dy - \int_0^L \big(\sigma_2(\varphi_x,\varphi_y) - \ H_0\big)\ \delta\varphi\ dx \tag{5.2.2}$$

Here we assumed that $\varphi(x,0) = \chi(x)$ and therefore $\delta\phi(x,0) = 0$. When $\nabla\varphi$ does not hit a singularity of $\sigma(s,t)$ the first term gives the Euler-Lagrange equation:

$$\partial_x\sigma_1(\varphi_x,\varphi_y) + \partial_y\sigma_2(\varphi_x,\varphi_y) = 0 \tag{5.2.3}$$

The second term gives boundary constraint at $y = T$:

$$\sigma_2\big(\varphi_x(x,T),\varphi_y(x,T)\big) - H_0 = 0$$

The Surface Tension Function for $\Delta > 1$

The free energy and surface tension of the 6-vertex model in the $\Delta > 1$ regime was studied in detail in [BS] [No]. We summarize briefly the computations and relevant results.

For the critical value of magnetic field $H_0 = \pm\eta/2 = \pm\cosh^{-1}(\Delta)/2$ and any magnetization (slope), the roots of the Bethe ansatz equation lie on a closed contour in the complex plane and can be solved exactly by Fourier transform. Near the critical value of H_0, the Bethe ansatz equations can be solved perturbatively to yield the perturbative expansions for the free energy f and the surface tension σ.

In the phase diagram of the free energy f, the exact solutions correspond to the conical singularities of $f(H, V)$, at $(H_0, V_0) = (\pm\eta/2, \mp\eta/2)$ (see Figure (5.5a)). In the surface tension σ, the conical points correspond to critical lines (see Figure (5.5b)); each direction of approach to the conical point maps (by Legendre transform) to a slope (s, t) on the critical line. The critical lines in σ are given by the equation:

$$s = \frac{t \pm \tanh(u + \eta)}{1 \pm \tanh(u + \eta)t} \tag{5.2.4}$$

Near the critical line, the partial derivatives of the σ can be computed using the perturbative expressions given in [BS]. A long but straightforward calculation, which we omit, yields:

Lemma 11. *For slopes (s, t) on the critical lines (5.2.4):*

$$\sigma_{11}(s, t)\sigma_{22}(s, t) - \sigma_{12}(s, t)^2 = 0$$

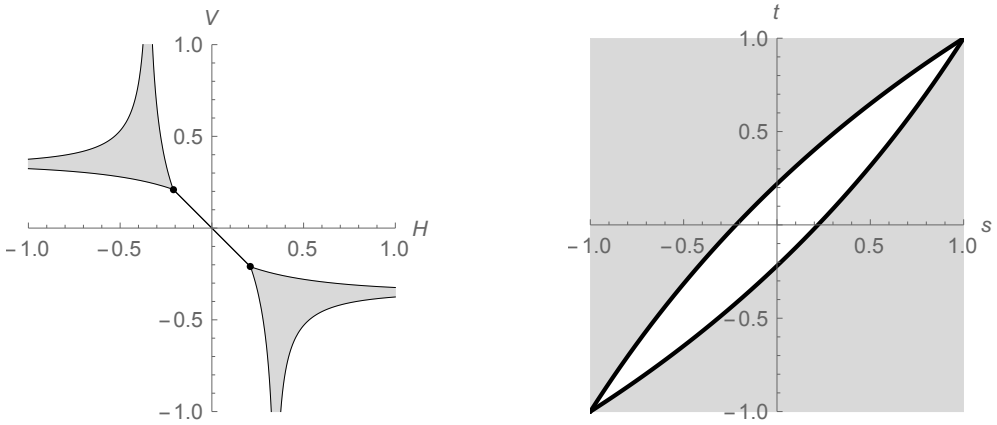

(a) (b)

Figure 5.5: (A) The phase diagram in the (H, V) plane. The shaded regions correspond to the liquid phase; the white regions are frozen. The dots are the location of the conical singularities in f. (B) The phase diagram in the (s, t) plane. The shaded regions correspond to the liquid phase. The bold lines correspond to the conical points. There are no pure states with slopes between these critical lines.

Degeneration to a Parabolic PDE

A crucial property of the function σ described in Appendix 5.2 is:

Lemma 12. *The Hessian of σ*[1] *when $\Delta > 1$ is vanishing on the curve $\sigma_2(s, t) = \pm H_0$.*

[1] $\text{Hess}\,(\sigma(s, t)) = \sigma_{11}(s, t)\sigma_{22}(s, t) - \sigma_{12}(s, t)^2$

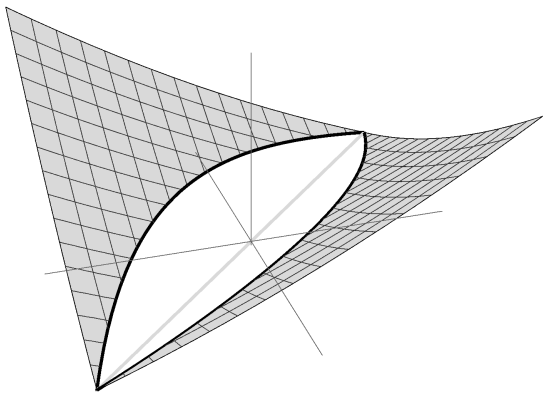

Figure 5.6: A Sketch of the σ, reproduced from [BS].

As a consequence, we have

Lemma 13. *The constant:*

$$\sigma_2\big(\varphi_x(x,y),\varphi_y(x,y)\big) = H_0 \quad \textit{(for all } (x,y) \in C_{LT}\textit{)}$$

is consistent with the Euler-Lagrange equations. This equation describes the minimizer of the functional $S[\varphi]$ which satisfies the free boundary condition at any given y.

Proof. Starting with the bulk equation of motion (5.2):

$$\begin{aligned}\partial_y\sigma_2 &= -\partial_x\sigma_1 \\ &= -\sigma_{11}\varphi_{xx} - \sigma_{12}\varphi_{xy} \\ &= -\frac{\sigma_{12}^2}{\sigma_{22}}\varphi_{xx} - \sigma_{12}\varphi_{xy}\end{aligned}$$

Here we used $\sigma_{11}\sigma_{22} - \sigma_{12}^2 = 0$ to eliminate σ_{11}.

$$\begin{aligned}&= -\frac{\sigma_{12}}{\sigma_{22}}\left(\sigma_{12}\varphi_{xx} + \sigma_{22}\varphi_{xy}\right) \\ &= -\frac{\sigma_{12}}{\sigma_{22}}\left(\partial_x\sigma_2\right) \\ &= 0\end{aligned}$$

□

Remark 5. *The fact that the uniform boundary condition gives the constraint $\sigma_2\big(\varphi_x,\varphi_y\big) = H_0$ that is preserved by the equations of motion is analagous (and is related) to the fact that the uniform boundary condition is a coeigenvector of the Markov process with maximal eigenvalue.*

Using the lemma, the first term in the bulk equation (5.2) vanishes, and the limit shape equation becomes parabolic:

$$\begin{aligned} 0 &= \partial_x \sigma_1(\varphi_x, \varphi_y) \\ &= \sigma_{11}(\varphi_x, \varphi_y)\ \varphi_{xx} + \sigma_{12}(\varphi_x, \varphi_y)\ \varphi_{xy} \end{aligned}$$

The partial derivatives of the surface tension can be computed exactly on the critical line [BS]. Alternatively, we can exploit the exact formula for the shape of the line (5.2.4):

Proposition 5. *Limit Shape Equation:*

$$\rho_y = -\frac{v^2 - 1}{(1 + v\rho)^2}\ \rho_x \tag{5.2.5}$$

where $\rho = \varphi_x$ *and:*

$$v = \frac{b_1 - b_2}{2 - b_1 - b_2}$$

Note that in Baxter's parametrization $v = \tanh(u + \eta)$.

Proof. Since $\sigma_2(\varphi_x, \varphi_y) = H_0$, the slopes must lie they must lie on the critical line (5.2.4):

$$\varphi_y = \frac{\varphi_x + \tanh(u + \eta)}{1 + \tanh(u + \eta)\varphi_x} \tag{5.2.6}$$

Differentiating with respect to x gives:

$$\varphi_{xy} = \frac{1 - \tanh(u + \eta)^2}{(1 + \tanh(u + \eta)\varphi_x)^2}\ \varphi_{xx}$$

Substituting $\rho = \varphi_x$ gives (5.2.5). □

Note that we are interested in periodic solutions to (5.2.5) with L-periodic initial conditions.

The ASEP Limit and Burgers Equations

It is well known [BF][Rez][GS] that in the hydrodynamic limit of ASEP, the time evolution of the ASEP height function is described by the inviscid Burgers' equation. This agrees with our result after taking in (5.2.5) the ASEP limit as described in section (5.1).

Letting $b_1 = \epsilon p$ and $b_2 = \epsilon q$, we expand (5.2.5) in ϵ:

$$\rho_t = \rho_x - \frac{1}{2}\epsilon(p - q)\rho\rho_x + O(\epsilon^2)$$

The limit $\epsilon \to 0$ corresponds to $u \to 0$. The first term $\rho_t = \rho_x$ is the transport equation and is the continuum limit of the cyclic shift operator (5.1.9).

They can be removed with a change of coordinates to $(\widetilde{x}, \widetilde{y})$:

$$x = \widetilde{x} \qquad y = \epsilon\widetilde{y} + x$$
$$\partial_x = \partial_{\widetilde{x}} \qquad \partial_y = \epsilon\partial_{\widetilde{y}} + \partial_{\widetilde{x}}$$

Then in the limit $\epsilon \to 0$:

$$\rho_{\widetilde{y}} = \frac{1}{2}(p-q)\ \rho\ \rho_{\widetilde{x}}$$

Note that in Baxter's parametrization $\frac{1}{2}(p-q) = 1$

5.3 Solutions to the Limit Shape equations

Recall $\rho = \partial_x \varphi$ satisfies $\rho \in [-1, 1]$. It is useful to write the limit shape PDE in conservation form:

$$\rho_y = \partial_x \left(F(\rho)\right) \tag{5.3.1}$$
$$= f(\rho)\ \rho_x \tag{5.3.2}$$

where f is as given in (5.2.5), and F is an antiderivative.

Note that when solutions are smooth and F is strictly convex, the PDE can be transformed into the inviscid Burgers' equation, letting:

$$u(x, y) = f(\rho(x, y)) \tag{5.3.3}$$

Then ρ satisfies (5.3.1) if and only if u satisfies $u_y = uu_x$.

Characteristics for Conservation Equations

Equations of form (5.3.1) can be solved by the method of characteristics. Assume the initial condition $\rho(x, 0) = \rho_0(x)$. Then, assuming the solution is smooth, the solution $\rho(x, y)$ is constant on the line in spacetime that passes through $(x_0, 0)$ with slope $dx/dy = f(\rho_0(x_0))$, i.e. on the line:

$$x = f\left(\rho(x_0)\right) y + x_0$$

In other words, a piece of fluid with "density" ρ moves with velocity $f(\rho)$.

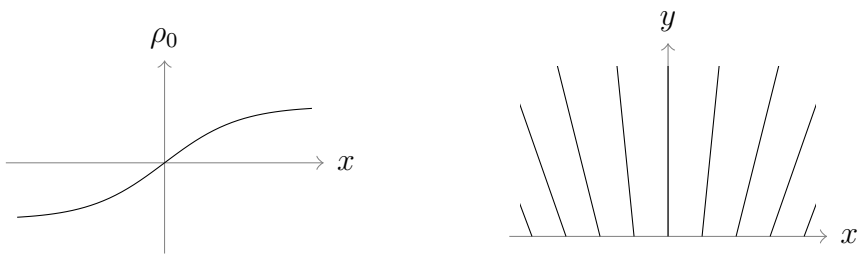

Figure 5.7: An initial condition ρ_0 and its characteristic lines with $f(\rho) = \rho$

Solutions to the Burgers equations with generic initial conditions typically develop discontinuities at later times. These discontinuities correspond to regions where the characteristics fail, either giving multiple solutions or no solutions. We instead look for weak solutions to the PDE [E].

Shocks

Intersecting characteristic lines give multiple values ρ for each point in space time. Thee correspond to a jump discontinuity in ρ called a shock. The precise location of the shock within a region of intersecting characteristics is determined by the *Rankine-Hugoniot* condition for the propogation of the shock. If $s(t)$ is the x coordinate of shock then:

$$\frac{ds}{dy}(y) = \frac{F(\rho_L(y)) - F(\rho_R(y))}{\rho_L(y) - \rho_R(y)} \qquad \rho_{L,R}(y) = \lim_{x \to s(y)^{\mp}} \rho(x, y)$$

Here ρ_L and ρ_R are the values of ρ just to the left and right side of the jump discontinuity. Note that the jump condition and propogation of the shock is not preserved by the transformation (5.3.3).

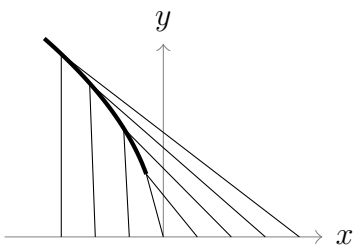

Figure 5.8: A shock (drawn in bold) caused by the intersecting characteristics.

Rarefaction Fans

Diverging characteristics lead to regions of spacetime where ρ is not determined by the characteristics. The correct solution for ρ in these regions, called rarefaction fans, is given by the *Lax-Oleinik* solution:

$$\rho(x, y) = f^{-1}\left(\frac{x}{y}\right) \qquad f(\rho_L) < \frac{x}{y} < f(\rho_R)$$

Here ρ_+ and ρ_- are the values of ρ just beyond the boundary of the rarefaction fan; in other words $F(\rho_L)$ and $F(\rho_R)$ are the slopes of the characteristics bounding the fan.

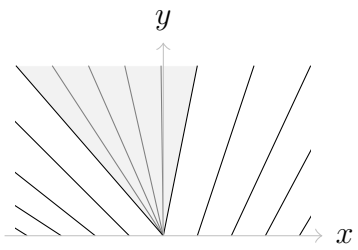

Figure 5.9: A rarefaction fan and its characteristics in gray.

Limit Shapes of the Stochastic Six Vertex Model with Domain Wall Initial Conditions

Recall that for the stochastic 6-vertex model:

$$F(\rho) = \frac{1}{v}\,\frac{1-v^2}{1+\rho\,v} \qquad f(\rho) = F'(\rho) = -\frac{1-v^2}{(1+v\rho)^2}$$

where

$$v = \frac{b_2 - b_1}{2 - b_2 - b_1}$$

Without loss of generality we assume $0 < b_1 < b_2 < 1$ so that $v \in (0,1)$. Then F is strictly convex since $F''(\rho) = f'(\rho) > 0$, see Figure 5.10.

The critical values of of $\rho = \pm 1$ correspond to "frozen" phases of the 6-vertex model. For these:

$$f(-1) = \frac{v+1}{v-1} = \frac{b_2 - 1}{b_1 - 1}$$
$$f(1) = \frac{v-1}{v+1} = \frac{b_1 - 1}{b_2 - 1}$$

The inverse of f is easily calculated:

$$f^{-1}(x) = \frac{-1 + \sqrt{\frac{1-v^2}{|x|}}}{v} \tag{5.3.4}$$

for $f(-1) < x < f(1) < 0$. For reference we also calculate:

$$F(f^{-1}(x)) = \sqrt{\left(1 - \frac{1}{v^2}\right)|x|}$$

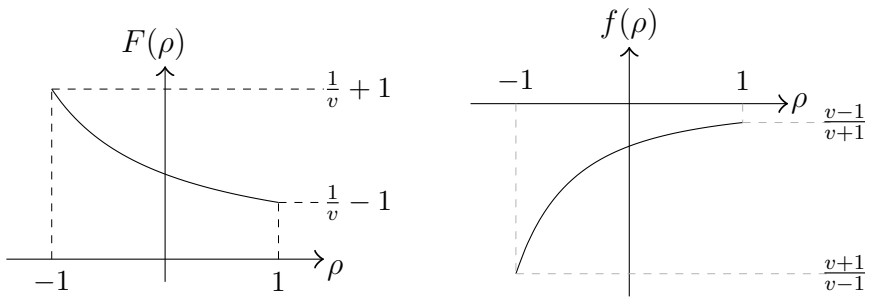

Figure 5.10: Plots of $F(\rho)$ and $f(\rho)$.

Example 1

Consider the step initial conditions on a line ($L = \infty, x \in \mathbb{R}$):

$$\rho_0 = \begin{cases} \rho_R & x \geq 0 \\ \rho_L & x < 0 \end{cases}$$

This means, the negative part of the real line is saturated by particles, with the positive side empty. When $\rho_L > \rho_R$ a shock forms and propagates from the origin with constant velocity:

$$\frac{ds}{dy} = \frac{F(\rho_L) - F(\rho_R)}{\rho_L - \rho_R} = v_0$$

The corresponding solution is:

$$\rho(x, y) = \begin{cases} \rho_R & x/y \geq v_0 \\ \rho_L & x/y < v_0 \end{cases}$$

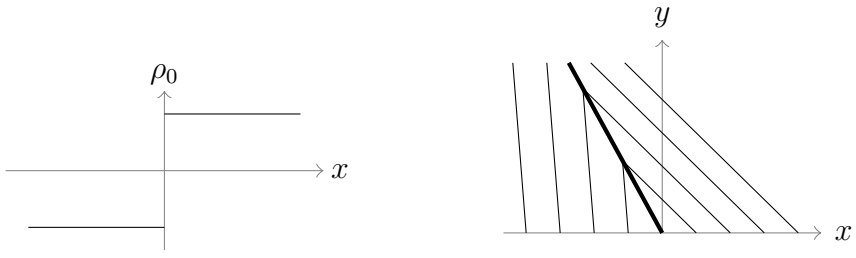

When $\rho_R = -1$ and $\rho_L = 1$ we have $v_0 = -1$.

Example 2

Consider now the step initial conditions on a line with $\rho_L < \rho_R$. In this case characteristic solutions do not span the region $f(\rho_L) < x/y < f(\rho_R)$ and instead we have

a rarefaction fan propagating in this region from the origin. Using the Lax-Oleinik formula and (5.3.4), we have the general solution:

$$\rho(x,y) = \begin{cases} \rho_R & x/y > f(\rho_R) \\ \frac{-1+\sqrt{\frac{1-v^2}{x/y}}}{v} & f(\rho_L) < x/y < f(\rho_R) \\ f(\rho_L) & x/y < f(\rho_L) \end{cases}$$

For critical densities $\rho_L = -1$, $\rho_R = 1$ we have

$$f(\rho_L) = \frac{v-1}{v+1}, \quad f(\rho_R) = \frac{v+1}{v-1}$$

and this solution correspond to the limit shape derived in [BCG].

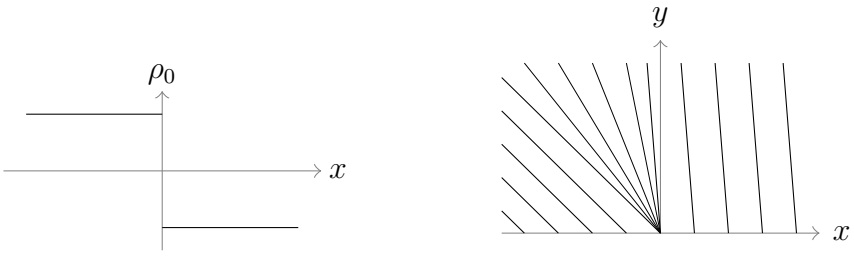

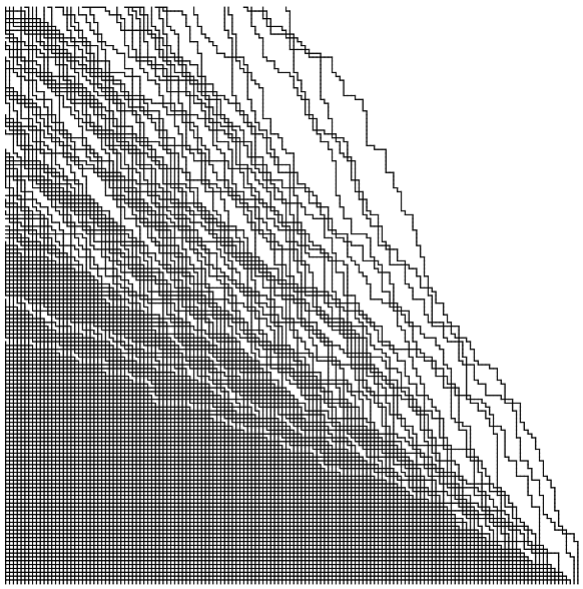

Figure 5.11: A numerical simulation

Example 3

We now consider domain wall type boundary conditions on the cylinder, with one segment of the circle is saturated with particles with the rest of the cylinder empty. The initial conditions are:

$$\rho_0 = \begin{cases} \rho_L & 0 < x < x_1 \\ \rho_R & x_1 < x < L \end{cases}$$

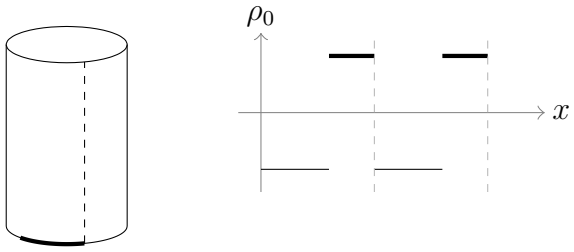

In the following analysis, we assume that $\rho_L = 1, \rho_R = -1$; and $x_1 > \frac{1}{2}L(1-v)$. The more general initial condition is similar. For these initial conditions, there is both a shock and a rarefaction fan. It is straightforward to solve the differential equations for the propogation of the shock; we omit the details and summarise the result, see Figure 5.12.

For $y \in [0, y_1]$ the shock moves with constant speed, as the "frozen" characteristics collide. From $y \in [y_1, y_2]$,the shock curves as the frozen characteristics collide with the rarefaction fan. For $y > y_2$, the shock asymptotes to a straight line with slope:

$$\lim_{y\to\infty} \frac{ds}{dy} = f\left(\rho_{\text{ave}}\right)$$

Here $\rho_{\text{ave}} = \frac{2x_1 - L}{L}$ is the asymptotic value of ρ, and the average density of ρ on the cylinder.

A similar picture occurs if $x_1 < \frac{1}{2}L(1-v)$, except that the frozen region corresponding to $\rho = 1$ vanishes first. For the critical value of $x_1 = \frac{1}{2}L(1-v)$ the frozen regions disappear at the same time $y_1 = y_2$.S

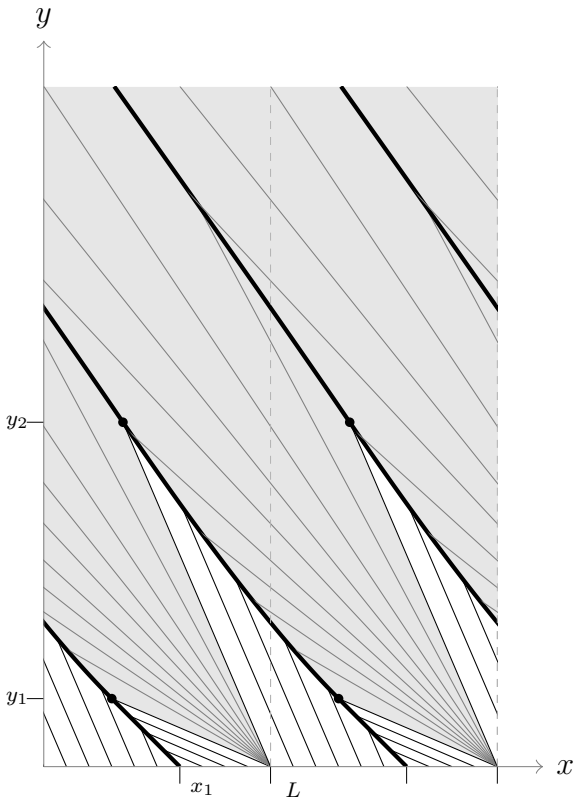

Figure 5.12: Step initial conditions on the cylinder.

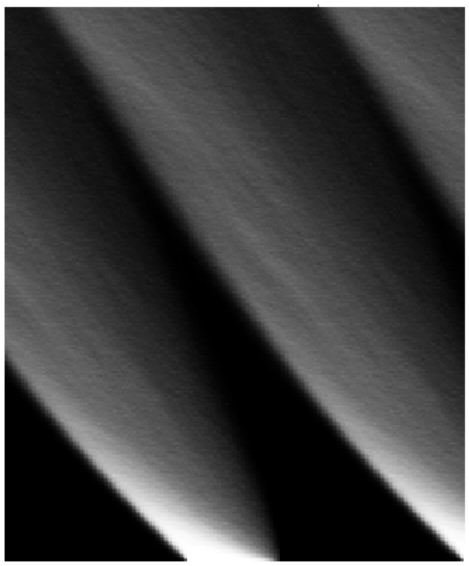

Figure 5.13: A numerical simulation. The brighter regions correspond to areas of higher density.

5.4 Conclusion

There are a few areas of further work that we plan to pursue in followup publications.

Firstly, note (see Section 5.1) that the uniform boundary state on the top of the cylinder is crucially a co-eigenstate of the transfer matrix with the eigenvalue 1, corresponding to the Markov property of the stochastic model. Similar results to those in this paper hold for the general 6-vertex model, with the ground co-state being the boundary state for the top end of the cylinder.

Secondly, we expect that similar results hold for the higher spin 6-vertex models.

Finally, for the generic phases of the 6-vertex and dimer model, the statistical fluctuations about the limit shape are conjecturally described by the Gaussian free field determined by surface tension functional near the limit shape. The degeneracy of the surface tension function at the stochastic point (see Lemma 12) explains the appearance of the KPZ scaling as computed in [BCG]. Fluctuations for TASEP model near shocks were described recently in [BL]. Translation invariant Gibbs measures for the stochastic six vertex model were studied recently in [A]. We expect that the fluctuations in the limit shapes studied in this paper will be given by Baik-Rains along the characteristic lines and exponential decay in other directions. From our point of view this is the line where the quadratic variation of the "effective action" (5.2.1) is non-degenerate.

Chapter 6

Asymptotic Determinants of Discrete Laplace Operators

On a graph $X = (V, E)$, the graph laplacian is an operator that acts on the space of functions $f : V \to \mathbb{R}$ as:

$$\Delta f(u) = \sum_{[u,v]\in E} f(v) - f(u) \tag{6.0.1}$$

The determinants of graph laplacians have been well studied in many different contexts. For instance, in spectral graph theory, Kirchoff's theorem relates the determinant of the graph laplacian on X to the number of rooted spanning trees on X. Similarly, by Temperley's trick and its generalizations, the determinant of the graph laplacian on certain graphs X computes the number of perfect matchings on a related graph X' [KPW00]. In each case, the determinant of the laplacian is the partition function of an associated model in statistical mechanics.

When X is the graph of a regular lattice, the asymptotics of the determinant have been investigated in many papers. In particular, when X is a rectangular subgraph of $\mathbb{Z}^2$ with $N \times M$ vertices, the determinant of the laplacian (with Dirichlet boundary conditions) as $N, M \to \infty$ is computed by [DD] in the context of Hamiltonian walks on the grid. The asymptotic expansion is:

$$\log\det\Delta_{NM} = NM\frac{4G}{\pi} + 2(N+M)\log(\sqrt{2}-1) + \frac{1}{4}\log(NM) + O(1) \tag{6.0.2}$$

where G is the Catalan constant. More generally, the asymptotics of the determinants of laplacians on rectilinear regions of $\mathbb{Z}^2$ have been computed in [Ken00]. When appropriately rescaled, this graph laplacian can be understood as a finite difference approximation of the laplacian $\frac{\partial^2}{\partial x^2} + \frac{\partial^2}{\partial y^2}$ of Eulidean space.

In this chapter, we study a generalized graph laplacians in $\mathbb{Z}^2$ that can be regarded as finite difference approximations of Laplace-Beltrami operators induced by a Riemannian metric g. These laplacians arise as follows: on any graph X, the cochain complex $(C^*(X), d)$ can be regarded as a combinatorial version of the de Rham complex. We

define a Riemannian structure on X as a set of inner products $\langle , \rangle_{C^*(X)}$ on the cochain spaces. On such a graph with Riemannian structure, we define a combinatorial Guassian field theories, as outlined in section §6.1. The partition function of the boson field theory is $Z = \det \Delta$, where the combinatorial laplacian Δ is by $\langle df, df \rangle_{C^*(X)} = \langle \Delta f, f \rangle_{C^*(X)}$ for all $f \in C^0(X)$.

Assume now that the underlying space $M \subset \mathbb{R}^2$ of X is endowed with a metric $g = g_{xx}\, dx^2 + g_{yy}\, dy^2$. By square subdivision of X, we have a sequence $\{X^i\}$ of graphs with mesh $\epsilon_i \to 0$. Assume that the $\{X^i\}$ have Riemmanian structure such that the combinatorial laplacian Δ^i on X^i is a good approximation of the laplacian induced by g on M (see section 6.1). This can be regarded as discretization of a massless scalar field theory on a nontrivial background metric. We show that the determinant of Δ^i has the asymptotic expansion (Theorem 3):

$$\log \det \Delta^i = \frac{1}{\epsilon_i^2} \int_M F(g)\, dx\, dy + \frac{1}{\epsilon_i} \int_{\partial M} B(g) \cdot ds + \frac{1}{2} \log(\epsilon^i) + O(1) \tag{6.0.3}$$

where the functions F and B are given in equation (6.2.2).

The outline of this paper is as follows: In section 1, we describe the notion of a Riemannian structure on a graph, and define the combinatorial codifferential and combinatorial laplacian. We explain how a Riemannian manifold can be approximated by a sequence of graphs with Riemannian structure. Then we outline the definition of a combinatorial Gaussian free field theory on a graph and describe the relation to the dimer model of statistical physics. In section 3, we focus on the bosonic field theory on (M, g), when M is a rectangular region in $\mathbb{R}^2$ endowed with a diagonal metric g, and set up the calculation of the determinant. Sections §6.3 and §6.4 are more technical sections: §6.3 is devoted to estimating the inverse $(\Delta^i)^{-1}$ as $i \to \infty$; in §6.4 we prove the main theorem, equation (6.0.3). Finally in §6.5, we conclude with some general remarks and further research directions.

6.1 Discrete Laplacians

Let X be a cell decomposition of a simply connected region $M \subset \mathbb{R}^2$, with q-cells X_q for $q = 0, 1, 2$. The space of q-chains $C_q(X)$ for $q = 0, 1, 2$ is the real vector spaces with canonical basis X_q. The dual space space $C^q(X) = C_q(X)^*$ is the space of functions $X_q \to \mathbb{R}$. There is an isomorphism $C_q(X) \simeq C^q(X)$ induced by the canonical basis on $C_q(X)$. For any subcomplex $L \subset X$, there is a natural projection $p : C^q(X) \to C^q(L)$ given by restriction to L. Define $C^q(X, L) = \ker(p) \subset C^q(X)$. The boundary of X is the 1-dimensional subcomplex ∂X contained in ∂M.

On an oriented complex, there is a natural boundary operator $\partial_q : C_q(X) \to C_{q-1}(X)$. The coboundary $d_q : C^q(X) \to C^{q+1}(X)$ is the adjoint of ∂_q with respect to the pairing $C^q(X) \times C_q(X) \to \mathbb{R}$. The coboundary operator satisfies $d_{q+1} d_q = 0$ and the complex $(C^*(X), d)$ can be regarded as a discrete analog of the de Rham complex of a smooth manifold.

In the remainder, we assume for simplicity that X is embedded such that image of each 2-cell is a simple convex polygon. In this case the 1-skeleton of X then defines a simple planar graph embedded in M.

The dual and double of a graph

We define the dual complex $\widetilde{X}$ as the complex found by truncating the standard dual, so that $\widetilde{X}$ is also a cell complex of M (see figure **??**). Note that as usual, there is a bijection from X_q and to $(\widetilde{X}\backslash\partial\widetilde{X})_{2-q}$, but in addition the truncation gives a bijection of ∂X_q and $\partial\widetilde{X}_{1-q}$.

The double $D(X)$ of X is, roughly speaking, the union of the X and $*X$ (see figure **??**). Precisely, $D(X)$ is the complex consisting of: a 0-cell p_σ at the center of each $\sigma \in X$; a 1-cell $[p_\sigma, p_\tau]$ for each pair $\sigma \in X_i,\ \tau \in X_{i+1}$ with σ adjacent to τ; and a 2-cell $[p_\alpha, p_{\beta_1}, p_\gamma, p_{\beta_2}]$, for each set of $\alpha \in X_0,\ \beta_1, \beta_2 \in X_1,\ \gamma \in X_2$ pairwise adjacent. Note that the graph of $D(X)$ has a natural bipartite structure given by painting p_σ white if σ is a 1-cell, and black otherwise.

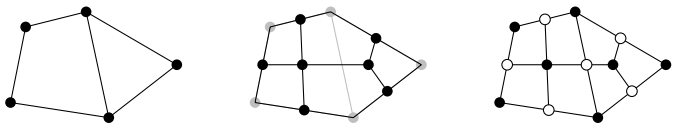

Figure 6.1: A graph, its dual, and its double.

Riemannian Structures on Graphs

Recall that the metric on a compact, oriented Riemannian manifold (M, g) induces a scalar product on the de Rham complex $\Omega^*(M)$: for $f, g \in \Omega^q(M)$

$$\langle f, g\rangle_{\Omega^q(M)} = \int_M f \wedge *g$$

where $* : \wedge^q T_pM \to \wedge^{2-q} T_pM$ is the Hodge dual. Continuing to view the cochain spaces $C^q(X)$ as the combinatorial analog of $\Omega^q(M)$, we define:

Definition 3. *A Riemannian structure on X is a set of scalar products $\langle , \rangle_{C^q(X)}$ for $q = 0, 1, 2$.*

The scalar products can be required to satisfy certain additional axioms. In particular, recall that the scalar product on $\Omega^q(M)$ is local in the sense that it is the integral of a fiberwise scalar product. We consider more generally the combinatorial notion of a fiberwise map $\Omega^q(M) \to \Omega^r(M)$ as follows:

Definition 4. *A map $T : C^q(X) \to C^r(X)$ is said to m-local if the matrix elements $T_{\sigma,\tau}$ in the canonical basis of $C^*(X)$ vanishes whenever the graph theoretic distance between $p_\sigma, p_\tau \in D(X)$ is greater than $2m$.*

Definition 5. *A Riemannian structue $\langle , \rangle_{C^q(X)}$ is local if the corresponding dual operator $C^q(X) \to C^q(X)$ is m-local for some m. A Riemannian structure is said to be diagonal if it is 0-local.*

A diagonal Riemannian structure can be understood as an assignment of a volume weight $|\sigma| = \langle \sigma, \sigma \rangle_{C^q(X)}$ to each cell $\sigma \in X_q$.

Approximation theory

We now consider how a Riemannian manifold can be approximated by a graph with Riemannian structure. We assume as before that X is a cell decomposition of a region $M \subset \mathbb{R}^2$, but in addition assume that M is endowed with a smooth Riemannian metric g. Define the mesh of X is $\epsilon_X = \sup\{ \operatorname{diam}(\tau) \mid \tau \in X\}$. The embedding of X in M defines a surjection, namely the de Rham integration map $I_X : \Omega^q(M) \to C^q(X)$:

$$I_X \omega = \sum_{\alpha \in X_q} \alpha \int_\alpha \omega$$

for $\omega \in \Omega^q(M)$.

Let $\{X^i\}_{i \in \mathbb{N}}$ be a sequence of complexes in M, such that $\epsilon_{X^i} \to 0$, for example generated by iterated subdivision of an initial complex. A sequence of Riemannian structures on the $\{X^i\}$ is said to be consistent if the integration maps I_{X^i} approaches an isometry of spaces $\Omega^q(M)$ and $C^q(X^i)$ as $i \to \infty$. More precisely:

Definition 6. *A sequence of Riemannian structures on $\{X^i\}$ is consistent if for any $f \in \Omega^q(M)$ there exists a constant η_f such that, for all i:*

$$\left| \langle I_{X^i} f, I_{X^i} f \rangle_{C^q(X^i)} - \langle f, f \rangle_{\Omega^q(M)} \right| \leq \eta_f \, \epsilon_{X^i}$$

The Combinatorial Laplacian

Let X be a complex with a Riemannian structure. Let $L \subset \partial X$ be a subcomplex of ∂X. Let $d_{q,L} : C^q(X, L) \to C^q(X, L) = \pi_L d$ where $\pi_L : C^q(X) \to C^q(X, L)$ is orthogonal projection. The combinatorial codifferential combinatorial codifferential $\delta_{q,L} : C^q(X) \to C^{q-1}(X)$ is defined the adjoint of d_q:

$$\langle d_{q,L} f, g \rangle_{C^{q+1}(X,L)} = \langle f, \delta_{q+1,L} g \rangle_{C^q(X,L)}$$

for all $f \in C^q(X), g \in C^{q+1}(X)$.

Remark 6. *Choosing the canonical basis for the $C^*(X)$ and writing the scalar products $\langle , \rangle_{C^q(K)}$ as matrices g_q, the codifferential δ_q can be written in matrix form as:*

$$\delta_q = g_{q-1}^{-1} d_q^T g_q$$

From this, it is clear that generally δ_q is m-local (for any m!) only if the scalar product g_{q-1} is diagonal.

Duality

In this section, we briefly explain how Hodge duality arises in this combinatorial framework. Let X be a complex with a diagonal Riemannian structure, and as above $L \subset \partial X$. Let $\widetilde{L} \subset \partial \widetilde{X}$ be the complement of the image of L under the bijection $\partial X_q \to \partial \widetilde{X}_{1-q}$, and $\widetilde{X}_L$ be the complex found by removing from $\widetilde{X}$ the image of L under both bijections $X_q \to (\widetilde{X} \backslash \partial \widetilde{X})_{2-q}$ and $\partial X_q \to \partial \widetilde{X}_{1-q}$.

There is a bijection of $X_q \backslash L_q$ and $X_{2-q} \backslash \widetilde{L}_{2-q}$, which induces an isomorphism $\phi : C_q(X, L) \to C_{2-q}(\widetilde{X}_L, \widetilde{L})$. Putting a Riemannian structure on $\widetilde{X}_L$ via the isomorphism, ϕ becomes an isomorphism of chain complexes $(C_q(X, L), d_L)$ and $(C_{2-q}(\widetilde{X}_L, \widetilde{L}), \delta_{\widetilde{L}})$; ie. $\phi \circ d_{q,L} = \widetilde{\delta}_{q,\widetilde{L}} \circ \phi$ and $\phi \circ \delta_{q,L} = \widetilde{d}_{q,\widetilde{L}} \circ \phi$.

The Combinatorial Laplacian

The combinatorial Laplacian is defined as $\Delta_{q,L} = \delta_{q+1,L} d_{q,L} + d_{L,q-1} \delta_{q,L}$. This Laplacian should be understood as corresponding to mixed boundary conditions, with relative (Dirichlet) boundary conditions on L and absolute (Neumann) boundary conditions on $\partial X \backslash L$. In particular, since we focus attention on 0-forms, we let:

$$\Delta_L = \delta_{1,L} d_{0,L}$$

For a diagonal Riemannian structure, it follows by straightforward computation that for $p \in X_0 \backslash L$, the combinatorial laplacian can be written:

$$\Delta_L f(p) = \sum_{\substack{\sigma \in X_1 \\ p \cap \sigma \neq 0 \\ \sigma \cap L = 0}} \frac{|\sigma|}{|p|} \left(f(q) - f(p) \right) \tag{6.1.1}$$

Consistency of the Combinatorial Laplacian

Fix a submanifold $L \subset \partial M$, and let Δ be the Laplace-Beltrami operator acting on C^∞ functions with Dirichlet boundary conditions on L and Neumann on $\partial M \backslash L$. Consider a sequence of graphs $\{X_i\}$ approximating (M, g) as in Section 6.1, and such that for each i there is a subcomplex $L_i \subset \partial X_i$ that is a decomposition of L. In this context:

Definition 7. *The sequence of combinatorial laplacians Δ_i on X_i is said to be consistent if for any $f \in C^\infty(M)$ there exists a constant η_f such that, for all i:*

$$\left| \Delta_L^i I_{X_i} f - I_{X_i} \Delta f \right| \leq \eta_f \, \epsilon_{X_i}^2 \tag{6.1.2}$$

Gaussian Field Theories on Graphs

In this section, we briefly outline the definition of discrete Guassian field theories on graphs with Riemannian struture.

Bosonic Free Field Theory

Let X be a complex with a Riemannian structure. The (massless) free field action, or Dirichlet energy, is the quadratic form $S : C^0(X) \to \mathbb{R}^+$:

$$S(f) = \langle df, df \rangle_{C^1(X)}$$

for $f \in C^0(X)$.

The space of fields $\mathcal{H} \subset C^0(X)$ of the discrete field theory is given by prescribing boundary conditions as follows: let $L \subset \partial X$ be a nonempty subcomplex and let $\mathcal{H} = C^0(X, L)$.The Bosonic scalar field theory is then defined by the partition function:

$$Z_b(X, L) = \int_{\mathcal{H}} e^{-S(\psi)} \, \mathcal{D}\psi$$

where the measure $\mathcal{D}\psi$ on $\mathcal{H}$ is induced by the scalar product on $C^0(X)$. The correlation functions are defined in the usual way as:

$$\langle \psi(p_1) \cdots \psi(p_n) \rangle = \frac{1}{Z_b(X, L)} \int_{\mathcal{H}} \psi(p_1) \cdots \psi(p_n) e^{-S(\psi)} \, \mathcal{D}\psi$$

Using standard Gaussian integral formulae give:

$$\log Z_b(X, L) = -\frac{1}{2} \log \det(\Delta_L) + \frac{1}{2} \left(\dim \mathcal{H}\right) \log(2\pi)$$

Similarly, correlation functions can be expressed in terms of matrix elements of Δ_L^{-1}. For exampe, the two point function:

$$\langle \psi(p_1) \psi(p_2) \rangle = \left(\Delta_L^{-1}\right)_{p_1, p_2}$$

Fermionic Free Field Theory

As before, let $L \subset \partial X$ be a subcomplex of ∂X. Let $S^+ = C^0(X, L) \oplus C^2(X, L)$ and $S^- = C^1(X, L)$. The combinatorial Dirac operator $D_L : S^+ \to S^-$ is the restriction of $d_L + \delta_L$ to S^+, and the adjoint $D_L^\dagger$ is the restriction of $d_L + \delta_L$ to S^-. This operator should be regarded as a combinatorial analog of the Hodge-Dirac operator.

The space of fields for the free fermionic field theory is $\mathcal{H}^+ = C^0(X, L) \oplus C^2(X, L)$ and $\mathcal{H}^- = C^1(X, L)$. The theory is defined by partition function given by the Grassmanian integral over $\mathcal{H} = \wedge(\mathcal{H}^+ \oplus \mathcal{H}^-)$:

$$Z_f(X, L) = \int_{\mathcal{H}^+} \int_{\mathcal{H}^-} \exp\left(\frac{1}{2} \langle \psi, D_L \chi \rangle\right) \mathcal{D}\chi \mathcal{D}\psi \tag{6.1.3}$$

where the measure $\mathcal{D}\chi \, \mathcal{D}\psi$ is induced by the scalar products on S^+ and S^-. Correlation functions are once again defined by insertions into the path integral:

$$\begin{aligned} &\langle \psi(p_1)\chi(p_1) \cdots \psi(p_n)\chi(p_n) \rangle \\ &\qquad = \frac{1}{Z_f(X, L)} \int_{\mathcal{H}^+} \int_{\mathcal{H}^-} \psi(p_1)\chi(p_1) \cdots \psi(p_n)\chi(p_n) \exp\left(\frac{1}{2} \langle \psi, D_L \chi \rangle\right) \mathcal{D}\chi \end{aligned}$$

We can explicitly calculate as follows. Choosing the standard basis $\{\chi_i\} = X_1 \backslash \partial X_1$ for $\mathcal{H}^-$ and $\{\psi_j\} = X_0 \backslash \partial X_0 \cup X_2$ for $\mathcal{H}^+$, one can write the measure as:

$$\mathcal{D}\chi\mathcal{D}\psi = \prod_i \frac{1}{\sqrt{|\chi_i|}}\, d\chi_i \;\; \prod_j \frac{1}{\sqrt{|\psi_j|}}\, d\psi_i$$

Using the standard Grassman integral formulae, the partition function (6.1.4) can be evaluated as:

$$Z_f(X, L) = \frac{\prod \sqrt{|\psi_i|}}{\prod \sqrt{|\chi_j|}} \det\left(D_L\right) \tag{6.1.4}$$

The fermionic field theory is closely related to the bosonic theory. First define the dual fermionic theory as:

$$\widetilde{Z}_f(X, L) = \int_{\mathcal{H}^+} \int_{\mathcal{H}^-} \exp\left(\frac{1}{2}\langle D_L\psi, \chi\rangle\right) \mathcal{D}\chi\mathcal{D}\psi \tag{6.1.5}$$

Then it is straightforward to show that:

$$Z_f(X, L)\widetilde{Z}_f(X, L) = \left(Z_b(\widetilde{X}_L, \widetilde{L})\; Z_b(X, L)\right)^{-1}$$

The Dimer Model

The free fermionic theory defined above is closely related to the dimer model of statistical mechanics. First we briefly recall the definition of the dimer model. On a graph G with positive edge weights $w \in C^1(G)$, a perfect matching M of G is a subset $M \subset G_1$ of edges such that each vertex v is contained in exactly one edge $e \in M$. The weight of the matching M is $\prod_{e\in M} w(e)$. This defines a Gibbs measure μ on the set $\mathcal{M}$ of all perfect matchings: the probability of a matching M is:

$$\mu(M, w) = \frac{w(M)}{Z(G, w)}$$

where the partition function $Z(G, w) = \sum_{M\in\mathcal{M}} \omega(M)$. A gauge transformation of the dimer model is a function $\lambda \in C^0(G)$ that acts on the edge weights as $(\lambda \cdot w)\big([p_1, p_2]\big) = w([p_1, p_2])\lambda(p_1)\lambda(p_2)$. The gauge transformation leaves the measure μ invariant, but transforms the partition function as:

$$Z\left(G, (\lambda \cdot w)\right) = \left(\prod_{p\in G_0} \lambda(p)\right) Z(G, w) \tag{6.1.6}$$

The dimer model is exactly solvable by the Kasteleyn technique as follows: for simplicity, assume G is bipartite with black vertices $\{b_i\}_{i=1\cdots n}$ and white vertices $\{w_i\}_{j=1\cdots n}$. A Kasteleyn orientation is a function $\widetilde{w} : G_1 \to \{1, -1\}$, such that the product of $\widetilde{w}$ on edges around any face is either -1 if the number of edges is divisible by four, or $+1$

otherwise. The Kasteleyn matrix is the $n \times n$ matrix with columns and rows indexed by black and white vertices respectively, and with matrix elements

$$K_{b_i w_j} = \widetilde{w}([b_i w_j]) w([b_i, w_j])$$

when b_i and w_j are adjacent, and zero otherwise.

Kasteleyn's theorem is that the partition function of the dimer model is given by $Z(G, w) = \det(K)$. In addition, the Kasteleyn matrix encodes the statistics of dimer model via the local statistics theorem, which gives correlation functions of the dimer model in terms of the inverse Kasteleyn matrix.

We now define a dimer model on the double of a complex X endowed with a local Riemannian structure. As before, let $L \subset \partial X$ be a non-empty subgraph of the boundary. Define an the edge weight function $w_r \in C^1(D(X))$ on the double as:

$$w_r([p_\sigma, p_\tau]) = \sqrt{\frac{\langle \sigma, \sigma \rangle_{C_q(G)}}{\langle \tau, \tau \rangle_{C_{q+1}(G)}}}$$

In writing the above formula, we have assumed σ is of smaller dimension than τ in X. Let $D(X)'$ be the graph found by attaching to each p_σ with $\sigma \in \partial X$ a unit weighted edge and an additional univalent vertex. (See figure **??**). Let $Z_d(X, w_r, L)$ be the dimer partition function of the dimer model defined by the graph $D(X)'$ with weight w_r.

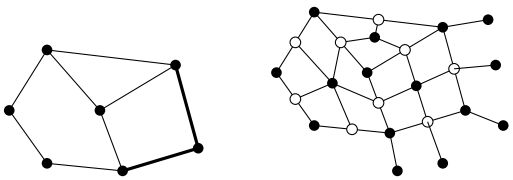

Figure 6.2: A graph with boundary conditions in bold and the associated dimer model.

Proposition 6.

$$Z_d(X, w_r, L) = Z_f(X, L)$$

This proposition states essentially that $D_{\mathcal{L}}$ is a Kasteleyn matrix for the dimer model $(D(X)', w_r, L)$. It follows then that the correlation functions of the fermionic theory also give the correlation functions of the dimer model.

Proof. First, note that the dimer model on $D(X)'$ is equivalent to the dimer model found by removing from $D(X)$ vertices p_σ with $\sigma \in L$, and edges adjacent to them. In addition, applying the gauge transformation

$$\lambda(p_\sigma) = \begin{cases} 1/\sqrt{|\sigma|} & \text{if } \sigma \in X_0, X_2 \\ \sqrt{|\sigma|} & \text{if } \sigma \in X_1 \end{cases}$$

on the remaining vertices transforms the edge weights into:

$$w'\left([p_\sigma, p_\tau]\right) = \begin{cases} 1 & \text{if } \sigma \in X_0, \tau \in X_1 \\ |\sigma|/|\tau| & \text{if } \sigma \in X_1, \tau \in X_2 \end{cases}$$

Comparing the action of the gauge transformation (6.1.6) and the explicit formula for the fermionic partition function (6.1.4), it remains to show that:

$$Z_d(D(X)\backslash L, w') = \det(D_L)$$

Recall that the double $D(X)$ has a bipartite structure. Regarding $D_{\mathcal{H}}$ as map operator from white vertices in $D(X)$ (edges in X) to black vertices $D(X)$ (vertices and faces in X we compute for $\tau \in X_1$:

$$D\tau = \sum_{\sigma \in X_0} (-1)^{(\sigma,\tau)}\sigma + \sum_{\sigma \in X_2} (-1)^{(\sigma,\tau)} \frac{|\sigma|}{|\tau|}\sigma$$

where $(-1)^{(\sigma,\tau)}$ is the function that is 0 if σ is not adjacent to τ, and is ± 1 if the orientations of σ and τ are compatible. That is, up to a sign, the matrix element $D_{\sigma,\tau}$ is equal to the edge weight $w'([p_\sigma, p_\tau])$. It remains to check that the signs of the matrix elements of D satisfy the Kasteleyn orientation condition. Since every face in the double $D(X)$ is quadrilateral, the Kasteleyn condition requires the number of minus signs around each is odd. This follows from $d^2 = 0$ and $\delta^2 = 0$. □

6.2 Combinatorial Laplacians in Rectangular Graphs

In the remainder of this paper, we focus on the particular case that U is a rectangular region with a diagonal metric $g = g_{xx}\, dx^2 + g_{yy}\, dy^2$, approximated by subgraphs of $\mathbb{Z}^2$. For simplicity, we assume that both the metric and the induced Riemannian distance function are analytic. In addition, denote by ∂M_i for $i = 1, \cdots, 4$ be the four straight segments of ∂M, and let boundary conditions be specified by $L \subset \partial M$, where L is the union of a non-empty subset of $\{\partial M_i\}$.

Let X^0 be the cell decomposition of M, consisting of four 0-cells placed at the corners of U, four 1-cells, and one 2-cell. Let $\{(X^i, \langle , \rangle_{C^q(X^0)})\}_{i \in \mathbb{N}}$ be a sequence of subdivisions by iteratively taking doubles, endowed with a local, consistent Riemannian structure and consistent combinatorial laplacians Δ_L^i.

Theorem 3. *In the above setting, the determinant of the combinatorial laplacian Δ^i has the following expansion:*

$$\log\det\Delta^i = \frac{1}{\epsilon_i^2}\int_M F(g)\, dx\, dy + \frac{1}{\epsilon_i}\int_{\partial M} B(g)\cdot ds + \frac{1}{2}\log(\epsilon^i) + O(1) \tag{6.2.1}$$

where:

$$\begin{aligned} F(g_{xx}, g_{yy}) &= \frac{2}{\pi}\Im\left(\mathrm{Li}_2\left(i\sqrt{\frac{g_{yy}}{g_{xx}}}\right) + \mathrm{Li}_2\left(i\sqrt{\frac{g_{xx}}{g_{yy}}}\right)\right) - \log\left(\sqrt{g_{xx}g_{yy}}\right) \\ B_x(g_{xx}, g_{yy}) &= -\frac{1}{2}\log(\sqrt{g_{xx}g_{yy}} + \sqrt{g_{xx}g_{yy} + g_{yy}}) \\ B_y(g_{xx}, g_{yy}) &= -\frac{1}{2}\log(\sqrt{g_{xx}g_{yy}} + \sqrt{g_{xx}g_{yy} + g_{yy}}) \end{aligned} \tag{6.2.2}$$

where Li_2 *is the dilogarithm function.*

The approach to calculate the determinant is to study variations of the metric g. Under a variation $g \to g + \delta g$ we have:

$$\frac{\delta}{\delta g}\log\det\Delta_L^i = \mathrm{Tr}\left((\Delta_L^i)^{-1}\frac{\delta\Delta_L^i}{\delta g}\right) \tag{6.2.3}$$

In the next section §6.3, we compute an estimate of the combinatorial Green's function Δ_L^i, which we use in section §6.4 to compute an estimate of (6.2.3). The asymptotic expansion (6.2.1) follows by integrating (6.2.3), with the constant of integration fixed by the expansion (6.0.2), corresponding to the case that $g = dx^2 + dy^2$.

We conclude this section by estimating the matrix elements of the combinatorial laplacians Δ_L^i as $i \to \infty$.

Asymptotics of the Combinatorial Laplacian

First, we fix some useful notation borrowed from the finite difference calculus. For clarity, we leave implicit superscripts indicating the level of subdivision when there is no danger of confusion, for example $C^0(X)$ for $C^0(X^i)$, ϵ for ϵ_{X^i}, etc. For $p \in X_0\backslash\partial X_0$ with coordinates $(x, y) \in \mathbb{R}^2$, define the finite difference operators:

$$\begin{aligned} D_x f(x,y) &= \frac{1}{2}\left(f(x+\epsilon, y) - f(x-\epsilon, y)\right) \\ D_x^2 f(x,y) &= f(x+\epsilon, y) - 2f(x,y) + f(x-\epsilon, y) \end{aligned}$$

and similar operators in the y-directions. These operators are consistent: for every $f \in C^\infty(U, \partial U)$, there are constants η_f such that

$$\begin{aligned} \left|\frac{1}{\epsilon}D_x I_X f(x,y) - I_X\partial_x f(x,y)\right| &\le \epsilon^2\eta_f \\ \left|\frac{1}{\epsilon^2}D_x^2 I_X f(x,y) - I_X\partial_x^2 f(x,y)\right| &\le \epsilon^2\eta_f \end{aligned} \tag{6.2.4}$$

Proposition 7. *Then the laplacian has the following asymptotic asymptotic expansion:*

$$\begin{aligned} \epsilon^2\Delta^i = \frac{1}{\sqrt{g_{yy}g_{xx}}}\left(\sqrt{\frac{g_{yy}}{g_{xx}}}\,D_x^2 + \sqrt{\frac{g_{xx}}{g_{yy}}}\,D_y^2 + \epsilon\,\partial_x\sqrt{\frac{g_{yy}}{g_{xx}}}\,D_x + \epsilon\,\partial_y\sqrt{\frac{g_{xx}}{g_{yy}}}\,D_y\right) \\ + O(\epsilon^2)D_x^2 + O(\epsilon^2)D_y^2 + O(\epsilon^3)D_x + O(\epsilon^3)D_y \end{aligned} \tag{6.2.5}$$

Proof. It is straightforward to check that on the square lattice, the combinatorial laplacian (6.1.1) can be written as a sum of finite difference operators D_x^2, D_y^2, D_x and D_y. (In fact, any operator that couples only nearest neighbor vertices and and annihilates constant functions can be written in terms of these finite difference operators). The proposition then follows from comparing the consistency of the finite difference operators (6.2.4), and consistency of the laplacian (6.1.2). □

6.3 Inverse of Combinatorial Laplacian

In this section, we derive an estimate for the combinatorial Green's function Δ_L^i. The approach can be summarized as follows. Since the combinatorial Laplacian is a consistent approximation of Δ, the smooth Green's function G is an approximation of the combinatorial Green's function where it is smooth. However, the Green's function $G(p,q)$ is logarithmically divergent where $p \to q$. We construct an approximate inverse matrix $\widetilde{G}^i$ by replacing these logarithmic divergences with a lattice regularized logarithm function. We show that $\widetilde{G}^i$ is a "parametrix," in the sense that for sufficiently large i, the error

$$R = I - \Delta^i G^i$$

tends to zero, and for sufficiently large i, the inverse Δ_i^{-1} can be written as

$$(\Delta_L^i)^{-1} = G^i(I + R + R^2 + \cdots) \tag{6.3.1}$$

We begin first by recalling some facts about the Greens function of the smooth setting.

Smooth Green's Function

Recall that when the Riemmanian distance function $d : M \times M \to \mathbb{R}$ is smooth away from the diagonal, G can be written neatly in terms of d. Define $\omega : M \times M \to \mathbb{R}$ as satisfying

1. $\Delta\omega(p_1, p_2) = 0$
2. $\omega(p_1, p_2) = -\frac{\sqrt{g(p_1)}}{4\pi} \log(d^2(p_1, p_2))$ for p_2 or $p_1 \in \partial M$

Then the Green's function can be written:

$$G(p_1, p_2) = -\frac{\sqrt{g(p_1)}}{4\pi} \log\left(d^2(p_1, p_2)\right) + \omega(p_1, p_2) \tag{6.3.2}$$

In this decomposition, both terms are divergent: the logarithmic term contains divergences as $p_1 \to p_2$ while ω contains divergences as $p_1, p_2 \to \partial M$.

To understand the divergent behaviour as $p_1 \to p_2$, one can expand the distance function using the Hamilton-Jacobi equation. Letting $(x, y) = p_2 - p_1$, we calculate that as $(x, y) \to 0$:

$$\begin{aligned} d^2(p_1, p_2) =& g_{xx}\, x^2 + g_{yy}\, y^2 \\ &+ \frac{1}{2}\partial_x g_{xx}\, x^3 + \frac{1}{2}\partial_y g_{xx}\, x^2 y + \frac{1}{2}\partial_x g_{yy}\, xy^2 + \frac{1}{2}\partial_y g_{yy}\, y^3 \cdots \end{aligned} \tag{6.3.3}$$

Then for the logarithm of the distance function:

$$\log\left(d^2(p_1, p_2)\right) = \log\left(g_{xx}x^2 + g_{yy}y^2\right) + \log\left(1 + \frac{O(|p_1 - p_2|^3)}{g_{xx}\, x^2 + g_{yy}\, y^2}\right) \tag{6.3.4}$$

as $(x, y) \to 0$. The term on the right is bounded, so we have isolated the divergence into the first term.

Turning to ω, recall that although for fixed p_1, $\omega(p_1, \cdot)$ is smooth, as $p_1 \to \partial M$ the function and its partial derivatives diverge. One can understand the behaviour of $\omega(p_1, \cdot)$ as $p_1 \to \partial M$ using the method of images.(citation?). Define the reflected and the corner distance functions as:

$$d_{R_i}(p_1, p_2) = \inf\{d(p_1, b) + d(b, p_2) \mid b \in \partial M_i\} \tag{6.3.5}$$

$$\begin{aligned} d_{R_{ij}}(p_1, p_2) =& \inf\{d(p_1, b_1) + d(b_1, b_2) + d(b_2, p_2) \\ &\mid b_1 \in \partial M_i, b_2 \in \partial M_j \text{ or } b_1 \in \partial M_j, b_2 \in \partial M_i\} \end{aligned} \tag{6.3.6}$$

The reflected distance function is well defined for all p_2 when $d(p_1, \partial M_i)$ is sufficiently small, and similarly for the corner distance function. By definition, they satisfy $d_{R_i}(p_1, p_2) = d(p_1, p_2)$ when $p_1 \in \partial M_i$, and $d_{R_{ij}}(p_1, p_2) = d_{R_i}(p_1, p_2)$ when $p_2 \in \partial M_j$. In addition, they satisfy the Hamilton-Jacobi equation, so that $\Delta \log(d_{R_i}(p_1, p_2)) = 0$ and $\Delta \log(d_{R_{ij}}(p_1, p_2)) = 0$.

Fix δ such that reflected distance function is well defined when $d_{R_i}(p_1, \cdot)$ is well defined for all i and p_1 with $d(p_1, \partial M_i)$. Let $B_i = \{p | d(p, \partial M_i) < \delta\}$ for all i, $B = \cup_i B_i$. For $i \neq j$ let $C_{ij} = B_i \cap B_j$. Redefine ω by the decomposition:

1. For $p \in C_{ij}$:

$$\begin{aligned} G(p_1, p_2) =& -\frac{1}{4\pi}\log\left(d^2(p_1, p_2)\right) + \frac{1}{4\pi}\log\left(d^2_{R_i}(p_1, p_2)\right) \\ &+ \frac{1}{4\pi}\log\left(d^2_{R_j}(p_1, p_2)\right) - \frac{1}{4\pi}\log\left(d^2_{R_{ij}}(p_1, p_2)\right) + \omega(p_1, p_2) \end{aligned}$$

2. For $p \in B_i$:

$$G(p_1, p_2) = -\frac{1}{4\pi}\log\left(d^2(p_1, p_2)\right) + \frac{1}{4\pi}\log\left(d^2_{R_i}(p_1, p_2)\right) + \omega(p_1, p_2)$$

3. For $p \notin B$:

$$G(p_1, p_2) = -\frac{1}{4\pi}\log\left(d^2(p_1, p_2)\right) + \omega(p_1, p_2)$$

With this redefinition, it can be shown from a Schauder estimate that $\omega(p_1, \cdot)$ is smooth and bounded for all $p_1 \in M$, so that the divergences have been pushed into the reflected distance functions.

We can compute the expansion of the reflected distance functions as before, using the Hamilton-Jacobi equations. Write the coordinates $p_j = (x_j, y_j)$ for $j = 1, 2$, and for simplicity assume that ∂M_i is aligned with the y-axis, and ∂M_j is aligned with the x-axis. Then:

$$d^2_{R_i}(p_1, p_2) = g_{xx}(p_1)\ (x_1 + x_2)^2 + g_{yy}(p_1)\ (y_2 - y_1)^2 + O(x_1^2) + O(|p_1 - p_2|^2)$$
$$d^2_{R_{ij}}(p_1, p_2) = g_{xx}(p_1)\ (x_1 + x_2)^2 + g_{yy}(p_1)\ (y_1 + y_2)^2 + O(x_1^2 + y_1^2) + O(|p_1 - p_2|^2)$$

so that:

$$\log\left(d^2_{R_i}(p_1, p_2)\right) = \log\left(g_x^{-1}(x_1 + x_2)^2 + g_y^{-1}(y_2 - y_1)^2\right) + \cdots \tag{6.3.7}$$
$$\log\left(d^2_{R_{ij}}(p_1, p_2)\right) = \log\left(g_x^{-1}(x_1 + x_2)^2 + g_y^{-1}(y_1 + y_2)^2\right) + \cdots \tag{6.3.8}$$

where the remaining terms are continuous as $p_1, p_2 \to \partial M$.

Combinatorial Green's Function

Now we construct the parametrix G^i for the combinatorial Green's function. It is based on lattice regularized logarithm function, which is a special case of a general formula given in [Ken02], arising in the theory of discrete complex analysis. It is defined as follows:

Definition 8. *For a, b positive real numbers, define $Ł_{(a,b)} : \mathbb{Z}^2 \to \mathbb{R}$ for $(x, y) \in \mathbb{Z}^2$ as:*

$$Ł_{(a,b)}(x, y) = -\frac{\sqrt{ab}}{8\pi^2 i} \int_C \frac{\log(z)}{z} \left(\frac{z + e^{iw}}{z - e^{iw}}\right)^{|x|+|y|} \left(\frac{z + e^{-iw}}{z - e^{-iw}}\right)^{|x|-|y|} dz \tag{6.3.9}$$

where $w = \tan^{-1}\left(\sqrt{b/a}\right)$ and where C is a curve that encircles the points $\pm e^{iw}$ and $\pm e^{-iw}$, but not the origin.

This function satisfies the following properties, the proofs of which can be found in [Ken02],[Buc07]:

1. $Ł_{(a,b)}(0, 0) = 0$
2. $\left(\frac{1}{a}D_x^2 + \frac{1}{b}D_y^2\right) Ł_{(a,b)}(x, y) = \delta_{0x}\delta_{0y}$
3. $Ł_{(a,b)}(x, y)$ has the asymptotic expansion for $x, y \to \infty$:

$$Ł_{(a,b)}(x, y) = -\frac{\sqrt{ab}}{4\pi} \log\left(\frac{16\gamma^2}{a + b}\right) - \frac{\sqrt{ab}}{4\pi} \log\left(ax^2 + by^2\right) - \frac{\sqrt{ab}}{24\pi} \frac{ab\left(bx^4 - (a + b)x^2y^2 + ay^4\right)}{(b\ x^2 + a\ y^2)^3} + O\left(\frac{1}{(x^2 + y^2)^2}\right)$$

where $\gamma_l = \exp(\gamma_e)$ is the exponential of the Euler gamma γ_e.

4. The finite difference derivatives of $\text{Ł}_{(a,b)}$ have the asymptotic expansion:

$$\begin{aligned}
D_x\text{Ł}_{(a,b)}(x,y) &= \frac{\sqrt{ab}}{2\pi}\frac{ax}{ax^2+by^2} + O\left(\frac{1}{(x^2+y^2)^{3/2}}\right)\\
D_x^2\text{Ł}_{(a,b)}(x,y) &= \frac{\sqrt{ab}}{2\pi}\frac{ab\,y^2-a^2x^2}{(ax^2+by^2)^2} + O\left(\frac{1}{(x^2+y^2)^2}\right)\\
D_y\text{Ł}_{(a,b)}(x,y) &= \frac{\sqrt{ab}}{2\pi}\frac{by}{ax^2+by^2} + O\left(\frac{1}{(x^2+y^2)^{3/2}}\right)\\
D_y^2\text{Ł}_{(a,b)}(x,y) &= \frac{\sqrt{ab}}{2\pi}\frac{ab\,x^2-b^2y^2}{(ax^2+by^2)^2} + O\left(\frac{1}{(x^2+y^2)^2}\right)
\end{aligned} \tag{6.3.10}$$

(Here it is understood that in the finite difference operators $\epsilon = 1$.)

5. At the origin, the derivative is:

$$\begin{aligned}
D_x\text{Ł}_{(a,b)}(0,0) &= 0\\
D_x^2\text{Ł}_{(a,b)}(0,0) &= \frac{2a}{\pi}\tan^{-1}\left(\sqrt{\frac{b}{a}}\right)\\
D_y\text{Ł}_{(a,b)}(0,0) &= 0\\
D_y^2\text{Ł}_{(a,b)}(0,0) &= \frac{2b}{\pi}\tan^{-1}\left(\sqrt{\frac{a}{b}}\right)
\end{aligned}$$

Green's function on X^i

We now utilize the lattice logarithm defined above to construct the Green's function on X^i. Roughly speaking, we replace all logarithmic divergences identified in §6.3 with corresponding lattice logarithm functions. For some notational simplicity, we fix:

$$\begin{aligned}
L(p_1,p_2) &= -\frac{\sqrt{g(p_1)}}{4\pi}\log\left(g_{xx}(p_1)x^2 + g_{yy}(p_2)y^2\right)\\
\text{Ł}(p_1,p_2) &= \text{Ł}_{g(p_1)}\left(\frac{x}{\epsilon},\frac{y}{\epsilon}\right)
\end{aligned} \tag{6.3.11}$$

where $(x,y) = p_2 - p_1$. We define also $L_{R_i}, L_{R_{ij}}$ and $\text{Ł}_{R_i}, \text{Ł}_{R_{ij}}$ in the obvious way based on the expansions (6.3.7).

Then, define $G^i : X_0^i \times X_0^i \to \mathbb{R}$ as:

1. For $p \in C_{ij}$:

$$\begin{aligned}
G^i(p_1,p_2) = G(p_1,p_2) &- L(p_1,p_2) + \text{Ł}(p_1,p_2)\\
&- L_{R_i} + \text{Ł}_{R_i}(p_1,p_2)\\
&- L_{R_j} + \text{Ł}_{R_j}(p_1,p_2)\\
&+ L_{R_{ij}} - \text{Ł}_{R_{ij}}(p_1,p_2)
\end{aligned}$$

2. For $p \in B_i$:

$$G^i(p_1,p_2) = G(p_1,p_2) - L(p_1,p_2) + Ł(p_1,p_2) \\ - L_{R_i} + Ł_{R_i}(p_1,p_2)$$

3. For $p \notin B$:

$$G^i(p_1,p_2) = G(p_1,p_2) - L(p_1,p_2) + Ł(p_1,p_2)$$

Here, when $p_1 = p_2$ we set $I_{X^i}(G(p_1,p_1) + L(p_1,p_1)) = 0$.

We now estimate the error $R^i = \Delta^i G^i - I$. The series converges if in the operator norm $|R^i|_{op} < 1$. We show the stronger condition that each column of R^i has L_1 norm of $O(\epsilon)$. It follows then that for sufficiently large i, $|R^i|_{op} < 1$.

Proposition 8. *Let $R : X_0^i \times X_0^i \to \mathbb{R}$ be defined as:*

$$R^i(p_1,p_2) = \Delta^i G^i(p_1,p_2) - \delta_{p\cdot}$$

Then there is a constant C such that:

$$\sum_{p_2 \in X_0^i} |R^i(p_1,p_2)| \le Ch$$

Proof. We assume that $p_1 \notin B$, and we split the sum

$$\sum_{p_2 \in X_0^i} |R^i(p_1,p_2)| = R^i(p_1,p_1) + \sum_{\substack{p_2 \in X_0^i \\ p_2 \neq p_1}} |R^i(p_1,p_2)| \tag{6.3.12}$$

When $p_1 \neq p_2$, we write $R^i(p_1,p_2)$ using the fact that $\Delta G(p_1,p_2) = 0$ as follows:

$$\begin{aligned} |R^i| &= |\Delta^i G - \Delta^i L + \Delta^i Ł| \\ &= |\Delta^i G - \Delta^i L - \epsilon^2(\Delta G - \Delta L) + \Delta^i Ł - \epsilon^2 \Delta L| \\ &\le \left|\Delta^i G - \Delta^i L - \epsilon^2(\Delta G - \Delta L)\right| + \left|\Delta^i Ł - \epsilon^2 \Delta L\right| \end{aligned} \tag{6.3.13}$$

We estimate the two terms seperately using the aymptotic expansion of (6.2.5) of Δ^i, along with the consistency properties of the finite difference operators for the first term, and the asymptotic formulas (6.3.10) of Ł for the second term.

We begin with the first term: $|\Delta^i G - \Delta^i L - \epsilon^2(\Delta G - \Delta L)|$. Recall that the errors of the first and second order finite difference operators are bounded by the third and fourth partial derivatives of $G(p_1,p_2)$ and $L(p_1,p_2)$, which diverge near the diagonal. However, we can estimate these divergent terms using the expansion of the distance function (6.3.3). Letting $(x,y) = p_2 - p_1$, as $(x,y) \to 0$ we have:

$$\begin{aligned} &G(p_1,p_2) - L(p_1,p_2) \\ &\qquad = -\frac{\sqrt{g(p_1)}}{4\pi} \log\left(1 + \frac{\frac{1}{2}\partial_x g_{xx}\, x^3 + \frac{1}{2}\partial_y g_{xx}\, x^2 y + \frac{1}{2}\partial_x g_{yy}\, xy^2 + \frac{1}{2}\partial_y g_{yy}\, y^3 \cdots}{g_{xx}x^2 + g_{yy}y^2}\right) \end{aligned} \tag{6.3.14}$$

(we ignore $\omega(p_1, p_2)$ since it is smooth). From this, we can calculate explicitly that the third and fourth partial derivatives behave as $p_2 \to p_1$ as:

$$\partial_x^m \partial_y^{3-m} G(p_1, p_2) - \partial_x^m \partial_y^{3-m} L(p_1, p_2) = O\left(\frac{1}{|p_2 - p_1|^2}\right)$$
$$\partial_x^m \partial_y^{4-m} G(p_1, p_2) - \partial_x^m \partial_y^{4-m} L(p_1, p_2) = O\left(\frac{1}{|p_2 - p_1|^3}\right)$$

Here the constant of proportionalities in the asymptotics can be written in terms of the metric g and its partial derivatives, which we omit writing for brevity. Then we have:

$$\left|D_x^2(G - L) - \epsilon^2 \partial_x^2 (G - L)\right| = \frac{O(\epsilon^4)}{|p_2 - p_1|^3}$$
$$\left|\epsilon D_x(G - L) - \epsilon^2 \partial_x (G - L)\right| = \frac{O(\epsilon^4)}{|p_2 - p_1|^2}$$

and similar expressions for the y-direction. It follows from this and equation (6.2.5) that:

$$|\Delta^i G(p_1, p_2) - \Delta^i L(p_1, p_2) - \epsilon^2 (\Delta G(p_1, p_2) - \Delta L(p_1, p_2))| = \frac{O(\epsilon^4)}{|p_2 - p_1|^3} \tag{6.3.15}$$

We turn now to $|\Delta^i Ł - \epsilon^2 \Delta L|$. First observe that the equations (6.3.10) can be rewritten as:

$$D_x^2 Ł(p_1, p_2) = \epsilon^2 \partial_x^2 L(p_1, p_2) + \frac{O(\epsilon^4)}{x^4}$$
$$\epsilon D_x Ł(p_1, p_2) = \epsilon^3 \partial_x L(p_1, p_2) + \frac{O(\epsilon^4)}{x^3}$$

and similar expressions for the y-direction. In addition, recall that for $p_1 \neq p_2$, we have $\left(\frac{D_x^2}{g_{xx}(p_1)} + \frac{D_y^2}{g_{yy}(p_1)} D_y^2\right) Ł(p_1, p_2) = 0$ and $\left(\frac{\partial_x^2}{g_{xx}(p_1)} + \frac{\partial_y^2}{g_{yy}(p_1)}\right) L(p_1, p_2) = 0$ Thus:

$$|\Delta^i Ł - \epsilon^2 \Delta L| = \left| \left(\Delta^i - \frac{D_x^2}{g_{xx}(p_1)} - \frac{D_y^2}{g_{yy}(p_1)}\right) Ł - e^2 \left(\Delta - \frac{\partial_x^2}{g_{xx}(p_1)} - \frac{\partial_y^2}{g_{yy}(p_1)}\right) L \right|$$

Using again the expression (6.2.5) for Δ^i, it follows that:

$$|\Delta^i Ł(p_1, p_2) - \epsilon^2 \Delta L(p_1, p_2)| = \frac{O(\epsilon^4)}{|p_2 - p_1|^3} \tag{6.3.16}$$

Putting together (6.3.16) and (6.3.15), we find for $p_1 \neq p_2$:

$$|R^i(p_1, p_2)| = \frac{O(\epsilon^4)}{|p_2 - p_1|^3} \tag{6.3.17}$$

We can estimate the sum by changing variables $p = (p_2 - p_1)/\epsilon$. Then:

$$\sum_{\substack{p_2 \in X_0^i \\ p_2 \neq p_1}} |R^i(p_1, p_2)| \leq O(\epsilon) \sum_{p \in \mathbb{Z}^2 \setminus 0} \frac{1}{|p|^3} \leq O(\epsilon) \left(\int_1^\infty \frac{2\pi |p|}{|p|^3} d|p| + 1 \right)$$
$$= O(\epsilon) \tag{6.3.18}$$

Lastly, we have the case $p_1 = p_2$. We compute explicitly:

$$\begin{aligned} \Delta^i Ł(p_1, p_1) &= 1 + O(\epsilon^2) \\ \Delta^i G(p_1, p_1) - \Delta^i(p_1, p_1) &= O(\epsilon^2) \end{aligned} \tag{6.3.19}$$

Putting together equations (6.3.16) and (6.3.18) completes the calculation. The case where $p \in B$ is identical except for the additional "image" charges that can be handled in precisely the same way.

□

6.4 Asymptotic Determinant of Laplacian

In this section, we derive an expression (6.4.21) for the variation of the determinant of the combinatorial laplacian. It is more convenient to write variations of g in terms of scaling variations and . Letting $\lambda = \sqrt{g_{xx} g_{yy}}$ and $\omega = \sqrt{g_{yy}/g_{xx}}$, we rewrite (6.2.5) as:

$$\begin{aligned} \Delta_L^i = \frac{1}{\lambda} \left(\omega \ D_x^2 + \omega^{-1} \ D_y^2 + \epsilon \partial_x \omega \ D_x + \epsilon \partial_y \omega^{-1} \ D_y \right) \\ + \left(O(\epsilon^2) D_x^2 + O(\epsilon^2) D_y^2 + O(\epsilon^3) D_x + O(\epsilon^3) D_y \right) \end{aligned}$$

Then we rewrite (6.2.3) as:

$$\begin{aligned} \mathrm{Tr}\left((\Delta_L^i)^{-1} \delta \Delta_L^i \right) = & \sum_{p \in X \setminus \partial X} -\frac{\delta \lambda}{\lambda} \Delta_L^i (\Delta_L^i)^{-1}(p,p) \\ & + \frac{1}{\lambda} \sum_{p \in X \setminus \partial X} \left(\delta\omega \ D_x^2 - \frac{\delta\omega}{\omega^2} \ D_y^2 + \epsilon \partial_x \delta\omega \ D_x - \epsilon \frac{\partial_y \delta\omega}{\omega^2} D_y \right) (\Delta_L^i)^{-1}(p,p) \\ & + \sum_{p \in X \setminus \partial X} \left(O(\epsilon^2) D_x^2 + O(\epsilon^2) D_y^2 + O(\epsilon^3) D_x + O(\epsilon^3) D_y \right) (\Delta_L^i)^{-1}(p,p) \end{aligned} \tag{6.4.1}$$

The finite difference derivatives of the Green's function $G(p,p)$ at the diagonal can be estimated using the results of the last section. The key is that all relevant terms are given by Ł:

Proposition 9. *Asymptotics of the partial derivatives of the Green's functions. For $p \in X_0$, let $r_{p,\partial M}$ be the Euclidean distance in $\mathbb{R}^2$ of p to ∂M. Then:*

$$D_x^2(\Delta^i)^{-1}(p,p) = D_x^2 Ł(p,p) + \frac{O(\epsilon^4)}{d^3}$$
$$D_x(\Delta^i)^{-1})(p,p) = O(\epsilon)$$

and similar expressions for the y-direction. When p is near the boundary, $d_{p,\partial M} \leq \delta_{\partial M}$, then we have a different estimate including the image charges. Let $p \in B_i$. Then:

$$D_x^2(\Delta^i)^{-1}(p,p) = D_x^2 Ł_(p,p) - D_x^2 Ł_{R_i}(p,p) + O(\epsilon^2)$$
$$D_x(\Delta^i)^{-1}(p,p) = D_x Ł_{R_i}(p,p) + O(\epsilon)$$

Finally when $p \in C_{ij}$, we have:

$$D_x^2(\Delta^i)^{-1}(p,p) = D_x^2 Ł_(p,p) - D_x^2 Ł_{R_i}(p,p) - D_x^2 Ł_{R_j}(p,p) + D_x^2 Ł_{R_{ij}}(p,p) + O(\epsilon^2)$$
$$D_x(\Delta^i)^{-1}(p,p) = -D_x Ł_{R_i}(p,p) - D_x Ł_{R_j}(p,p) + D_x Ł_{R_{ij}}(p,p) + O(\epsilon)$$

and similar expressions for the y-direction.

Proof. Recall that from (6.3.1) that:

$$(\Delta^i)^{-1} = G^i + G^i R^i + G^i R^i R^i \cdots$$

We estimate $D_x^2(\Delta^i)^{-1}(p,p)$ and $D_x(\Delta^i)^{-1}(p,p)$ by first calculating $D_x^2 G^i(p,p)$ and $D_x G(p,p)$. Then we show that the higher order terms only contribute at $O(\epsilon^2)$.

As before, we assume that $p \notin B$. Recall that $G^i(p_1,p_2) = G(p_1,p_2) - Ł(p_1,p_2) + Ł(p_1,p_2)$. By direct computation using the expansion (6.3.14) for $G - L$, we find:

$$D_x^2 G(p,p) - D_x^2 L(p,p) + D_x^2 Ł(p,p) = D_x^2 Ł(p,p) + O(\epsilon^2) D_x G(p,p) - D_x L(p,p) + D_x Ł(p,p) = O(\epsilon)$$

and similar expressions for the y-direction.

We turn now to the second order term:

$$D_x^2 G^i R^i(p_1,p_1) = \sum_{p_2 \in X_0^i} D_x^2 G^i(p_1,p_2) R(p_2,p_1)$$

Fix r to be the (euclidean) distance to the boundary, ie $r = \inf\{|p - p_2| \;\big|\; p_2 \in \partial M\}$. We break the sum:

$$\sum_{p_2 \in X_0^i} D_x^2 G^i(p_1,p_2) R(p_2,p_1) = D_x^2 G^i(p_1,p_1) R^i(p_1,p_1) \tag{6.4.2}$$
$$+ \sum_{0<|p_2-p_1|\leq r} D_x^2 G^i(p_2,p_1)\; R^i(p_1,p_2) \tag{6.4.3}$$
$$+ \sum_{|p_2-p_1|>r} D_x^2 G(p_2,p_1) R^i(p_1,p_2) \tag{6.4.4}$$

and estimate each term seperately.

We begin with the region $|p_2 - p_1| > r$. We can estimate $R^i(p_1, p_2)$ as before with equation (6.3.16):

$$|R^i(p_1, p_2)| = \frac{O(\epsilon^4)}{|p_2 - p_1|^3}$$

To estimate $D_x^2 G^i(p_2, p_1)$, we use (6.3.15) and (6.3.10) to find:

$$D_x^2 G^i(p_2, p_1) = \frac{O(\epsilon^2)}{|p_2 - p_1|^2}$$

Thus we find:

$$\begin{aligned}\sum_{|p_2-p_1|>r} D_x^2 G(p_2, p_1) R^i(p_1, p_2) &= \sum_{|p-p_1|>r} \frac{O(\epsilon^6)}{|p_2 - p_1|^5} \\ &= \frac{O(\epsilon^4)}{r^3}\end{aligned} \tag{6.4.5}$$

Next, we turn to the region $0 < |p_2 - p_1| < r$. This region requires more work because there is considerable cancellation. We first find a more refined estimate for $R^i(p_1, p_2)$ and show that largest terms of $O(\epsilon)$ in $R^i(p_1, p_2)$ are antisymmetric about p_1 (ie. odd as a function of $(x, y) = p_2 - p_1$). We show that $D_x^2 G^i(p_1, p_2)$, on the other hand is symmetric about p_1. Thus, the sum (6.4.3) vanishes at $O(\epsilon)$.

As before, we write $R^i(p_1, p_2)$ as in (6.3.13). Considering the term:

$$|\Delta^i G(p_1, p_2) + \Delta^i L(p_1, p_2) - \Delta G(p_1, p_2) - \Delta L(p_1, p_2)| \tag{6.4.6}$$

we can use the expansion (6.3.13) and expand for small (x, y):

$$1 + \frac{\frac{1}{2}\partial_x g_{xx}\, x^3 + \frac{1}{2}\partial_y g_{xx}\, x^2 y + \frac{1}{2}\partial_x g_{yy}\, xy^2 + \frac{1}{2}\partial_y g_{yy}\, y^3}{g_{xx}x^2 + g_{yy}y^2} + \cdots$$

The first term is clearly odd in (x, y), and the fourth partial derivatives of the higher order terms are only $O(1/(p_2 - p_1)^2)$ as $p_2 \to p_1$. Consequently, using (6.2.5) again, we write:

$$|\Delta^i G(p_1, p_2) + \Delta^i L(p_1, p_2) - \Delta G(p_1, p_2) - \Delta L(p_1, p_2)| = O(\epsilon^4) f(p_1, p_2) + \frac{O(\epsilon^4)}{|p_2 - p_1|^2} \tag{6.4.7}$$

for a function f that is anti symmetric with about p_1 and $f(p_1, p_2) = O(\frac{1}{|p_1 - p_2|^3}$ as $p_2 \to p_1$. Next, compute a similar estimate for $\Delta^i \mathfrak{L}$. Since both $\mathfrak{L}(p_1, p_2)$ and $L(p_1, p_2)$ are even about p_1 it follows

$$\begin{aligned} &D_x^2 \mathfrak{L}(p_1, p_2) - \partial_x^2 L(p_1, p_2) \\ &D_y^2 \mathfrak{L}(p_1, p_2) - \partial_y^2 L(p_1, p_2)\end{aligned}$$

are even. Since, as before we have $g(p_1)D_x^2 + g(p_1)D_y^2 Ł = 0$ we find using (**??**) that

$$\Delta^i \mathfrak{L}(p_1, p_2) - \Delta L(p_1, p_2) = \epsilon^4 f_2(x, y) + \frac{O(\epsilon^2)}{|p_2 - p_1|} \tag{6.4.8}$$

for a function f_2 that is odd and $f_2(x, y) = O(\frac{1}{|p_1 - p_2|^3})$. Putting together equations (6.4.7) and (6.4.8), we find:

$$R^i(p_1, p_2) = \epsilon^4 f_1(p_1, p_2) + \frac{O(\epsilon^4)}{|p_2 - p_1|^2} \tag{6.4.9}$$

where $f_1(p_1, p_2)$ is an odd function, bounded by $\frac{1}{|p_1 - p_2|^3}$.

Next we estimate $D_x^2 G^i(p_2, p_1)$. Assume $p_2 \notin B$. First we have:

$$D_x^2 G(p_1, p_2) - D_x^2 L(p_1, p_2) = \frac{O(\epsilon^2)}{|p_1 - p_2|}$$

Turning to $D_x^2 \mathfrak{L}(p_2, p_1)$, recall that:

$$D_x^2 \mathfrak{L}(p_2, p_1) = D_x^2 \mathfrak{L}_{g(p_2)}(x/\epsilon, y\epsilon)$$

We can expand out the dependence on the metric as:

$$D_x^2 \mathfrak{L}_{g(p_2)}(x/\epsilon, y/\epsilon) = D_x^2 \mathfrak{L}_{g(p_1)}(p_2, p_1) + \frac{O(\epsilon^2)}{|p_1 - p_2|}$$

Notice however that $D_x^2 Ł$ is an even function. If $p_2 \in B$, there are additional image charges are bounded by $\frac{O(\epsilon^2)}{r^2}$. In either case, we can write:

$$D_x^2 G^i(p_1, p_2) = \epsilon^2 f_2(p_1, p_2) + \frac{O(\epsilon^2)}{|p_1 - p_2|} \tag{6.4.10}$$

for a function f_3 even about p_1.

Putting the estimates (6.4.10) and (6.4.9) into (6.4.3), we have finally:

$$\sum_{0<|p_2-p_1|\leq r} D_x^2 G^i(p_2, p_1) = \sum_{0<|p_2-p_1|\leq r} \epsilon^6 f_2(p_1, p_2) f_1(p_1, p_2) + \frac{O(\epsilon^6)}{|p_2 - p_1|} = O(\epsilon^5)$$

where the first term vanishes due to the even-odd.

The contribution of the higher order terms in (6.3.1) can be estimated using (6.3.16) and we omit the details. □

Returning to equation (6.4.1), note first that there are $O(\frac{1}{\epsilon^2})$ vertices as $\epsilon \to 0$, so that any summand of $O(\epsilon^2)$ in will contribute at most a constant term in the asymptotic expansion, which we neglect. Recall that B, C. Thus using Proposition (9), we drop irrelevant terms, and rearrange equation (6.4.1) as:

$$\mathrm{Tr}\left((\Delta_L^i)^{-1} \delta \Delta_L^i\right) = \sum_{p \in X \setminus L} [\text{bulk}] + \sum_{p \in B} [\text{boundary}] + \sum_{p \in C} [\text{corner}] \tag{6.4.11}$$

where the summands are:

$$[\text{bulk}] = -\frac{\delta\lambda}{\lambda} + \frac{1}{\lambda}\left(\delta\omega\ D_x^2 - \frac{\delta\omega}{\omega^2}\ D_y^2\right) Ł(p_1, p_1) \tag{6.4.12}$$

$$[\text{boundary}] = \left(\frac{\delta\omega}{\lambda}D_x^2 - \frac{\delta\omega}{\lambda\omega^2}D_y^2 + \epsilon\partial_x\delta\omega D_x - \epsilon\delta\left(\frac{\partial_y\omega}{\omega^2}\right)D_y\right) Ł_{R_i}(p_1, p_2) \tag{6.4.13}$$

$$[\text{corner}] = \left(\frac{\delta\omega}{\lambda}D_x^2 - \frac{\delta\omega}{\lambda\omega^2}D_y^2 + \epsilon\partial_x\delta\omega D_x - \epsilon\delta\left(\frac{\partial_y\omega}{\omega^2}\right)D_y\right) Ł_{R_ij}(p_1, p_2) \tag{6.4.14}$$

we compute each of these sums in the following subsections. To compute these sums, we utilize the Euler-MacLaurin formula, which we write as:

Proposition 10. *Let $f \in C^\infty([0,1])$, and $N \in \mathbb{N}$, then:*

$$\sum_{i=1}^{N-1} f(i/N) = N\int_0^1 f(x)dx - \frac{1}{2}(f(0)+f(1)) + O\left(\frac{1}{N}\right)$$

Let $S = [0,1]\times[0,1]$ be the unit square and $g \in C^\infty(S)$. Then

$$\sum_{i=1}^{N-1}\sum_{j=1}^{M-1} g(i/N, j/N) = N^2\int_S g(x,y)\ dx\ dy - \frac{N}{2}\int_{\partial S} g(s)ds + O(1)$$

Bulk Term

The bulk sum is:

$$\begin{aligned}&\sum_{p\in X\setminus L} -\frac{\delta\lambda}{\lambda} + \frac{1}{\lambda}\left(\delta\omega\frac{2\lambda}{\pi\omega}\tan^{-1}(\omega) - \frac{\delta\omega}{\omega^2}\frac{2\lambda\omega}{\pi}\tan^{-1}\left(\frac{1}{\omega}\right)\right)\\ =&\sum_{p\in X\setminus L} -\frac{\delta\lambda}{\lambda} + \frac{2\ \delta\omega}{\pi\ \omega}\left(\tan(\omega) - \tan^{-1}(\omega^{-1})\right)\end{aligned}$$

Using the Euler-MacLaurin formula, we find that the bulk contribution to the asymptotic determinant is:

$$\begin{aligned}&\frac{1}{\epsilon^2}\int_M -\frac{\delta\lambda}{\lambda} + \frac{2\ \delta\omega}{\pi\ \omega}\left(\tan(\omega) - \tan^{-1}(\omega^{-1})\right)\ dx\ dy\\ &\quad - \frac{1}{2\epsilon}\int_{\partial M} -\frac{\delta\lambda}{\lambda} + \frac{2\ \delta\omega}{\pi\ \omega}\left(\tan(\omega) - \tan^{-1}(\omega^{-1})\right) ds\end{aligned} \tag{6.4.15}$$

Boundary Term

We will compute the contribution of one boundary region B_i. We first sum in the normal direction of the boundary ∂M_i, and then sum along the boundary using the Euler-Maclaurin formula. We assume is aligned with the y-axis. We choose coordinates (x, y) chosen so that ∂M_i is on the y-axis with the interior of M in the region $x > 0$.

Observe that in the boundary summand (6.4.13) by symmetry the term $D_y Ł_{R_i}$ vanishes. In addition, $\left(\frac{\omega}{\lambda}D_x^2 + \frac{1}{\lambda\omega}D_y^2\right) Ł_{R_i}$. So we rewrite (6.4.13) as:

$$2\frac{\delta\omega(p_1)}{\lambda(p_1)}D_x^2 Ł_{R_i}(p_1,p_1) + \epsilon\frac{\partial_x\delta\omega(p_1)}{\lambda(p_1)}D_y Ł_{R_i}(p_1,p_1) \tag{6.4.16}$$

We expand the terms in the x-coordinate, normal to the boundary:

$$\begin{aligned}\frac{\delta\omega(x,y)}{\lambda(x,y)} &= \frac{2\delta\omega(0,y)}{\lambda(0,y)} + x\,2\frac{\partial_x\delta\omega(0,y)\lambda(0,y) - \partial_x\lambda(0,y)}{\lambda(0,y)^2} + \cdots \\ \frac{\partial_y\delta\omega(x,y)}{\lambda(x,y)} &= \frac{\partial_x\delta\omega(x,0)}{\lambda(x,0)} + \cdots\end{aligned}$$

Recall that $Ł_{R_i}(p_1,p_1) = Ł_{g(x,y)}(2x/\epsilon,0)$. We can expand the spatial dependence in the metric $g(x,y)$ as:

$$D_x^2 Ł_{g(x,y)}(2x/\epsilon,0) = D_x^2 Ł_{g(x,0)}(2x/\epsilon) - \frac{1}{8\pi}\frac{\epsilon\,\partial_x\lambda(x,0)}{x} + \frac{O(\epsilon^3)}{x^2} \tag{6.4.17}$$

This expression can be justified with using the definition of Ł and the equation (6.3.9), but it is easy to guess from the asymptotic expression (6.3.10), which we rewrite in terms of λ and ω as:

$$\begin{aligned}D_x^2 Ł_{g(x,y)}(2x/\epsilon,0) &= -\frac{\lambda(x,y)\epsilon^2}{8\pi x^2} + \frac{O(\epsilon^4)}{x^4} \\ D_x Ł_{g(x,y)}(2x/\epsilon,0) &= \frac{\lambda(x,y)\epsilon^2}{4\pi x} + \frac{O(\epsilon^3)}{x^2}\end{aligned}$$

Using these expansions in (6.4.16), we find that all terms of order $\frac{O(\epsilon)}{x}$ cancel so that we have for (6.4.16):

$$\frac{2\delta\omega(0,y)}{\lambda(0,y)}D_x^2 Ł_{g(x,0)}(2x/\epsilon,0) + \frac{O(\epsilon^3)}{x^2}$$

We now sum normal to the boundary:

$$\begin{aligned}&\sum_{x=\epsilon}^{\delta}\left(\frac{2\delta\omega(0,y)}{\lambda(0,y)}D_x^2 Ł_{g(x,0)}(2x/\epsilon,0) + \frac{O(\epsilon^3)}{x^2}\right) \\ &\qquad = -\frac{\delta\omega(0,y)}{2\sqrt{1+\omega(0,y)^2}} + \frac{2\delta\omega(0,y)}{\pi\omega(y,0)}\tan^{-1}(\omega) + O(\epsilon)\end{aligned}$$

Finally, we sum along the boundary using the Euler-Maclaurin formula:

$$\frac{1}{\epsilon}\int_{\partial M_i}\left(-\frac{\delta\omega}{2\sqrt{1+\omega^2}} + \frac{2}{\pi}\frac{\delta\omega}{\omega} + \frac{\delta\omega}{\pi\omega}(\tan^{-1}(\omega) - \tan^{-1}(\omega^{-1})\right)dy + O(1)$$

For the other boundary segments oriented along the x-axis, we have the same formula but with $\omega \to \frac{1}{\omega}$. We summarise this by writing:

$$\delta B_x = -\frac{\delta\omega}{2\sqrt{1+\omega^2}} + \frac{\delta\omega}{\omega} \tag{6.4.18}$$

$$\delta B_y = \frac{\delta\omega}{2\omega\sqrt{1+\omega^2}} - \frac{\delta\omega}{\omega} \tag{6.4.19}$$

And writing the boundary contribution as:

$$\frac{1}{\epsilon}\int_{\partial M} \delta B_\perp \ + \frac{\delta\omega}{\pi\omega}(\tan^{-1}(\omega) - \tan^{-1}(\omega^{-1})ds + O(1) \tag{6.4.20}$$

Corner Term

Using methods very similar to the previous subsection, it is straightforward to check that the corner terms (6.4.14) do not contribute to the asymptotic expansion. We omit the details.

Determinant

We now compile together (6.4.15) and (6.4.20) into equation (6.4.11). The boundary term in (6.4.12) cancels with part of (6.4.13). So we have in total:

$$\delta \log\det\Delta = \frac{1}{\epsilon^2}\int_M \delta F dx\ dy \ + \frac{1}{\epsilon}\int_{\partial M} \delta B_\perp ds + O(1) \tag{6.4.21}$$

where:

$$\delta F = -\frac{\delta\lambda}{\lambda} + \frac{2\ \delta\omega}{\pi\ \omega}\left(\tan(\omega) - \tan^{-1}(\omega^{-1})\right)$$

$$\delta B_x = -\frac{\delta\omega}{2\sqrt{1+\omega^2}} + \frac{\delta\omega}{\omega} - \frac{\delta\lambda}{\lambda}$$

$$\delta B_y = \frac{\delta\omega}{2\omega\sqrt{1+\omega^2}} - \frac{\delta\omega}{\omega} - \frac{\delta\lambda}{\lambda}$$

To compute the determinant, we integrate (6.4.21). The constant of integration is fixed when $\lambda = 1$ and $\omega = 1$ by the expansion (6.0.2). We find:

$$\log\det\Delta = \frac{1}{\epsilon^2}\int_M F dx\ dy \ + \frac{1}{\epsilon}\int_{\partial M} B_\perp ds + O(1)$$

where

$$F = \log(\lambda) + \frac{2}{\pi}\Im\left(Li_2\left(i\omega\right) + Li_2\left(i\omega^{-1}\right)\right)$$

$$B_x = -\log(1+\sqrt{1+\omega^{-2}}) - \log(\lambda)$$

$$B_y = -\log(1+\sqrt{1+\omega^{2}}) - \log(\lambda)$$

Substituting $\lambda = \sqrt{g_{xx}g_{yy}}$ and $\omega = \sqrt{g_{yy}/g_{xx}}$ yields (6.2.2).

6.5 Conclusions

There are many areas where we believe this work can be improved or generalized. We conclude by outlining some of these areas.

In this paper, we have focused on the square lattice on which one can approximate diagonal metrics. To study more general metrics, one could for example add the diagonal edges of the square lattice. Our methods do not generalize easily to this case - the difficulty is in calculating boundary contributions. In fact,the case where the metric is constant but nondiagonal has not been computed in the literature. One could also consider massive Laplacian operators of the form $\Delta + m^2$ or even more generally $\Delta + V(x)$ for some potential function $V \in C^\infty(M)$. In this case, we expect the asymptotic expansion to the be same up to logarithmic terms, although we have not tried to prove this in this paper. For results in this direction, see [Cha06].

Another avenue for generalization is to study the combinatorial Laplacian on non-rectangular regions, for instance, rectilinear regions in $\mathbb{Z}^2$. We conjecture that the asymptotic expansion for this case is the obvious generalization of (6.0.3). An approach to this would be to derive gluing formulas for the asymptotic expansions. Similar gluing formulas were derived in [Ken00] by exploiting the relation to the spanning tree model. Alternatively, gluing formulas for determinants can be written in terms of the discrete Dirichlet-to-Neumann operator, which could be studied in the asymptotic limit using estimates for the discrete Green's function given in this paper.

In this paper, we have focused on the laplacian and have not studied the discrete dirac operator, and dimer model on graphs with Riemannian structure. We plan to study this in a future publication. Existing results already give the leading order contribution in the asymptotic partition function and also the average height function [Ken09], but we believe it is possible to strengthen these results for the dimer models defined in this paper.

Finally, as we have previously mentioned, we have not attempted to investigate the constant term in the asymptotic expansion of the determinant. It is clear that the constant term depends on details of the combinatorial Laplacian not fixed by requiring its consistency. However, for the pure graph laplacian on the square lattice, corresponding to a Euclidean metric, it is known that the constant term in the expansion is equal to the ζ-regularized determinant of the analytic laplacian. We question if there is a natural condition on combinatorial Laplacians for which the constant term in the asymptotic expansion of the determinant is equal to the ζ-regularized determinant. Identifying such a condition would be a step towards defining a free Gaussian field theory as the regularized limit of discrete Gaussian field theories.

Bibliography

[A] Amol Aggarwal. *Current Fluctuations of the Stationary ASEP and Six-Vertex Model.* arXiv:1608.04726

[AR] D. Allison, N. Reshetikhin. *The 6-vertex model with fixed boundary conditions* , Annales de l'institut Fourier. Vol. 55. No. 6. 2005. arXiv:cond-mat/0502314.

[BL] Jinho Baik, Zhipeng Liu. *TASEP on a ring in sub-relaxation time scale*, arXiv:1608.08263.

[Ba] R.J. Baxter. *Exactly Solved Models in Statistical Mechanics*, 1982 , Dover Publications, London.

[BCG] A. Borodin, I. Corwin, V. Gorin. *Stochastic six-vertex model.* Duke Math. J. 165, no. 3 (2016), 563-624

[BF] A. Benassi, J. P. Fouque, *Hydrodynamic limit for the asymmetric simple exclusion process.* Ann. Prob. 15:546-560 (1987)

[BFK] D. Burghelea, L. Friedlander, and T. Kappeler *On the determinant of elliptic differential and finite difference operators in vector bundles over* S^1. Comm. Math. Phys. Volume 138, Number 1 (1991), 1-18.

[BLZ] V. Bazhanov, S. Lukyanov, A. Zamolodchikov. *Integrable structure of conformal field theory, quantum KdV theory and thermodynamic Bethe ansatz.* Comm. Math. Phys. Volume 177, Number 2 (1996), 381-398.

[BS] D.J. Bukman and J.D. Shore, *The conical Point in the Ferroelectric Six-Vertex Model.* J. Stat. Phys. 78, 1277-1309, 1995.

[Buc07] U. Bucking, *Approximation of conformal mappings by circle patterns and discrete minimal surfaces* Ph.D. thesis, Technische Universitat Berlin, 2007

[CaPes] J. Cardy. I Peschel. *Finite-size dependence of the free energy in two-dimensional critical systems.* Nuclear Physics B Volume 300, 1988, pp. 377392.

[CEP] H. Cohn, N. Elkies, J. Propp. *Local statistics for random domino tilings of the Aztec diamond.*, Duke Mathematical Journal 85 (1996), 117-166 arXiv:math/0008243

[Cha06] Chaumard, Laurent *Discrtisation de zeta-dterminants d'oprateurs de Schrdinger* Bull. Soc. Math. France 134 (2006), no. 3, 327355.

[CJK10] G. Chinta, J. Jorgenson, and A. Karlsson *Zeta functions, heat kernels, and spectral asymptotics of degeenerating families of discrete tori* Nagoya Math J. 198 (2010), 121-172.

[CKP] H. Cohn, R. Kenyon, J. Propp. *A variational principle for domino tilings*, Journal of the American Mathematical Society 14.2 (2001): 297-346. arXiv:math/0008220

[CoPr] F. Colomo, A.G. Pronko. *The arctic curve of the domain-wall six-vertex model.* Journal of Statistical Physics 138.4-5 (2010): 662-700. arXiv:0907.1264

[CPZJ] F. Colomo, A.G. Pronko, P. Zinn-Justin *The arctic curve of the domain-wall six-vertex model in its anti-ferroelectric regime* . Journal of Statistical Mechanics: Theory and Experiment 2010.03 (2010): L03002. arXiv:1001.2189

[CR] D. Cimasoni, N. Reshetikhin. *Dimers on surface graphs and spin structures.* Communications in Mathematical Physics 275.1 (2007): 187-208. arXiv:0704.0273

[DD] B. Duplantier; F. David. *Exact partition functions and correlation functions of multiple Hamiltonian walks on the Manhattan lattice.* J. Stat. Phys. 51 (1988), pp 327-434.

[DEC] M. Desbrun, A. Hirani, M. Leok, J.E. Marsden *Discrete Exterior Calculus* Differential Geometry (math.DG); Numerical Analysis (math.NA).

[E] C. Evans, *Partial Differential Equations.* Providence: American Mathematical Society, ISBN 0-8218-0772-2.

[F] L.D. Faddeev. *Algebraic Aspects of Bethe-Ansatz.* Int. J. Mod. Phys. A 10 no. 13 (1995) pp. 1845-1878, arXiv:hep-th/9404013

[For92] R. Forman. *Determinants, finite-difference operators and boundary value problems.* Communications in Mathematical Physics. July (II) 1992, Volume 147, Issue 3, pp 485-526

[FT] L.D. Faddeev, L. A. Takhtajan. *The quantum method for the inverse problem and the XY Z Heisenberg model.* (Russian) Uspekhi Mat. Nauk 34 (1979); no. 5(209), 13-63, 256.

[GS] L-H. Gwa, Herbert Spohn. *Bethe solution for the dynamical-scaling exponent of the noisy Burgers equation.* Phys. Rev. A, v. 46, n. 2, 844-854, 1992.

[HWKK] H.Y. Huang, F. Y. Wu, H. Kunz, D. Kim. *Interacting dimers on the honeycomb lattice: An exact solution of the five-vertex model.* Physica A: Statistical Mechanics and its Applications 228.1 (1996): 1-32. arXiv:cond-mat/9510161

[JM] M. Jimbo, T. Miwa. *Algebraic Analysis of Solvable Lattice Models*. Vol. 85. American Mathematical Soc., 1994.

[Ka] P. Kasteleyn. *Graph theory and crystal physics*, 1967 Graph Theory and Theoretical Physics pp. 43-110 Academic Press, London

[Ken00] R. Kenyon *The asymptotic determinant of the discrete Laplacian*. Acta Mathematica.(2000), Volume 185, Issue 2, pp 239-286.

[Ken02] R. Kenyon *The Laplacian and Dirac operators on critical planar graphs*. Invent. math. (2002), 409-439.

[Ken09] R. Kenyon *Lectures on Dimers*. arXiv:0910.3129 [math.PR]

[KO] R. Kenyon and A. Okounkov. *Limit shapes and the complex burgers equation.*, Acta Mathematica 199.2 (2007): 263-302. arXiv:math-ph/0507007

[KOS] R. Kenyon, A. Okounkov and S. Sheffield. *Dimers and Amoebae*, Annals of mathematics (2006): 1019-1056. arxiv:math-ph/0311005

[KPW00] R. Kenyon; J. Propp; D.B. Wilson; *Trees and matchines*. Electron. J. Combin. 7 (2000), Research Paper 25, 34 pp.

[LL] L.D. Landau, E.M. Lifhitz. *Statistical Physics. Vol. 5* (1980) Butterworth-Heinemann. ISBN 978-0-7506-3372-7.

[LW] E. Lieb, F. Y. Wu. *Two-dimensional ferroelectric models.* Phase transitions and critical phenomena, pp.331-490

[Mer07] Discrete Riemann Surfaces C. Mercat *Discrete Riemann Surfaces* arXiv:0802.1612 [math.CV]

[MW] B. McCoy, T. Wu. *The Two-Dimensional Ising Model* 1973, Harvard University Press.

[NK] J.D. Noh, D. Kim. *Finite size scaling and the toroidal partition function of the critical asymmetric six-vertex model*, Physical Review E 53.4 (1996): 3225. arXiv:cond-mat/9511001

[No] I. M. Nolden, *The Asymmetric Six-Vertex Model*, J. Statist. Phys., v. 67, 155, 1992

[OR] A. Okounkov, N. Reshetikhin. *Random skew plane partitions and the Pearcey process*. Communications in mathematical physics 269.3 (2007): 571-609. arXiv:math/0503508

[PR] K. Plamarchuk, N. Reshetikhin. *The 6-vertex model with fixed boundary conditions* , arXiv:1010.5011

[Re] N. Reshetikhin. *Lectures on the integrability of the 6-vertex model.* arXiv:1010.5031

[Rez] F. Rezakhanlou. *Hydrodynamic limit for attractive particle systems on* $\mathbb{Z}^d$, Commun. Math. Phys. 40:417-448 (1991)

[RS15] N. Reshetikhin, A. Sridhar. *Integrability of Limit Shapes in the Six Vertex Model*, arXiv:1510.01053 [math-ph]

[RS16] N. Reshetikhin, A. Sridhar. *Integrability of Limit Shapes in the Six Vertex Model*, arXiv:1510.01053 [math-ph]

[Sh] S. Sheffield, PhD Thesis, Stanford Univ. 2003.

[Sk] E. K. Sklyanin. *Quantum Inverse Scattering Method. Selected Topics.* Quantum Group and Quantum Integrable Systems: Nankai Lectures on Mathematical Physics : Nankai Institute of Mathematics, China 2-18 April 1991 (World Scientific 1992), pp 63-97

[Sm] S. Smirnov. *Discrete Complex Analysis and Probability* arXiv:1009.6077

[Til13] B. de Tiliere *Critical Ising model and spanning trees partition functions* arXiv:1312.7026 [math-ph]

[ZJ] P. Zinn-Justin. *The Influence of Boundary Conditions in the Six-Vertex Model*, arXiv:cond-mat/0205192